

AD \_\_\_\_\_

Award Number: W81XWH-05-2-0027

TITLE: Imaging and Molecular Markers for Patients with Lung Cancer: Approaches with Molecular Targets, Complementary/Innovative Treatment, and Therapeutic Modalities

PRINCIPAL INVESTIGATOR: Waun Ki Hong, M.D.  
Roy Herbst, M.D., Ph.D.

CONTRACTING ORGANIZATION: University of Texas M.D. Anderson Cancer Center  
Houston, TX 77030

REPORT DATE: February 2011

TYPE OF REPORT: Annual

PREPARED FOR: U.S. Army Medical Research and Materiel Command  
Fort Detrick, Maryland 21702-5012

DISTRIBUTION STATEMENT: Approved for public release; distribution unlimited

The views, opinions and/or findings contained in this report are those of the author(s) and should not be construed as an official Department of the Army position, policy or decision unless so designated by other documentation.

REPORT DOCUMENTATION PAGE				Form Approved OMB No. 0704-0188	
Public reporting burden for this collection of information is estimated to average 1 hour per response, including the time for reviewing instructions, searching existing data sources, gathering and maintaining the data needed, and completing and reviewing this collection of information. Send comments regarding this burden estimate or any other aspect of this collection of information, including suggestions for reducing this burden to Department of Defense, Washington Headquarters Services, Directorate for Information Operations and Reports (0704-0188), 1215 Jefferson Davis Highway, Suite 1204, Arlington, VA 22202-4302. Respondents should be aware that notwithstanding any other provision of law, no person shall be subject to any penalty for failing to comply with a collection of information if it does not display a currently valid OMB control number. <b>PLEASE DO NOT RETURN YOUR FORM TO THE ABOVE ADDRESS.</b>					
1. REPORT DATE (DD-MM-YYYY) 01-02-2011		2. REPORT TYPE Annual		3. DATES COVERED (From - To) 1 FEB 2010 - 31 JAN 2011	
4. TITLE AND SUBTITLE  Imaging and Molecular Markers for Patients with Lung Cancer: Approaches with Molecular Targets, Complementary/Innovative Treatment, and Therapeutic Modalities				5a. CONTRACT NUMBER	
				5b. GRANT NUMBER W81XWH-05-2-0027	
				5c. PROGRAM ELEMENT NUMBER	
6. AUTHOR(S) Waun Ki Hong, M.D. Roy Herbst, M.D., Ph.D.  E-Mail: whong@mdanderson.org				5d. PROJECT NUMBER	
				5e. TASK NUMBER	
				5f. WORK UNIT NUMBER	
7. PERFORMING ORGANIZATION NAME(S) AND ADDRESS(ES) University of Texas M.D. Anderson Cancer Center Houston, TX 77030				8. PERFORMING ORGANIZATION REPORT NUMBER	
9. SPONSORING / MONITORING AGENCY NAME(S) AND ADDRESS(ES) U.S. Army Medical Research and Materiel Command Fort Detrick, Maryland 21702-5012				10. SPONSOR/MONITOR'S ACRONYM(S)	
				11. SPONSOR/MONITOR'S REPORT NUMBER(S)	
12. DISTRIBUTION / AVAILABILITY STATEMENT Approved for Public Release; Distribution Unlimited					
13. SUPPLEMENTARY NOTES					
14. ABSTRACT The projects in this proposal specifically target several signal transduction pathways known to be critical for NSCLC pathogenesis including the EGFR pathway and the more downstream ras/raf/Mek/ERK pathway. These projects combine targeted approaches using molecular and imaging techniques to validate activity against a target and monitor response using imaging modalities specific to the receptor using either small molecules or targeted peptide approaches.					
15. SUBJECT TERMS Lung cancer, molecular markers, molecular imaging, targeted therapy					
16. SECURITY CLASSIFICATION OF:			17. LIMITATION OF ABSTRACT  UU	18. NUMBER OF PAGES  113	19a. NAME OF RESPONSIBLE PERSON USAMRMC
a. REPORT U	b. ABSTRACT U	c. THIS PAGE U			19b. TELEPHONE NUMBER (include area code)

## TABLE OF CONTENTS

<b>INTRODUCTION .....</b>	<b>2</b>
<b>BODY .....</b>	<b>3</b>
<b>Project 1 .....</b>	<b>3</b>
<b>Project 2 .....</b>	<b>5</b>
<b>Project 3.....</b>	<b>7</b>
<b>Project 4.....</b>	<b>7</b>
<b>Project 5.....</b>	<b>8</b>
<b>Project 6 .....</b>	<b>11</b>
<b>Core B Biostatistics and Data Management.....</b>	<b>12</b>
<b>Core C Molecular Pathology and Specimen Procurement.....</b>	<b>13</b>
<b>Developmental Research Project 1.....</b>	<b>16</b>
<b>Developmental Research Project 2.....</b>	<b>20</b>
<b>Career Development Project 1.....</b>	<b>21</b>
<b>KEY RESEARCH ACCOMPLISHMENTS .....</b>	<b>26</b>
<b>REPORTABLE OUTCOMES.....</b>	<b>28</b>
<b>CONCLUSIONS.....</b>	<b>29</b>
<b>REFERENCES.....</b>	<b>30</b>
<b>APPENDICES.....</b>	<b>31</b>
<b>Appendix     I           Publications</b>	
<b>Appendix     II          IPQA Manufacturing Process</b>	
<b>Appendix     III         IPQA Clinical Trial Protocol</b>	

**IMPACT: Imaging and Molecular Markers for Patients with Lung Cancer: Approaches with Molecular Targets, Complementary, Innovative and Therapeutic Modalities**

**INTRODUCTION**

Lung cancer is the most prevalent cancer worldwide and the leading cause of cancer-related mortality in both men and women in the United States. Conventional multimodality therapies (surgery, radiation and chemotherapy) have reached a therapeutic ceiling in improving the five-year overall survival rate of non-small cell lung cancer (NSCLC) patients, clinically in large part due to chemo- and radiation-resistant locoregional and metastatic spread but ultimately due to poor understanding of the disease and its resistance to the therapy.

Lung cancer is a heterogeneous disease, resulting from accumulated genetic abnormalities over years, which thus requires a coordinated attack in a truly integrated fashion on multiple altered signal pathways. Emerging targeted therapy aims to target key molecular abnormalities in cancer and has succeeded in some tumor types such as chronic myeloid leukemia (CML) (Druker et al., 2004; Druker and Sawyers et al., 2001; Druker and Talpaz et al., 2001), gastrointestinal stromal tumor (Demetri et al., 2002), colon cancer (Hurwitz et al., 2003), and breast cancer (Howell et al., 2005). Thus, the incorporation of targeted therapy into conventional treatments appears to be a new promising approach to treatment of lung cancer.

The program project IMPACT has proposed to integrate targeted therapy in the lung cancer research program when initial clinical results showed disappointing response rates and survival benefit of epidermal growth factor receptor (EGFR) inhibitor gefitinib (Iressa™) for non-selected lung cancer patients (Herbst et al., 2002, 2003, 2004; Herbst, 2004; Kris et al., 2003; Giaccone et al., 2004). It aims to validate molecular mechanisms of targeted agents alone and in combination with chemo- and/or radiation therapies in preclinical and clinical settings. It also aims to develop effective molecular imaging and cancer cell-targeted peptide-based delivery tools to help improve efficacy of the targeted agents. Specifically, our objectives are:

- To validate preclinically and clinically several key signaling pathways and their agents for therapeutic potentials alone or in combination with each other or with chemo and /or radiotherapy
- To explore applications of molecular imaging for targeted therapy and identify cancer cell-targeted peptides for systemic delivery of therapeutic and imaging agents
- To discover and evaluate new molecular abnormalities and therapeutic predictors in lung cancer
- To develop an educational program for teens and young adults for smoking risk and resultant lung cancer occurrence.

IMPACT is composed of 6 research projects, 1 Biostatistics Core, 1 Molecular Pathology Core, 1 Molecular Imaging Core, 2 career development projects, and 2 developmental research projects. Here we present their scientific progresses in the sixth grant year as follows. We note that an additional no-cost extension for this grant has been requested, which is pending review, to allow completion of the clinical activities proposed in this report.

## **Project 1: Targeting epidermal growth factor receptor signaling to enhance response of lung cancer to therapeutic radiation.**

(PI and co-PI: Raymond E. Meyn, Ph.D., Ritsuko Komaki, M.D.)

In spite of significant technical advances including intensity-modulated radiation therapy (IMRT) and chemoradiation, locally advanced lung cancer continues to have a dismal prognosis as many patients' tumors appear to be resistant to radiation therapy. The molecular basis for radiation resistance is not fully understood, but tumor cells have an enhanced survival response that involves increased capacity for DNA repair and suppressed apoptosis. Both apoptosis propensity and DNA repair capacity are thought to be partly controlled by the upstream signal transduction pathways triggered by EGFR activation, which is constitutively activated in many NSCLCs, and its activation leads to a radiation-resistant phenotype. We hypothesize that the response of NSCLC to radiation can be improved through the use of inhibitors of EGFR signaling.

**Aim 1 To test the combination of external beam radiation and the selective EGFR-tyrosine kinase inhibitor erlotinib (Tarceva) in locally advanced NSCLC.**

### **Summary of Research Findings**

The clinical trial completed accrual with a total of 48 patients between November 2007 and July 2010. Seventeen patients were female (37%), the median age was 64 years, ranging from 46 years to 81 years. All patients had stage III medically or surgically (53%) inoperable lung cancer. Twenty-three patients (48%) had adenocarcinoma. All patients had good performance status of KPS 80 or higher (ECOG 0 or 1). Sixty percent of these patients were former- and 12.5% were never-smokers.

At present time, 46 patients have completed the entire treatment and they are evaluable for their response. These patients have an 80% response rate (CR 30% and PR 50%), with 9% of patients with stable disease or progressive disease, based on RECIST.

Although follow-up time is still short, with median follow-up 11 months for patients treated, overall survival of this trial is promising compared to chemoradiotherapy alone. The comparison was made for stage III NSCLC patients who were treated with 63 Gy in 7 weeks radiotherapy and concurrent weekly taxol and carboplatin, the same chemoradiation regimen as ID 2005-1023 but without Tarceva that was added to the regimen for this trial. Overall survival (at one year) is 85% in ID 2005-1023 (Taxol/Carboplatin and concurrent RT with Tarceva) compared to the historical control rate of 67% of patients who were treated by weekly Taxol/Carboplatin and concurrent RT without Tarceva (P=0.03).

### **Toxicity**

Toxicity data is available for 46 patients either having completed therapy, or who are presently receiving treatment. There have been no treatment-related deaths (Grade 5), although one patient died of pulmonary emboli which could not be differentiated from treatment-related or disease-related. Severe acute toxicities (grade 3 or higher according to CTC.3) related to treatments were recorded as the following events:

- Treatment skin reaction: Grade 2 in 6 patients and Grade 3 in 6 patients
- Acne, Grade 2 in 24 patients
- Acne, Grade 3 in 2 patients

- Diarrhea, Grade 2 in 4 patients
- Diarrhea, Grade 3 in 2 patient
- Pneumonitis, Grade 3 in 2 patients; Grade 4 in 1 patient
- Leukopenia, Grade 3 in 12 patients, Grade 4 in 1 patient
- Neutropenia Grade 3 in 5 patient, Grade 4 in 2 patients
- Thrombocytopenia, Grade 3 in 1 patient
- Hypomagnesemia, Grade 3 in 1 patient
- Hypokalemia, Grade 3 in 2 patient
- Pneumonia, Grade 3 in 7 patients
- Dehydration, Grade 3 in 3 patients.

Once the clinical trial reached the target patient accrual, we elected to extend the project to test whether EMT may govern the radiosensitizing abilities of EGFR antagonists and may also directly regulate tumor cell radiosensitivity itself. We hypothesized that these relationships extend to NSCLC patients treated with EGFR inhibitors, e.g., erlotinib, in combination with radiation and to patients treated with radiotherapy alone. To do this, we enlisted the expertise of Dr. Ignacio Wistuba (Core C) to analyze the biopsy specimens from the phase II clinical trial for biomarkers associated with response to EGFR TKI and tumor's epithelial or mesenchymal status and correlate the results with patient response. Tumor response in this trial was 14 (30%) CR, 23 (50%) PR, and 9 (20%) stable or progressive disease. Five in 41 pts (12%) had EGFR mutation (EGFR-M), all adenocarcinoma with 2 females, compared to none with squamous histology ( $p=0.05$ ). At present time, 39.1% (18/46) of patients are alive without any evidence of disease, 34.8% (16/46) of patients are alive with disease, and 26.1% (12/46) of patients are dead. The median overall survival (OS) and progressive-free survival (PFS) were 25.8 months & 13.6 months, respectively. One-year & 2-year OS rates were 84% & 75%, respectively, and 1- and 2-year PFS rates were 54% & 32%, respectively. We plan to analyze the pre-treatment biopsy specimens and correlate findings with response as well as with patterns of failure outside the scope of this project. Further results of this study will be reported in Cores B and C.

**Aim 2      To test the hypothesis that activation of the EGFR pathway leads to radiation resistance in NSCLC cells due to an enhanced capacity for repairing DNA lesions.**

**Summary of Research Findings**

This aim was completed as reported in the previous annual report.

**Aim 3      To test the hypothesis that clinically useful inhibitors of EGFR signaling abrogate DNA repair capacity, restore apoptotic response and radiosensitize NSCLC cells.**

**Summary of Research Findings**

This aim was completed as reported in the previous annual report.

**Aim 4      To test the hypothesis that targeting both EGFR and its downstream signaling pathways will have at least an additive radiosensitizing effect on NSCLC.**

**Summary of Research Findings**

This aim was completed as reported in the previous annual report.

**Aim 5 To test whether the strategies developed in Specific Aims 2-4 have efficacy in a xenograft tumor model.**

**Summary of Research Findings**

This aim was completed as reported in the previous annual report.

**Key Research Accomplishments**

- Completed patient enrollment to the ID 2005-1023 trial.
- Analyzed biopsy specimens from the phase II clinical trial for biomarkers associated with response to EGFR TKI and tumor's epithelial or mesenchymal status.
- Analyzed the pre-treatment biopsy specimens and correlated findings with response as well as with patterns of failure.

**Conclusions**

This prospective phase II clinical study demonstrated an excellent 1-year overall survival of 84 % and median overall survival of 25.8 months. All EGFR-M were seen in adenocarcinomas. Erlotinib demonstrated a radiosensitization effect. We will further analyze the activity of EMT to see if it has a direct role in the regulation of tumor cell radiosensitivity, and these results will be reported by Cores B and C in the next year's report.

**Project 2: Molecular Imaging of EGFR Expression and Activity in Targeting Therapy of Lung Cancer**

(PI and co-PI: Juri Gelovani, M.D., Ph.D.; Roy Herbst, M.D., Ph.D.)

**Aim 1 To synthesize novel pharmacokinetically optimized  $^{124}\text{I}$  and  $^{18}\text{F}$ -labeled IPQA derivatives for PET imaging of EGFR kinase activity and conduct *in vitro* radiotracer accumulation studies in tumor cells expressing different levels of EGFR activity.**

**Summary of Research Findings**

This aim was completed and summarized in the previous reports.

**Aim 2 To assess the biodistribution (PK/PD) and tumor targeting by novel  $^{124}\text{I}$  and  $^{18}\text{F}$ -labeled EGFR kinase-specific IPQA derivatives using PET imaging in orthotopic mouse models of lung cancer and compare *in vivo* radiotracer uptake/retention with phospho-EGFR levels *in situ*.**

**Summary of Research Findings**

This aim was completed as reported in the previous annual report.

**Aim 3 Using selected  $^{124}\text{I}$  or  $^{18}\text{F}$ -labeled IPQA derivative, to conduct pre-clinical studies in animals with orthotopic models of lung cancer xenografts with different levels of EGFR expression/activity, and to assess the value of PET imaging as the inclusion criterion for therapy by EGFR inhibitors, as well as for monitoring the efficacy of treatment with EGFR-targeted drugs.**

**Summary of Research Findings**

This aim was completed as reported in the previous annual report.

**Aim 4** Perform pilot clinical PET imaging studies with the optimized  $^{124}\text{I}$  or  $^{18}\text{F}$ -labeled IPQA derivative under the RDRC guidelines in patients with NSCLC undergoing adjuvant therapy before tumor resection or biopsy. Compare PET image-based measures of EGFR activity with immunohistochemical measures of phospho-EGFR *in situ*.

#### **Summary of Research Findings**

We have completed all required development work of this novel imaging agent in order to translate it into a clinical trial through an IND application (current regulation). The main development work includes a formal GLP toxicology study (summarized in previous report), clinical phase I trial protocol (summarized in previous report), and clinical grade automated manufacturing process under the current regulation (summarized in Appendix II). The clinical trial protocol (attached in Appendix III) has been reviewed and approved with contingencies by IRB, and the protocol is now being reviewed by DoD. Upon completion of the review, the institutional IND office will submit the complete IND document to FDA for approval to allow us to proceed with the phase I clinical trial.

A complete IND document including the following chapters have been prepared:

- Cover Sheet
- Table of Contents
- Introductory Statement and General Investigational Plan
- Protocol
- Chemistry, Manufacturing, and Control Information (CMC)
- Pharmacology and Toxicology Information
- Previous Human Experience with the Investigational Drug
- Additional information
- Relevant information

The proposed timeline for IND submission, clinical trial activation and completion of the IPQA study is as follows:

IRB review and approval	February 2011 (completed)
DoD review and approval	Feb-Mar 2011
IND submission to FDA	April 2011
FDA review	30 days, April-May 2011
Addressing FDA's comments and FDA approval for trial	May-June 2011
Trial activation	June-July 2011
Estimated trial completion	December 2011

#### **Key Research Accomplishments**

- Received institutional IND approval for the Phase I clinical trial.
- Received IRB approval with contingencies for the Phase I clinical trial.
- Submitted the clinical trial to the DoD for review and approval.

#### **Conclusions**

We have successfully submitted the IPQA imaging clinical trial to our IRB for review and approval during the current project period. Once we receive approval from the DoD, we will submit the IND to the FDA for review and approval to activate the trial. We have requested an

additional no-cost extension of this grant to allow us to activate and complete this trial, and will report the results of this small study (n=18 patients) at the end of this extended grant period.

### **Project 3: Targeted Peptide-based Systemic Delivery of Therapeutic and Imaging Agents to Lung Cancer**

(PI and co-PI: Renata Pasqualini, Ph.D., Wadih Arap, M.D., Ph.D.)

The studies outlined in this proposal focus on the use of peptide sequences with selective lung tumor-targeting properties. We will seek to validate these probes as delivery vehicles in drug and gene-targeting approaches. This approach directly selects *in vivo* for circulating probes capable of preferential homing into tumors. The strategy will be to combine homing peptides in the context of phage as gene therapy vectors. Given that many of our peptides also target angiogenic vasculature in addition to tumor cells, these studies are likely to enhance the effectiveness of therapeutic apoptosis induction and imaging technology.

**Aim 1 To select peptides targeting primary and metastatic tumors in lung cancer patients.**

#### **Summary of Research Findings**

This aim was completed as reported in the previous annual report.

**Aim 2 To validate receptors for targeting human lung cancer.**

#### **Summary of Research Findings**

This aim was completed as reported in the previous annual report.

**Aim 3 To design tools for molecular imaging of lung tumors.**

#### **Summary of Research Findings**

This aim was completed as reported in the previous annual report.

### **Project 4: Inhibition of bFGF Signaling for Lung Cancer Therapy**

(PI: Reuben Lotan, Ph.D.)

The survival of lung cancer patients is poor because this cancer is diagnosed at advanced stages. Therefore, improvements in early detection through the identification of molecular markers for diagnosis and for intervention combined with targeted chemoprevention are urgently needed. While the molecular events involved in lung cancer pathogenesis are being unraveled by ongoing large scale genomics, proteomics, and metabolomics studies, it is already well recognized that proliferation-, survival- and angiogenesis- promoting signaling pathways are amplified in lung cancer. Among the angiogenesis signaling pathways, the basic fibroblast growth factor (bFGF) and its transmembrane tyrosine kinase receptors (FGFRs) are playing important roles in addition to the well-studied vascular endothelial growth factor (VEGF) and its receptors (VEGFRs). Both types of angiogenesis signaling pathways, the VEGF/VEGFR and the bFGF/FGFR, have been detected in NSCLC and associated with lung cancer development. However, most efforts in preclinical and clinical trials have been directed to the VEGF/VEGFR pathway.

We hypothesize that bFGF triggers signaling pathways that contribute to malignant progression of lung cancers by stimulating tumor cell and endothelial cell proliferation and survival and augmenting angiogenesis. Therefore, agents that intervene in this pathway may be useful for lung cancer therapy either alone or in combination with agents that target the VEGF/VEGFR signaling pathways and/or with cytotoxic agents. We will address the following specific aims in order to understand the mechanism(s) underlying the *in vitro* and *in vivo* effects of bFGF on lung cancer and endothelial cells and the ability of bFGF inhibitors to suppress the growth of NSCLC *in vitro* and *in vivo*.

**Aim 1      Determine the effects of bFGF on *in vitro* growth, survival, motility, invasion and angiogenesis of NSCLC cells and endothelial cells.**

**Summary of Research Findings**

This aim was completed and summarized in the previous reports.

**Aim 2      Evaluate the relative potency of several inhibitors of bFGF binding to receptor (i.e., TMPP and analogs) in inhibiting effects of bFGF detected in Specific Aim 1 and evaluate the effects of these inhibitors in combination with paclitaxel on *in vitro* growth and survival of tumor cells.**

**Summary of Research Findings**

This aim was completed and summarized in the previous reports.

**Aim 3      Evaluate anti-tumor activity (growth inhibition, apoptosis, suppression of angiogenesis) of the most effective inhibitor identified in Specific Aim 2 when used alone and in combination with paclitaxel in an orthotopic lung cancer model using luciferase-expressing NSCLC cells for *in vivo* bioluminescence imaging of tumor growth and response to treatment.**

**Summary of Research Findings**

This specific aim was abandoned as previously reported.

**Aim 4      To investigate the expression of bFGF signaling components (bFGF, FGFR-1, FGFR-2, heparan sulfate, syndecan-1, and FGFR-3) by IHC staining of tissue microarrays (TMAs), and correlate the expression of bFGF/bFGFRs between tumor and non-malignant epithelial cells with angiogenesis.**

**Summary of Research Findings**

This aim was completed and summarized in the previous reports.

**Project 5: Targeting mTOR and Ras signaling pathways for lung cancer therapy**

(Project Co-leaders: Shi-Yong Sun, Ph.D., Suresh Ramalingam, M.D.)

It should be noted that Dr. Suresh Ramalingam assumed the leadership of Project 5 following Dr. Fadlo Khuri's decision to step down due to increased administrative responsibilities; this administrative change was approved by the DoD in November 2009. Following is a summary of our research progress:

**Aim 1 To determine whether an mTOR inhibitor inhibits the growth of human NSCLC cells via G1 growth arrest or induction of apoptosis, and to identify the molecular determinants of mTOR inhibitor sensitivity.**

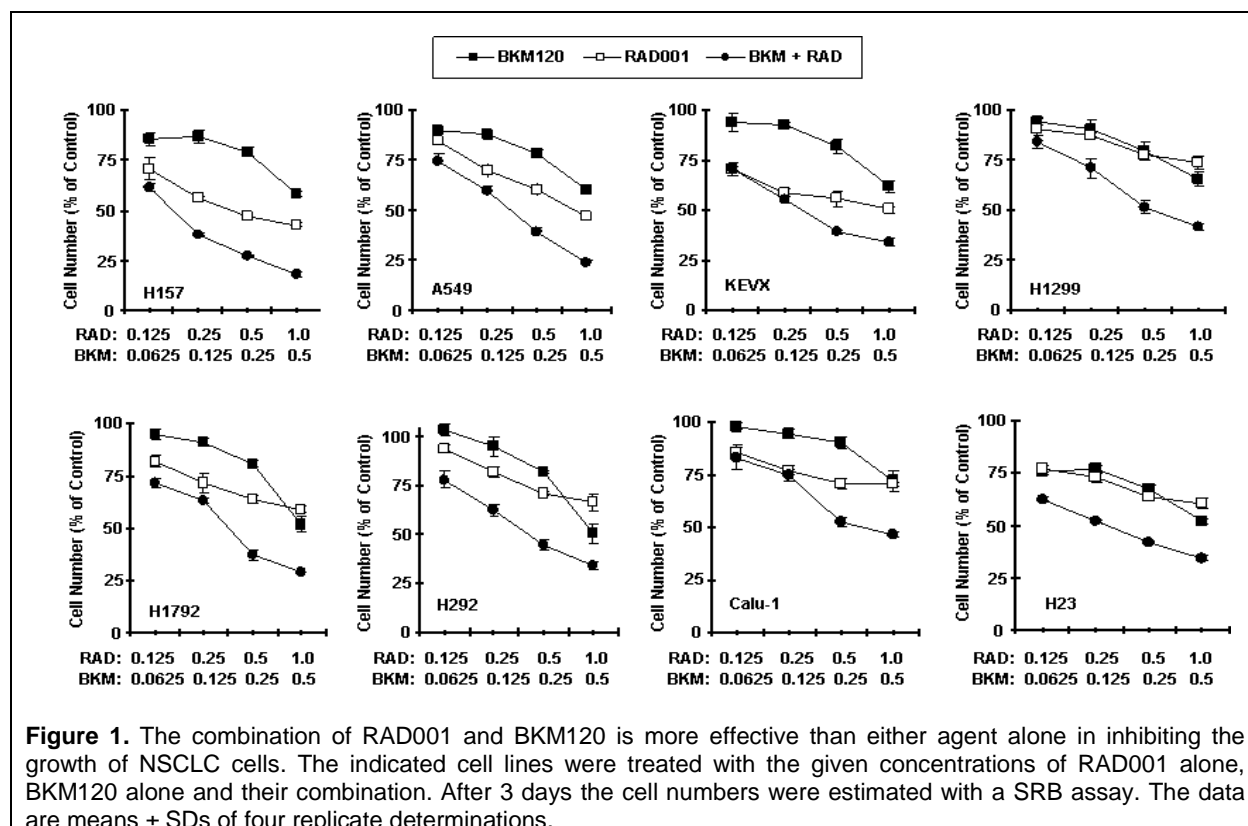
### Summary of Research Findings

This aim was completed and summarized in the previous reports.

**Aim 2 To determine whether the effect of mTOR inhibitors on the growth of human NSCLC cells is enhanced in the presence of a PI3K inhibitor or a MAPK inhibitor.**

### Summary of Research Findings

The combination of RAD001 and BEZ235 on the growth of human NSCLC cells as summarized in the last report has been summarized in a manuscript. The manuscript has been submitted to Novartis for review and is now ready to be submitted for publication.



Moreover, we recently obtained BKM120, a novel PI3K inhibitor under clinical testing, from Novartis and tested the effect of its combination with RAD001 on the growth of NSCLC cells. We found that the combination of low doses of RAD001 and BKM120 was much more effective than either agent alone in inhibiting the growth of a panel of NSCLC cells (Figure 1). The combinational effects appear synergistic as the combination indexes are  $< 1$ . The combinational effects were further confirmed in a long-term colony formation assay (12 day). These findings further support our notion that co-targeting the mTOR and PI3K signaling pathway generates enhanced anticancer activity. Thus, our findings warrant further evaluation outside the scope of this grant to study the combination of RAD001 and BKM120 *in vivo* and in clinical trials.

Based on our findings on the combination of a rapalog and a PI3K inhibitor, including the combination of RAD001 and BKM120 from the IMPACT, we have developed another project to co-target the mTOR and PI3K signaling in NSCLC (Project 1 in our recently submitted lung cancer P01 competitive renewal). The goal of the project is to translate our lab findings from bench to bedside.

**Aim 3 To evaluate the efficacies of the combinations of rapamycin with LY294002 or U0126 in nude mice models of lung cancer xenografts *in vivo*.**

#### **Summary of Research Findings**

This aim was completed as reported in the previous annual report.

**Aim 4 To conduct a pilot clinical biochemical induction trial to investigate the effect of RAD001 in operable NSCLC patients and identify molecular determinants of RAD001 sensitivity and prognosis.**

#### **Summary of Research Findings**

This project involves a clinical trial that is designed to evaluate the biological activity of RAD001 in patients with early stage non-small lung cancer. Briefly, the patients undergo a biopsy, followed by 3-4 weeks of therapy with RAD001 and then undergo surgical resection. The specimens from pre-treatment and post-treatment time points are then analyzed for various biomarkers of the mTOR pathway. Initially, we enrolled a total of 12 patients to the 5mg/ day dose of RAD001. The treatment was tolerated well overall with no undue safety concerns. Analysis of biomarkers at this time point revealed that levels of p-AKT were predictably up-regulated with RAD001 therapy. However, down-regulation of the downstream markers was not consistently noted across tumor specimens. One possible explanation for this observation was the fact that the dose of RAD001 (5 mg/day) might have been insufficient for marker modulation. In order to address this issue, we expanded the trial to include a cohort of patients treated with higher dose of 10 mg/day. This cohort began accrual after the amendment was approved by the institutional review board. We have already enrolled two patients to the higher dose level and are screening the third patient. We intend to have approximately 10 patients at the 10mg dose level to test this hypothesis. The need for an additional experimental biopsy has caused the trial accrual to be slower than originally anticipated. However, the exciting biological findings so far could help explain the modest levels of RAD001 activity in patients with non-small cell lung cancer. Once the accrual is complete, the dose-response effect could guide all current and future trials of RAD001 in non-small lung cancer.

#### **Key Research Accomplishments**

- Demonstrated synergistic inhibitory effects on the growth of human NSCLC cells through the combination of RAD001 and BKM120.
- Developed a new project for our P01 renewal (5P01CA116676) titled “Targeting PI3K and mTOR signaling in lung cancer” based on our IMPACT findings.
- Enrolled 14 patients to the RAD001 clinical trial.

#### **Conclusions**

The co-targeting the mTOR and PI3K singling is an effective strategy to achieve enhancement of mTOR-targeted cancer therapy. From our RAD001 clinical trial, we have discovered that further research is needed to study the sensitivities of this drug in NSCLC to discover a dose-response for future clinical studies.

## **Project 6: Identification and Evaluation of Molecular Markers in Non-Small Cell Lung Cancer (NSCLC)**

(PI and co-PI: Ralf Krahe, Ph.D., Li Mao, M.D)

A better understanding of the lung cancer biology and an identification of genes involved in tumor initiation, progression and metastasis are an important first step leading to the development of new prognostic markers and targets for therapy. In the same context, identification of reliable predictive markers for response or resistance to therapy in NSCLC patients is also desperately desired for optimal delivery of targeted therapy and/or standard chemotherapy. The proposed studies aim to identify the two types of markers that would eventually help develop smarter clinical trials, which will selectively recruit patients who are more likely to respond to one regimen over another and lead to improvement of overall therapeutic outcomes.

**Aim 1 To expression profile by DNA microarray technology aerodigestive cancers - with primary focus on adenocarcinoma and squamous cell carcinoma (SCC) of the lung, and head and neck squamous cell carcinoma (HNSCC), including primary tumors and normal adjacent tissue, and (where available) metastatic lesions.**

### **Summary of Research Findings**

This aim was completed as reported in the previous annual report.

**Aim 2 To DNA profile the same samples by complementing DNA approaches to stratify RNA expression profiles on the basis of their corresponding DNA profiles.**

### **Summary of Research Findings**

This aim was completed as reported in the previous annual report.

**Aim 3 To evaluate the contribution of promoter hypermethylation and transcriptional inactivation of known cancer genes subject to epigenetic silencing to cancer phenotype.**

### **Summary of Research Findings**

This aim was completed as reported in the previous annual report.

**Aim 4 To determine protein signatures of treatments of erlotinib and other therapeutic agents, alone or in combination, in NSCLC and identify molecular predictors of response.**

### **Summary of Research Findings**

This aim was completed as reported in the previous annual report.

**Aim 5 To determine a clinical utility of the molecular predictors.**

### **Summary of Research Findings**

This aim was completed and summarized in previous reports.

## **Core B: Biostatistics & Data Management Core**

(Core Director: J. Jack Lee, Ph.D.)

The Biostatistics and Data Management Core has continued to work with all IMPACT Projects in their research efforts, especially in the area of biostatistical support in clinical trial design, implementation, and analysis of experimental results. We also developed statistical methods to enhance the design and analysis pertinent to the lung cancer research.

### **Specific Aims:**

1. To ensure that the results of all projects are based on well-designed experiments and are appropriately interpreted by providing experimental design; sample size estimates; power calculations; and integrated, comprehensive analysis for each basic science, pre-clinical, and clinical study.
2. To develop a data management system that integrates clinical, pathological, and basic science data while providing data integrity through process tracking and quality control.
3. To provide statistical and data management support for genomic and imaging studies including microarray, proteomics, and molecular targeted imaging.
4. To develop and adapt innovative statistical methods pertinent to biomarker-integrated translational lung cancer studies.
5. To produce statistical reports for all projects.
6. To collaborate and assist all project investigators with the publication of scientific results.

### **Summary of Research Findings**

For Project 1: “Targeting epidermal growth factor receptor signaling to enhance response of lung cancer to therapeutic radiation,” Core B continues to provide statistical support in the conduct and interim efficacy and toxicity analyses of the clinical trial proposed in Project 1: “A Phase I/II Study of Tarceva (erlotinib) in Combination with Chemoradiation in Patients with Stage III A/B Non-Small Cell Lung Cancer” (PI: Dr. Ritsuko R. Komaki). This study has reached the target accrual of 48 patients. We have performed preliminary analysis and an abstract summarizing the study results has been submitted to the Annual Meeting of ASCO 2011.

For Project 2 “Molecular Imaging of EGFR Expression and Activity in Targeting Therapy of Lung Cancer,” Core B has worked closely with Drs. Juri Gelovani, David Stewart, and Bijun Yang in the development of a three-stage design for the protocol “A phase I study of 18F-Fluoro-PEG6-IPQA as a PET Imaging Agent for Active/Mutant EGFR Expression in Tumors (2009-0832).” This protocol has been approved by MDACC CRC and is IRB-approved with contingencies. It will be submitted to the FDA as soon as it is approved by MDACC IRB.

For Project 3: “Targeted Peptide-based Systemic Delivery of Therapeutic and Imaging Agents to Lung Cancer,” we have been working in collaboration with Drs. Pasqualini, Arap, and Wistuba. The IHC staining of lung cancer TMAs (390 cases) has been completed. We are working with investigators to analyze the marker EphA5. The association of the levels of EphA5 expression with histology, smoking history, pathological stage, recurrence-free survival and overall survival are being analyzed.

For Project 4: “Inhibition of bFGF Signaling for Lung Cancer Therapy,” most of the statistical analysis for the study has been completed. We continue to work with Dr. Lotan on the synergy

analysis of cell line studies and developing the statistical methods for analyzing data from combination studies.

For Project 6: “Identification and Evaluation of Molecular Markers in Non-Small Cell Lung Cancer (NSCLC),” statistical support was provided for genomic analysis.

In addition, we continue to provide statistical support for the development project study “Treatment of Malignant Pleural Effusion with ZD6474 a Novel Vascular Endothelial Growth Factor Receptor (VEGFR) and Epidermal Growth Factor Receptor (EGFR) Tyrosine Kinase Inhibitor” (PI: Dr. Roy Herbst). The study has accrued a total of 20 patients. This study has been closed to accrual.

We have requested an additional unfunded grant period to allow continued support to complete the study analyses described above.

### **Key Research Accomplishments**

- Continued to provide statistical support in the clinical trials for Project 1 and DRP-1.
- Provided statistical support for Projects 2, 3, 4, 6, and Pathology Core.
- Determined synergistic, additive, and antagonistic effects of combination drug treatments in synergy studies for Project 4 (PI: Dr. Reuben Lotan).
- Developed a Bayesian dose-finding trial design with multiple drug combinations (Project 2).

### **Conclusions**

Core B continued to provide statistical analysis and data management support for all research projects in the IMPACT study.

### **Core C: Pathology Core**

(Director: Ignacio Wistuba, M.D.)

The IMPACT interdisciplinary research proposal for studying targeted therapy of lung cancers has required extensive histopathologic, IHC, and molecular studies of cell and tissues specimens, which have been assisted, coordinated or performed by the Pathology Core. One of the most important roles of the Pathology Core has been to provide professional technical services for proper procurement, storage and use of human and animal tissues, as well as technical assistance for IHC analysis. In addition, the Pathology Core has provided assistance for collection and evaluation of tissue specimens in IMPACT clinical trials in lung cancer patients.

**Aim 1 Develop and maintain repository of tissue, cell and serum specimens from patients with lung neoplasia, as requested by the various component projects.**

### **Summary of Research Findings**

For the IMPACT clinical trial using erlotinib (Tarceva), chemotherapy, and radiotherapy in advanced NSCLC patients (Protocol 2005-1023; Principal Investigator: R. Komaki), the Pathology Core assisted in the evaluation of tumor tissue specimens of 35 NSCLC cases with adequate tissue for biomarker analysis. *EGFR* mutation (exons 18-21) was detected in 4 tumors and *KRAS* (codons 12-13) mutation in 2 tumors with adenocarcinoma histology. *EGFR* copy number increase by FISH (high polysomy and gene amplification, FISH+) was detected in 10 (30%) out of 34 tumors successfully tested, including 9 tumors with high polysomy and 1 with

gene amplification. Additionally, the expression of EGFR and phosphorylated-EGFR were examined by immunohistochemistry (IHC) using a semi-quantitative score (range 0-400) addressing intensity and extension of the membrane and cytoplasmic expression in malignant cells. EGFR and p-EGFR expression positive cells (score  $\geq 200$ ) were detected in 11 (31%) and 10 (29%) out of the 35 cases examined, respectively. Recently, the protein expression of epithelial-mesenchymal transition (EMT) IHC markers were optimized and are currently being tested in 25 tumor specimens with histology sections available for analysis. These results will be reported in the next and final annual report.

**Aim 2 Develop innovative tissue and cell reagents from lung cancer patients for the investigation and validation of the molecular endpoints relevant to each component project.**

#### **Summary of Research Findings**

The development of new tissue and cell reagents from lung cancer patients was completed in 2008. These reagents and data are available for future analysis of molecular abnormalities of lung cancer, including tissue microarrays (TMA), lung cancer cell lines repository, lung cancer heterotransplants (in collaboration with L. Mao), and pleural fluid specimens from lung cancer patients (in collaboration with C. Jimenez). In particular, the repository of pleural fluid specimens from 120 patients have been fully characterized from the cytology standpoint and the clinical information has been annotated.

**Aim 3 Process human and animal cell and tissues for histopathological, immunohistochemical (IHC) and molecular analyses, including tissue microdissection, as required by each component project.**

#### **Summary of Research Findings**

As indicated in the other Aims, most of the collaborations with the IMPACT research projects have been completed as reported previously. The preparation and processing of tissue specimens for research projects are described in Aim 4 and includes mostly histopathological, IHC, and molecular analysis.

**Aim 4 Perform and evaluate IHC analysis in human and animal cell and tissue specimens, as required by the various component projects.**

#### **Summary of Research Findings**

The collaborative work with the other IMPACT projects was completed in 2007 and 2008. During the current project period, we have collaborated with the IMPACT investigators to finalize the preparation of manuscripts for publications (see below, a to d).

Completed or published projects during the current project period in collaboration with IMPACT research projects.

**a) Analysis of GRP78, IL-11R and Eph5A markers in human NSCLC tissue specimens** (Collaboration with Project 3, R. Pasqualini). This project was completed and a manuscript is in preparation by Dr. Pasqualini's lab.

**b) Molecular abnormalities (protein expression and methylation) analysis of *TCF21* gene in NSCLC** (Collaboration with Project 6, R. Krahe). From this work, a paper by Richards et al. was published in 2010 *Cancer*.

**c) Analysis VEGFR-2 gene (KDR) copy number and mutation in NSCLC.** We studied the role of vascular endothelial growth factor-2 (VEGFR-2) gene (*KDR*) abnormalities in malignant cells of surgically resected non-small cell lung carcinoma (NSCLC) tissues and correlated with patients' outcome after platinum adjuvant chemotherapy. We studied tissues obtained from 248 surgically resected NSCLCs. *KDR* copy number gain (CNG) was examined by quantitative PCR (qPCR) and fluorescence *in situ* hybridization (FISH). VEGFR-2 protein expression and microvascular density were studied by IHC. In NSCLC cell lines, *KDR* CNG (n=75) and VEGFR-2 levels (n=63) were quantified and correlated with *in vitro* sensitivity to platinum drugs. *KDR* mutation (exons 7, 11 and 21) and single nucleotide polymorphisms (SNPs; 889G/A, 1416A/T and -37A/G) were genotyped by PCR-based sequencing. Malignant cells demonstrated *KDR* CNG in 32% of NSCLC tumors. *KDR* CNG detected by qPCR was confirmed by FISH analysis. *KDR* CNG in malignant cells was associated with poor overall survival (OS) (HR=4.0;  $P=0.001$ ) and worse recurrence-free survival (HR=1.83;  $P=0.044$ ) in multivariate analysis. *KDR* CNG predicted worse OS (HR=5.16;  $P=0.003$ ) in patients who received platinum adjuvant therapy but not in untreated patients ( $P=0.349$ ). In cell lines, *KDR* CNG and high VEGFR-2 expression correlated significantly with resistance to platinum. Recently, we have established that in NSCLC cell lines that inhibition of *KDR* expression using *KDR* siRNA produced a modest effect on improving cells sensitivity to platinum, but induced a significant inhibition of cell migration and invasion. Our preliminary analysis suggests that the association of *KDR* CNG and VEGFR-2 overexpression correlate with angiogenesis by inducing HIF-1 $\alpha$  protein overexpression by Western blot in malignant cells. *KDR* mutations were not detected in NSCLC tumor tissues. The *KDR* variant genotypes SNPs 1416 AT/TT and -37 AG/GG were associated with a favorable OS in lung adenocarcinoma. The association between *KDR* CNG and worse outcome in platinum adjuvant therapy-treated NSCLC patients suggests that *KDR* might be a potential biomarker for predicting the efficacy of adjuvant chemotherapy in this disease. From this work, a paper by F. Yang et al. was submitted and is currently being reviewed by *Cancer Research* (see attached manuscript).

**d) Role of NKX2-1 (TTF-1) gene amplification and protein overexpression in lung cancer and its association with EGFR abnormalities.** A paper with this data was published by X. Tang and H. Kadara et al. in 2010 in *Clinical Cancer Research*.

#### **Key Research Accomplishments**

- Completed the molecular biomarker analysis on the Project 1 clinical trials using NSCLC tissue specimens from 34 patients enrolled in the clinical trial, and demonstrated that *KDR* CNG and VEGFR-2 overexpression correlated with angiogenesis and patients' outcome when treated with adjuvant chemotherapy.
- Published research findings on the molecular abnormalities analysis of TCF21 gene in NSCLC.
- Published research findings on the role of NKX2-1 (TTF-1) gene amplification and protein overexpression in lung cancer and its association with EGFR abnormalities NSCLC.

#### **Conclusions**

The Pathology Core has assisted and collaborated actively with several research projects to perform multiple histopathological, immunohistochemical, and genetic studies in a large series of lung cancer tissue, including the collection and processing of prospectively collected samples from two ongoing clinical trials. In addition, the Pathology Core has managed to complete and publish several research activities, which fully integrate with some of the IMPACT research projects. The Pathology Core has successfully fulfilled the goals proposed for the sixth year of the IMPACT program.

### **DRP-1: Treatment of Malignant Pleural Effusion with ZD6474, a Novel VEGFR and EGFR TK Inhibitor**

(PI and co-PI: Roy Herbst, M.D., Ph.D., Carlos Jimenez, M.D.)

Recurrent malignant pleural effusion is a debilitating clinical problem that requires palliation with repeated therapeutic thoracentesis or pleurodesis (Putnam, J Surg Clin North Am 2002). Malignant pleural effusions have been associated with high levels of VEGF. Treatment with a VEGFR tyrosine kinase inhibitor resulted in a decrease in the amount of pleural effusion in an animal model (Yano, CCR 2000). We hypothesize that malignant pleural effusion formation in cancer patients can be decreased with ZD6474 (AstraZeneca), a VEGFR and EGFR tyrosine kinase inhibitor.

**Aim 1 To determine clinical effect of ZD6474.**

**Aim 2 To investigate biological correlates.**

**Aim 3 To investigate radiographic correlates.**

**Aim 4 To assess quality of life.**

#### **Summary of Research Findings**

The amended single arm, open-label study to evaluate the efficacy of ZD6474 on the management of pleural effusion in NSCLC patients was activated in June of 2007.

The study was closed early, on July 19, 2010, with 28 patients enrolled. Early closure was due to the company's decision not to continue development of this agent in this setting. Eight patients are excluded from the ongoing clinical analysis based on the following factors:

- Seven patients did not receive medication:
  - Non-compliance (1)
  - Benign pleural effusion (2)
  - Non-amenable for intrapleural catheter (IPC) placement (3)
  - Renal dysfunction (1)

One patient was not evaluable due to placement of a defective intrapleural catheter.

#### **Best response**

- Eleven patients had stable disease
- Two patients had partial response
- Seven patients had disease progression

#### **Days with intrapleural catheter in place**

Median time to intrapleural catheter removal was 35 days. IPC catheters were removed for the following reasons:

- Achievement of pleurodesis (16 patients)
- Pleurodesis failure (3 patients)

- Death (1 patient)

#### Related adverse events

- 5 patients with grade 3 QTc prolongation
- 1 patient with drug-related erythema multiforme and rash/desquamation
- 1 patient with grade 3 weight loss and anorexia

One patient stopped the medication at week 6 after developing neurological symptoms and hyponatremia. One patient with a defective intrapleural catheter was excluded from the study at week 6. One patient stopped the medication at week 7 due to recurrence of QTc prolongation after dose reduction. One patient has the IPC dislodged on day 15, and the IPC was later removed on day 23 due to emphysema.

*Systematic examination of pretreatment and changes in the plasma and pleural effusion angiogenic profiles consisting of a panel of proangiogenic cytokines and chemokines, soluble receptors, and potential biomarkers of endothelial damage.* We collected samples of pleural effusion and plasma from patients consenting to an optional specimen collection (see Table 1) and, in collaboration with Drs. John Heymach and Hai Tran, performed a cytokine and angiogenesis factor (CAF) analysis (Table 2) in the baseline and 2-week specimens, as described below.

**Table 1: Acquired samples**

Sample Type	Timepoint	Frequency	Percent
Plasma	2-Weeks	9	15.25
Plasma	Baseline	12	20.34
Pleural	2-Weeks	18	30.51
Pleural	Baseline	20	33.90

#### Methodology:

Multiplex bead-based technology enables the simultaneous quantitation of up to 100 analytes. This technology uses polystyrene beads internally dyed with differing ratios of two spectrally distinct fluorophores. Each fluorophore can have any of 10 possible levels of fluorescent intensity; thereby creating a family of 100 spectrally addressed bead sets. These assays contain dyed beads conjugated with monoclonal antibodies specific for a target protein or peptide such as a cytokine or a

phosphoprotein. Each of the 100 spectrally addressed bead sets can contain a capture antibody specific for a unique target protein. The antibody-conjugated beads are allowed to react with sample and a secondary, or detection, antibody in a microplate well to form a capture sandwich immunoassay. Multiplex assays can be created by mixing bead sets with different conjugated antibodies to simultaneously test for many analytes in a single sample. The use of this technique has been well documented in the literature and results are comparable to that of ELISA<sup>1-3</sup>. Analysis of these factors have been completed up to 23/27 proteins (Bio-Rad) from a single specimen have been completed from various matrices including: human serum and plasma and cell media from human cancer cell lines using Bio-Plex 200 system (Bio-Rad Laboratories, Hercules, CA) with the Bio-Plex Manager software. Currently, up to 50 human cytokines can be analyzed from 2 separate kits (2-plex, 21-plex & 27-plex). We also incorporated newly available markers of the EGFR axis including Amphiregulin, Betacellulin, EGF, EGFR, Epiregulin, FGF-basic, HB-EGF, PDGF-BB, PIGF, Tenascin C, and TGF- $\alpha$  (Table 3).

**Table 2: Cytokines and Angiogenic Factors Profiling (CAF)**

pro/antiangiogenic factors	EGF axis	chemokines	interleukins
VEGF, FGF-basic	EGF, EGFR, TGF- $\alpha$	MCP-1, -3	IL-1 $\alpha$ , -1 $\beta$ , -1RA
HGF, PDGF-bb	Amphiregulin, Betacellulin	MIP-1 $\alpha$ , $\beta$	IL-2, -2Ra
MMP-9, PIGF	HB-EGF	RANTES (CCL5)	IL3 - IL10
	<b>hypoxia</b>	MIP-2	IL-12 – IL18
<b>endothelial function/damage</b>	Osteopontin*	MIG (CXCL-9)	
sVEGFR-2	CA-9*	Eotaxin (CCL11)	<b>growth factors</b>
sE-selectin	<b>IGF axis</b>	IP-10 (CXCL10)	GM-CSF
VCAM-1	IGF-I*, -II*	SDF-1a (CXCR4)	G-CSF
	IGF-BP3*	KC (CXCL1)	M-CSF
<b>inflammation/adhesion</b>		GRO- $\alpha$	SCGF- $\beta$
sICAM-1		CTACK (CCL27)	SCF
IFN- $\alpha$ , $\gamma$			Beta-NGF
TNF- $\alpha$ , $\beta$			
MIF, LIF	*ELISA assays (Various)		

Depending on target protein, a typical calibration curve was generated covering the dynamic range from 2 to 32,000 pg/mL. Typical sample volume required for each sample well ranged from 50 – 100  $\mu$ L. Human CVD Biomarker Panel 1 (3-plex includes MMP-9, sICAM-1, and sE-Selectin) from Millipore (Catalog # HCVD1-67AK). The remaining analytes were determined by using validated, enzyme-linked immunosorbent assays (ELISA) assays. Soluble VEGFR1 and sVGFR2 was analyzed by EIA (Invitrogen,

Carlsbad, CA). For each plate, the standard curves were assessed to ensure that the expected assay range was achieved. For each individual sample, the mean concentration was calculated for duplicate samples, and the coefficient of variance % (CV%) calculated for each of the analytes. If the median CV% was greater than 25%, analysis of the sample was repeated. In the rare case that the repeat CV% is greater than 25%, one of the two analyses will be selected based on lower CV% and consistency with prior values.

#### Preliminary Results:

Data was sent to send to Biostatistics Core for analysis and a preliminary report was generated with the following results.

Several CAFs were observed to significantly change in specimens obtained at baseline compared to specimens obtained at 2-weeks after initiation of therapy from both pleural effusion and plasma samples from paired sets (Tables 3a and 3b).

**Table 3a: Pleural Effusion CAF changes over 2 weeks (baseline to 2 weeks)**

CAF	n	mean $\pm$ std, median(min, max)	pValue
PIGF	18	0.86 $\pm$ 0.61, 0.77 (-0.36, 2.18)	0
MCP-1	18	1.71 $\pm$ 1.66, 1.48 (-0.35, 4.97)	0.0005
MCP-3	18	1.83 $\pm$ 2.23, 1.41 (-2.48, 7.24)	0.0008
IL-8	18	1.57 $\pm$ 1.79, 1.66 (-1.84, 4.66)	0.0023
IL-18	18	0.22 $\pm$ 0.29, 0.15 (-0.38, 0.8)	0.0028
HGF	18	0.69 $\pm$ 0.88, 0.77 (-1.42, 2.42)	0.0047
M-CSF	18	0.71 $\pm$ 1.05, 0.79 (-1.19, 3.2)	0.009
Eotaxin	18	1.26 $\pm$ 1.61, 1.31 (-0.94, 4.95)	0.012
SCGF-b	18	0.21 $\pm$ 0.33, 0.12 (-0.3, 1.06)	0.0139
IGF-I	18	0.37 $\pm$ 0.55, 0.41 (-1.03, 1.22)	0.0139
b-NGF	18	0.61 $\pm$ 0.94, 0.74 (-1.48, 2.04)	0.0208
G-CSF	18	0.27 $\pm$ 0.83, 0.29 (-2.17, 1.79)	0.0268

IL-5	18	1.35 ± 2.64, 0.8 (-2.95, 7.56)	0.0268
IFN-α2	18	0.15 ± 0.34, 0.23 (-0.58, 0.65)	0.0304
HB-EGF	18	0.19 ± 0.34, 0.18 (-0.36, 0.93)	0.0395
IL-1Ra	18	-0.61 ± 0.44, -0.57 (-1.91, 0.13)	.0000
sEGFR	18	-0.3 ± 0.3, -0.28 (-1.05, 0.28)	.0003
CTACK	18	-0.33 ± 0.35, -0.23 (-1, 0.36)	.0016
Amphiregulin	18	-0.55 ± 0.79, -0.59 (-2.04, 1.2)	.0104

**Table 3b:** Plasma CAF changes over 2 weeks (baseline to 2 weeks)

CAF	n	mean ± std, median(min, max)	pValue
Eotaxin	9	0.46 ± 0.32, 0.44 (0.12, 0.89)	0.0039
PIGF	9	0.56 ± 0.44, 0.46 (0.07, 1.35)	0.0039
MCP-1	9	0.56 ± 0.57, 0.52 (-0.07, 1.51)	0.0117
IL-18	9	0.48 ± 0.53, 0.35 (-0.2, 1.54)	0.0195
IFN-α2	9	1.57 ± 2.64, 0.55 (-0.41, 7.64)	0.0273
sVEGFR2	9	-0.29 ± 0.21, -0.27 (-0.63, 0)	.0078
sEGFR	9	-0.24 ± 0.28, -0.18 (-0.83, 0.04)	.0117

Interestingly, the 5 factors that were increased in plasma, including Eotaxin, PIGF, MCP-1, IL-18 and IFN-α2, were also present and increased in the pleural effusion samples; only sEGFR was shown to be decreased from both sample types.

From our prior experience with vandetanib (ZD6474) in the front-line therapy with or without chemotherapy doublet for patients with NSCLC, a distinct pattern of plasma CAF correlated with either chemotherapy-based or vandetanib alone (1). It was reported that in the vandetanib treatment alone arm, plasma concentrations of VEGF increased at 3 week post and sVEGFR-2 was shown to be decreased at 8 days post initiation of therapy and progressively continue to declined, results that were associated with PFS. With our limited number of samples (n=9) in this trial, changes in VEGF were not significant but sVEGFR-2 significantly decreased over the first 2 weeks after starting vandetanib therapy (p=0.0078).

We then correlated baseline pleural effusion CAFs with both best therapeutic and best radiographic responses. Two factors, HB-EGF (p=0.073) and Eotaxin (p=0.053), from pleural effusions were associated with best therapeutic responses. For best radiographic responses, only GROα (p=0.035) was statistically significant, with other CAFs trending towards significance including Eotaxin (p=0.059), TNFα (p=0.097) and IGF-I (p=0.097).

For baseline plasma CAF, only IL-15 (p=0.040) was statistically significant, while IFN-γ (p=0.070) and IL1ra (p=0.070) were trending in correlation with best therapeutic responses. There were no associations noted with plasma CAF and best radiological responses. Additionally, there were no CAF levels significantly modulated (over the 2-week period from baseline) with either therapeutic or radiographic responses.

We have shown that the relative changes of CAFs over short period (up to 2 weeks) is very minimal, less than 10% (unpublished), in a small group of NSCLC cancer patients. Certainly, due to the small sample size in this study, some of these changes may be due to chance;

however, modulation with similar factors have been reported for two VEGFR tyrosine kinase inhibitors, vandetanib and pazopanib (1, 2).

### **Key Research Accomplishments**

- Completed patient enrollment to the clinical trial.
- Measured and analyzed all collected plasma and pleural effusion samples using magnetic multiplex bead-based and ELISA assays.
- Completed the preliminary biostatistics analysis.

### **Conclusions**

The amended single arm, open-label study to evaluate the efficacy of ZD6474 on the management of pleural effusion in NSCLC patients was closed on July 19, 2010, with 28 patients enrolled. Using the pleural effusion specimens collected from the 20 evaluable patients, we performed ELISA assays to determine that several CAFs from plasma and pleural effusions were associated with best responses (therapeutic and radiographic). Additional statistical analysis will be performed during the next year by the statistical core (Core B) to correlate CAFs from plasma and pleural effusion with overall survival.

## **DRP-2: TALK - Teens and Young Adults Acquiring Lung Cancer Knowledge**

(PI: Alexander V. Prokhorov, M. D., Ph.D.)

Ninety percent of lung cancer cases in adults are direct results of smoking. In children and young adults, tobacco use remains a major public health problem in spite of the recent declines in smoking prevalence among children and adolescents. Over the past 2-3 decades, numerous factors of smoking initiation among adolescents have been thoroughly investigated. A considerable volume of literature is currently available providing important clues with respect to designing tobacco prevention and cessation among youth.

Focusing on this major public health problem – tobacco use among young individuals and lack of in-depth knowledge of lung cancer issues – Project TALK (Teens and Young Adults Acquiring Lung Cancer Knowledge) was conceived and funded as a smoking cessation/prevention pilot project for culturally diverse high-risk young populations that include school drop-outs, economically disadvantaged, and underserved. Using modern technologies, the Departments of Behavioral Science and Thoracic/Head & Neck Medical Oncology have joined their efforts to conduct this developmental project under the leadership of Dr. Alexander V. Prokhorov. The project will assist in making major advances in lung cancer education and prevention among youth. Project TALK will produce a CD-ROM-based education/behavior change for teenagers and young adults (15-24 years of age).

We have thus been devoting our effort in 4 tasks as described in the Statement of Work based on the project timeline:

**Aim 1      Develop intervention program.** Focus groups will be held with adolescents and young adults to ensure we are capturing the essence of the program, using the right messages, and employing the appealing video and animated characters. (Years 1-2)

### **Summary of Research Findings**

This aim was completed and summarized in previous reports.

**Aim 2 Develop and beta-test CD-ROM.** This includes the design of the animation, illustrations, scripts and accompanying videos. (Years 1-2)

**Summary of Research Findings**

This aim was completed and summarized in previous reports.

**Aim 3 Implement program in agreed upon locations and recruit young adults to participate in the study.** (Years 3-4)

**Summary of Research Findings**

This aim was completed and summarized in previous reports.

**Aim 4 Collect and analyze data.** (Years 3-4)

**Summary of Research Findings**

This aim was completed and summarized in previous reports.

**Career Developmental Project (CDP1): Identification of Membrane Proteins in Bronchial Epithelia Cells as Biomarkers of Early Detection for Lung Cancer**

(PI: Ja Seok Peter Koo, Ph.D.)

Lung cancer is the leading cause of cancer deaths. Early detection of the malignant lesion leads to an improved 5-year survival rate after surgical resection. Therefore, advanced screening tools are needed urgently to detect lung cancer at an early stage to improve control of such deadly lung cancer.

It should be noted that Dr. Kang relocated to another institution after the beginning of the current project period. Dr. Ja Seok Koo has been appointed by the IMPACT Principal Investigator, Dr. Waun Ki Hong, to assume ongoing research of this project.

**Aim 1 To isolate membrane proteins uniquely expressed on the surface of squamous metaplasia using organotypically cultured bronchial epithelial cells.**

**Summary of Research Findings**

This aim was completed as reported in the previous annual report.

**Aim 2 To identify differentially represented proteins using proteomics.**

**Summary of Research Findings**

This aim was completed as reported in the previous annual report.

**Aim 3 To verify the differentially represented proteins using PCR, Western blotting, and immunocytochemistry.**

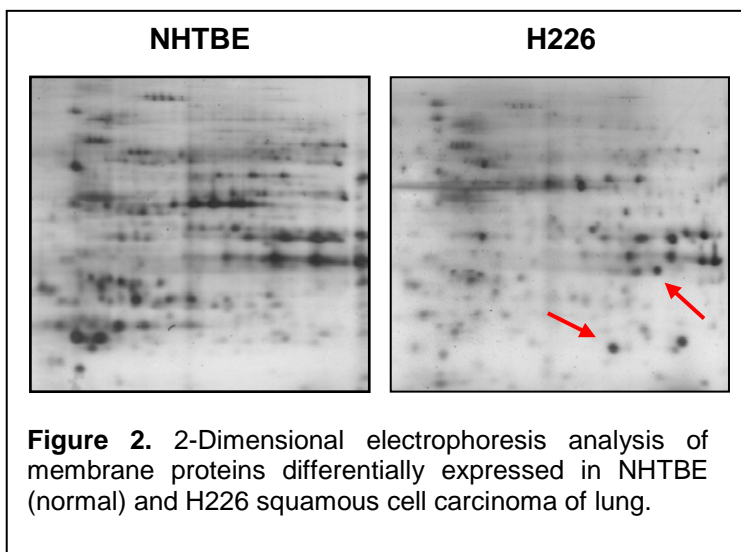
**Summary of Research Findings**

To identify cell-surface markers specific for lung cancer cells, as these proteins have strong potential for use as novel diagnostic and therapeutic biomarkers, we performed 2-Dimensional proteomics analysis using membrane fractions isolated from normal human bronchial epithelial

(NHBE) cells and non-small-cell lung cancer (NSCLC) cells. We performed the immunoblotting on cell lysates, following by immunohistochemistry and immunofluorescence using the A549, H1355, H1734, H520, H1703, H2228 and H460 cell lines. From this experiment, we conclude that increased expression levels of the receptor for activated kinase C (RACK1) in tumor tissue were observed in tumor but not normal lung cells, and was localized in the tumor cell cytoplasm. The expression of RACK1, which mediates protein–protein interactions for the regulation of cell motility, in NSCLC, and its interaction with several proteins that have important roles in cell growth and survival, makes RACK1 a candidate molecule to target as a potential therapeutic strategy for NSCLC. Details are described below.

*Proteomic identification of RACK1 (also known as GNB2L1, guanine nucleotide binding protein, or beta polypeptide 2-like 1) as a lung cancer cell-specific, membrane-associated protein.* Two-dimensional proteomics analysis using membrane fractions isolated from NHBE cells and NSCLC cells. Membrane proteins were isolated from *in vitro* models of squamous metaplastic bronchial epithelial cells and compared with those of normal mucocilliary bronchial epithelial cells by 2-dimensional polyacrylamide gel electrophoresis. Normal human tracheobronchial epithelial (NHTBE) cells from passage 3 were cultured by air-liquid interface method. Cells were harvested at 12 days after air-liquid formation. The NSCLC cell line H226 were grown on plastic plate in RPMI 1640 containing 10% fetal bovine serum. H226 and NHTBE cells were harvested at 80% confluence.

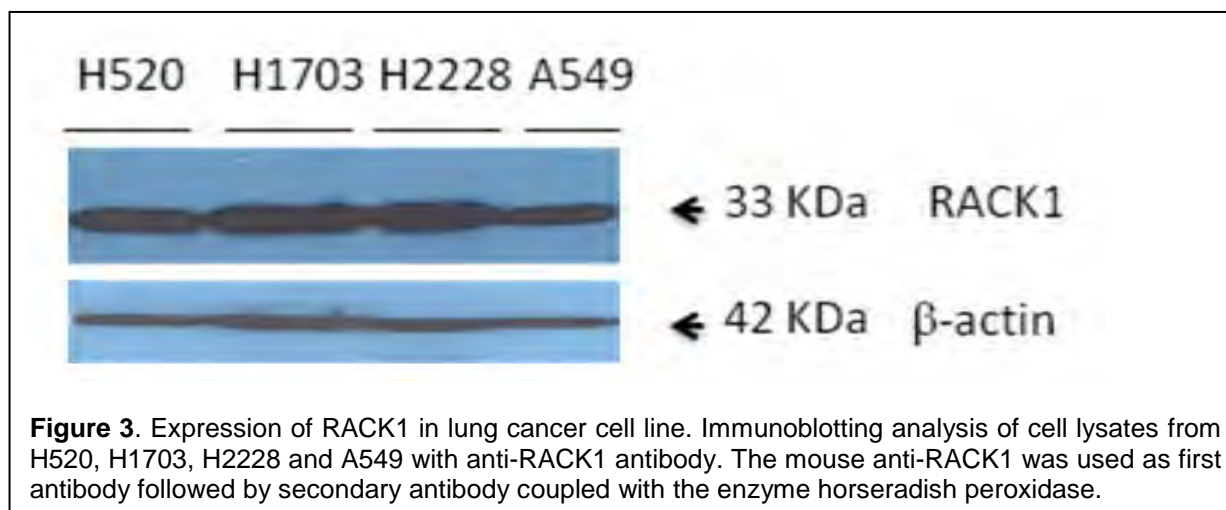
Using HPLC-tandem Mass Spectrometer in collaboration with the Proteomics Core facility at MD Anderson, we sequenced and determined the specific identity of the proteins isolated (Arrow marked in Figure 2). After being excised, the silver-stained spots were destained and digested in gel with 200 ng of modified trypsin (Promega). The resulting peptides were analyzed by nano-liquid chromatography-tandem mass spectrometry with on-line desalting with a Famos autosampler, an Ultimate nano-LC module, and a Switchos precolumn switching device (LC Packings/Dionex). Electrospray ion-trap mass spectrometry was done using an LTQ linear ion-trap mass spectrometer (Thermo). The fragment spectra were analyzed using the National Center for Biotechnology Information nonredundant protein database and the Mascot search engine (Matrix Science). After extensive database searching, we found that the protein in the lower spot was an unknown protein and identified the protein in the upper spot as a receptor for activated kinase C (RACK1).



RACK1 is ubiquitously expressed in a wide range of tissues, including the brain, liver, and spleen. Moreover, RACK1 has many other binding partners involved in the organization of adhesions and cell migration, including the cytoplasmic tail of  $\beta$ -integrins and PKC. These interactions support the role of RACK1 as a key scaffolding protein that mediates protein–protein interactions for the regulation of cell motility. Recent studies indicated that RACK1 reduced cell-cycle progression and the growth of colon carcinoma cells by negatively regulating

endogenous Src kinase activity, suggesting that RACK1 may be an attractive therapeutic target to treat cancer; thus, we explored its potential utility as a marker in lung cancer.

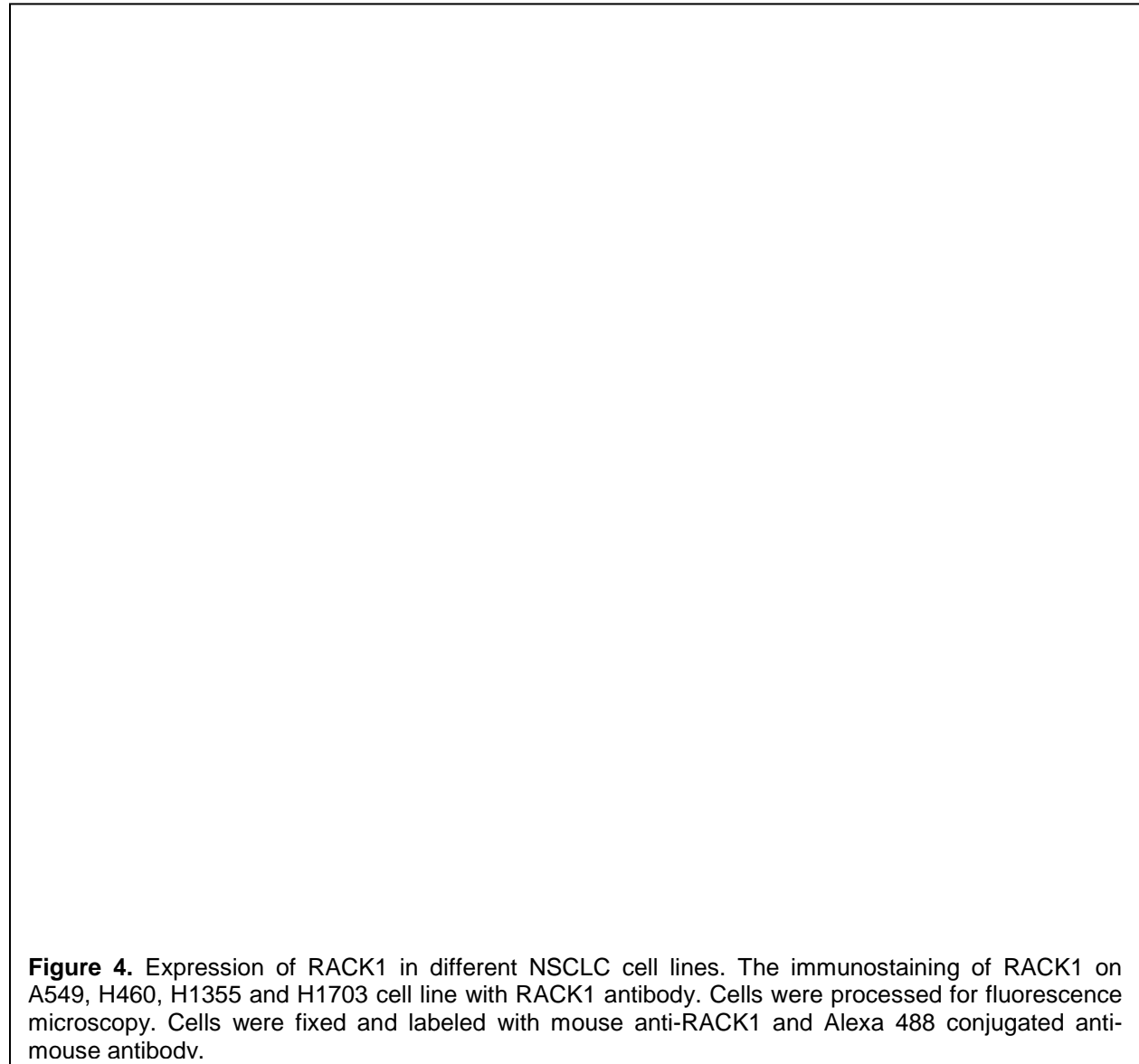
*Expression of RACK1 is detected in NSCLC cells.* We studied the expression of RACK1 in H520, H1703, H2228 and A549 NSCLC cell lines by Western blot analysis using the mouse anti-RACK1 antibody as the first antibody and cell lysates from the different cells lines (Figure 3). Proteins resolved by 1-dimensional electrophoresis were blotted onto nitrocellulose membranes (Bio-Rad) in a transfer buffer containing Tris, glycine (MP Biomedical). Membranes were blocked in 5% (wt/vol) skimmed milk in phosphate buffered saline 0.1% tween for 30min and probed with anti-RACK1 monoclonal antibody (Santa Cruz). After washing with phosphate-buffered saline 0.1% tween (vol/vol), the membranes were incubated with appropriate antibody conjugated with horseradish peroxidase and diluted at 1:1000, that is, anti-mouse immunoglobulin G (BioRad). The blot shows the reactivity of antibody with protein at 33KDa. The staining of RACK1 on cell lysates from H520, H1703 and H2228 appears stronger than the lysates from A549. This data suggests the presence of RACK1 in all the NSCLC cells tested with differences in expression levels.



*Immunofluorescence localization of the expression of RACK1.* Fluorescence experiments were performed to determine the localization of RACK1. The immunofluorescence was started with  $2.5 \times 10^4$  cells cultured in chamber slides. Cell lines were fixed for 10 minutes with 4% buffered glutaraldehyde at  $-20^\circ\text{C}$ , incubated for 30 minutes with 2% bovine serum albumin, and then with Anti-RACK1 antibodies (Santa-Cruz, CA) diluted 1:100 for 1 hour. Antibody binding was detected after 1 hour incubation at room temperature with an anti-mouse antibody Alexa-488 (1:200) (Invitrogen). Cells were imaged using fluorescence microscope equipped with X40 magnification. The staining shown in the cytoplasm of A549, H460, H1355 and H1703 cell lines confirm the presence of RACK1 in the cytoplasm of NSCLC cells (Figure 4). The positive control used shows the similar pattern of staining compare to the RACK1; the negative control shows no artifact of staining. This result confirmed the presence of RACK1 by showing the intense staining observed in cytoplasm of the NSCLC cells.


*Immunohistochemical staining.* To evaluate the expression of RACK1 as diagnostic marker in the tumor tissue, we studied IHC expression using the tissue of mouse pulmonary carcinomas from *KRAS*-mutant mice. IHC studies were performed on formalin-fixed, paraffin-embedded tissue sections using the streptavidin–biotin–peroxidase complex method. Sections were cut at  $4\mu\text{m}$  thickness and mounted on APES coated slides, dewaxed in xylene, and rehydrated in

graded ethanol. The sections were treated with 30% hydrogen peroxide for 10 minutes to inhibit endogenous peroxidase activity and washed in phosphate buffered saline (PBS). To retrieve antigen, the sections were immersed in 0.01M citrate buffer and heated by microwave or on a hot plate for 20 to 25 minutes, following by washing in water. Sections were preincubated with the primary antibody for 60 minutes at room temperature. The biotinylated secondary antibody (Invitrogen) was incubated for 30 minutes at room temperature. The sections were incubated with streptavidin–peroxidase complexes (Invitrogen kit) for 30 minutes at room temperature, followed by washing in PBS.



Staining results (Figure 5) show intense expression and localization of RACK1 in the cytoplasm observed in the lung epithelium and adenocarcinoma sections from *KRAS*-mutant mouse, but no obvious staining was observed in the lung sections from wild-type littermate control mice. Using mass spectrometry, we were able to identify RACK1 as a protein in plasma membrane fraction. RACK1 is also known as GNB2L1 (guanine nucleotide binding protein, beta polypeptide 2-like 1), lung cancer oncogene 7 or PIG21 (proliferation-inducing gene 21). We

verified expression of the RACK1 in lung cancer cells by immunoblotting that demonstrates the staining of protein at 33KDa, in H520, H1703, H2228 and A549. The data confirms the expression of RACK1 in the cell lysates of the different cells lines. Moreover, the fluorescence staining using NSCLC cell line confirms the presence of RACK1 in cytoplasm of these cell lines.



**Figure 5. Expression of RACK1 in mouse lung adenocarcinomas.** The marked expression of RACK1 was observed in the lung tumor sections from *KRAS*-mutant lung cancer mouse model. The RACK1 staining is not detected in the lungs from normal lung from control mice.

The expression of RACK1 was also verified in mouse tumor tissue obtained from *KRAS* lung cancer mouse model; a high staining and marked level of RACK1 were found in the tumor but not in the normal lung from wild-type mice. Moreover, RACK1 expression level was significantly associated with cell localization within the tumor. Further studies are needed to clarify the relationship between the expression of RACK1 and clinical outcome of adenocarcinoma.

#### **Key Research Accomplishments**

- Identified RACK1 as a protein that is uniquely expressed in squamous cell carcinoma cell lines and may be a therapeutic target to treat cancer.

#### **Conclusions**

We demonstrated increased expression levels of the RACK1 in tumor tissue in tumor but not normal lung cells, and this increased expression was localized in the tumor cell cytoplasm. RACK1 mediates protein–protein interactions for the regulation of cell motility, in NSCLC, and has interactions with several proteins that have important roles in cell growth and survival, making it a candidate molecule to target as a potential therapeutic strategy for NSCLC. Further extensive studies are warranted to clarify if RACK1 will have utility as a therapeutic target for lung cancer.

## **KEY RESEARCH ACCOMPLISHMENTS**

### **Project 1: Targeting epidermal growth factor receptor signaling to enhance response of lung cancer to therapeutic radiation.**

- Completed patient enrollment to the ID 2005-1023 trial.
- Analyzed biopsy specimens from the phase II clinical trial for biomarkers associated with response to EGFR TKI and tumor's epithelial or mesenchymal status.
- Analyzed the pre-treatment biopsy specimens and correlated findings with response as well as with patterns of failure.

### **Project 2: Molecular imaging of EGFR expression and activity in targeted therapy of lung cancer**

- Received institutional IND approval for the Phase I clinical trial.
- Received IRB approval with contingencies for the Phase I clinical trial.
- Submitted the clinical trial to the DoD for review and approval.

### **Project 5: Targeting mTOR and Ras signaling pathways for lung cancer therapy**

- Demonstrated synergistic inhibitory effects on the growth of human NSCLC cells through the combination of RAD001 and BKM120.
- Developed a new project for our P01 renewal (5P01CA116676) titled "Targeting PI3K and mTOR signaling in lung cancer" based on our IMPACT findings.
- Enrolled 14 patients to the RAD001 clinical trial.

### **Core B: Biostatistics & Data Management Core**

- Continued to provide statistical support in the clinical trials for Project 1 and DRP-1.
- Provided statistical support for Projects 2, 3, 4, 6, and Pathology Core.
- Determined synergistic, additive, and antagonistic effects of combination drug treatments in synergy studies for Project 4 (PI: Dr. Reuben Lotan).
- Developed a Bayesian dose-finding trial design with multiple drug combinations (Project 2).

### **Core C: Pathology Core**

- Completed the molecular biomarker analysis on the Project 1 clinical trials using NSCLC tissue specimens from 34 patients enrolled in the clinical trial, and demonstrated that *KDR* CNG and VEGFR-2 overexpression correlated with angiogenesis and patients's outcome when treated with adjuvant chemotherapy.
- Published research findings on the role of NKX2-1 (TTF-1) gene amplification and protein overexpression in lung cancer and its association with EGFR abnormalities NSCLC.
- Published research findings on the molecular abnormalities analysis of TCF21 gene in NSCLC.

### **DRP-1: Treatment of Malignant Pleural Effusion with ZD6474, a Novel VEGFR and EGFR TK Inhibitor**

- Completed patient enrollment to the clinical trial.
- Measured and analyzed all collected plasma and pleural effusion samples using magnetic multiplex bead-based and ELISA assays.
- Completed the preliminary biostatistics analysis.

**CDP1: Identification of Membrane Proteins in Bronchial Epithelia Cells as Biomarkers of Early Detection for Lung Cancer**

- Identified RACK1 as a protein that is uniquely expressed in squamous cell carcinoma cell lines and may be a therapeutic target to treat cancer.

## **REPORTABLE OUTCOMES**

### **Publications** *(attached in Appendix):*

Pal A, Balatoni JA, Mukhopadhyay U, Ogawa K, Gonzalez-Lepera C, Shavrin A, Volgin A, Tong W, Alauddin MM, Gelovani JG. Radiosynthesis and Initial In Vitro Evaluation of [(18)F]F-PEG (6)-IPQA-A Novel PET Radiotracer for Imaging EGFR Expression-Activity in Lung Carcinomas. *Molecular Imaging and Biology*. 2010 Sep 22. PMID: 20859697.

Richards KL, Zhang B, Sun M, Dong W, Churchill J, Bachinski LL, Wilson CD, Baggerly KA, Yin G, Hayes DN, Wistuba II, Krahe R. Methylation of the candidate biomarker TCF21 is very frequent across a spectrum of early-stage nonsmall cell lung cancers. *Cancer*. 2011 Feb 1;117(3):606-17. doi: 10.1002/cncr.25472. PMCID: PMC3023841.

Spivey KA, Banyard J, Solis LM, Wistuba II, Barletta JA, Gandhi L, Feldman HA, Rodig SJ, Chirieac LR, Zetter BR. Collagen XXIII: a potential biomarker for the detection of primary and recurrent non-small cell lung cancer. *Cancer Epidemiology, Biomarkers & Prevention*. 2010 May;19(5):1362-72. PMCID: PMC2880394.

Yeh HH, Ogawa K, Balatoni J, Mukhopadhyay U, Pal A, Gonzalez-Lepera C, Shavrin A, Soghomonyan S, Flores L 2nd, Young D, Volgin AY, Najjar AM, Krasnykh V, Tong W, Alauddin MM, Gelovani JG. Molecular imaging of active mutant L858R EGF receptor (EGFR) kinase-expressing nonsmall cell lung carcinomas using PET/CT. *Proceedings of the National Academy of Science U S A*. 2011 Jan 25;108(4):1603-8. PMCID: PMC3029752.

Yin G, Yuan Y. "Bayesian dose finding in oncology for drug combinations by copula regression." *Journal of the Royal Statistical Society*. 2009; 58: 211-224.

### **Abstracts** *(attached in Appendix):*

Komaki R, Blumenschein G, Wistuba II, Lee JJ, Allen P, Wei X, Tang XM, Meyn RE, Liu D, Hong WK. "The phase II trial of erotinib and radiotherapy following chemoradiotherapy for patients with stage III Non-Small Cell Lung Cancer has shown a favorable response profile." Submitted to the 2011 ASCO Annual Meeting.

## CONCLUSIONS

**Project 1:** This prospective phase II clinical study demonstrated an excellent 1-year overall survival of 84 % and median overall survival of 25.8 months. All EGFR-M were seen in adenocarcinomas. Erlotinib demonstrated a radiosensitization effect. We will further analyze the activity of EMT to see if it has a direct role in the regulation of tumor cell radiosensitivity, and these results will be reported in the next year.

**Project 2:** We have successfully submitted the IPQA imaging clinical trial to our IRB for review and approval during the current project period. Once we receive approval from the DoD, we will submit the IND to the FDA for review and approval to activate the trial. We have requested an additional no-cost extension of this grant to allow us to activate and complete this trial, and will report the results of this small study (n=18 patients) at the end of this extended grant period.

**Project 5:** The co-targeting the mTOR and PI3K singling is an effective strategy to achieve enhancement of mTOR-targeted cancer therapy. From our RAD001 clinical trial, we have discovered that further research is needed to study the sensitivities of this drug in NSCLC to discover a dose-response for future clinical studies.

**Biostatistics Core:** Core B continued to provide statistical analysis and data management support for all research projects in the IMPACT study.

**Pathology Core:** The Pathology Core has assisted and collaborated actively with several research projects to perform multiple histopathological, immunohistochemical, and genetic studies in a large series of lung cancer tissue, including the collection and processing of prospectively collected samples from two ongoing clinical trials. In addition, the Pathology Core has managed to complete and publish several research activities, which fully integrate with some of the IMPACT research projects. The Pathology Core has successfully fulfilled the goals proposed for the sixth year of the IMPACT program.

**DRP-1:** The amended single arm, open-label study to evaluate the efficacy of ZD6474 on the management of pleural effusion in NSCLC patients was closed on July 19, 2010 with 28 patients enrolled. Using the pleural effusion specimens collected from the 20 evaluable patients, we performed ELISA assays to determine that several CAFs from plasma and pleural effusions were associated with best responses (therapeutic and radiographic). Additional statistical analysis will be performed during the next year by the statistical core (Core B) to correlate CAFs from plasma and pleural effusion with overall survival.

**CDP1:** We demonstrated increased expression levels of the RACK1 in tumor tissue in tumor but not normal lung cells, and this increased expression was localized in the tumor cell cytoplasm. RACK1 mediates protein–protein interactions for the regulation of cell motility, in NSCLC, and has interactions with several proteins that have important roles in cell growth and survival, making it a candidate molecule to target as a potential therapeutic strategy for NSCLC. Further extensive studies are warranted to clarify if RACK1 will have utility as a therapeutic target for lung cancer.

## **References**

1. Hanrahan EO, Lin HY, et al. Distinct Patterns of Cytokine and Angiogenic Factor Modulation and Markers of Benefit for Vandetanib and/or Chemotherapy in Patients With Non–Small-Cell Lung Cancer. JCO January 10, 2010 vol. 28 no. 2 193-201.
2. Nikolinakos PG, Altorki N, et al. Plasma cytokine and angiogenic factor profiling identifies markers associated with tumor shrinkage in early-stage non-small cell lung cancer patients treated with pazopanib. Cancer Res. 2010 Mar 15;70(6):2171-9.

## **Appendix**

## RESEARCH ARTICLE

# Radiosynthesis and Initial *In Vitro* Evaluation of [ $^{18}\text{F}$ ]F-PEG<sub>6</sub>-IPQA—A Novel PET Radiotracer for Imaging EGFR Expression-Activity in Lung Carcinomas

Ashutosh Pal,<sup>1</sup> Julius A. Balatoni,<sup>1</sup> Uday Mukhopadhyay,<sup>1</sup> Kazuma Ogawa,<sup>2</sup> Carlos Gonzalez-Lepera,<sup>1</sup> Aleksandr Shavrin,<sup>1</sup> Andrei Volgin,<sup>1</sup> William Tong,<sup>1</sup> Mian M. Alauddin,<sup>1</sup> Juri G. Gelovani<sup>1</sup>

<sup>1</sup>Department of Experimental Diagnostic Imaging, University of Texas MD Anderson Cancer Center, 1515 Holcombe Blvd, Houston, TX 77030, USA

<sup>2</sup>Institute of Medical, Pharmaceutical and Health Sciences, Kanazawa University, Kakuma-machi, Kanazawa, Japan

### Abstract

**Introduction:** Epidermal growth factor receptor (EGFR)-targeted therapies with antibodies and small molecular EGFR kinase inhibitors have shown poor efficacy in unselected populations of patients with advanced non-small cell lung carcinomas (NSCLC). In contrast, patients with overexpression of EGFR and activating mutations in EGFR kinase domain demonstrated improved responses to EGFR kinase inhibitors. Therefore, we have developed a novel radiotracer, [ $^{18}\text{F}$ ]F-PEG<sub>6</sub>-IPQA for PET imaging of EGFR expression-activity in NSCLC, and have described its radiosynthesis and *in vitro* evaluation in two NSCLC cell lines with wild-type and L858R active mutant EGFR.

**Methods:** A mesylate precursor was synthesized in multiple steps and radiofluorinated using K<sup>18</sup>F/Kryptofix. The fluorinated intermediate compound was reduced to an amino derivative then treated with acryloyl isobutyl carbonate, followed by purification by HPLC to obtain the desired product.

**Results:** Decay-corrected radiochemical yields of [ $^{18}\text{F}$ ]F-PEG<sub>6</sub>-IPQA were 3.9–17.6%, with an average of 9.0% ( $n=11$ ). Radiochemical purity was >97% with specific activity of 34 GBq/ $\mu\text{mol}$  (mean value,  $n=10$ ) at the end of synthesis. The accumulation of [ $^{18}\text{F}$ ]F-PEG<sub>6</sub>-IPQA in H3255 cells was ten-fold higher than in H441 cells, despite a two-fold lower level of activated phospho-EGFR expression in H3255 cells compared with H441 cells. The accumulation of [ $^{18}\text{F}$ ]F-PEG<sub>6</sub>-IPQA in both cell lines was significantly decreased in the presence of a small molecular EGFR kinase inhibitor, Iressa, at 100  $\mu\text{M}$  concentration in culture medium.

Ashutosh Pal, Julius A. Balatoni, and Uday Mukhopadhyay shared equally in this work.

**Significance:** Non-small cell lung carcinoma (NSCLC) represents the majority of lung cancers. The response rate to EGFR inhibitors in patients with NSCLC exhibiting activating mutations of EGFR is approximately 85–90%, suggesting that these mutations, at least in part, may have caused malignant transformation and contribute in large to the tumor maintenance pathway. Therefore, we have been developing small molecular radiolabeled agents with preferential irreversible binding to active mutant EGFR kinases (i.e., L858R). Positron emission tomography imaging using such as selective radiolabeled agent could potentially allow for visualization of primary and metastatic tumor lesions expressing active mutant EGFR kinase, and for selection of patients who may benefit from therapy with EGFR kinase inhibitors.

Correspondence to: Juri G. Gelovani; e-mail: jgelovani@mdanderson.org

Published online: 22 September 2010

**Conclusion:** We have synthesized [ $^{18}\text{F}$ ]F-PEG<sub>6</sub>-IPQA and demonstrated its highly selective accumulation in active mutant L858R EGFR-expressing NSCLC cells *in vitro*. Further *in vivo* studies are warranted to assess the ability of PET imaging with [ $^{18}\text{F}$ ]F-PEG<sub>6</sub>-IPQA to discriminate the active mutant L858R EGFR-expressing NSCLC that are sensitive to therapy with EGFR kinase inhibitors vs NSCLC that express wild-type EGFR.

**Key words:** Radiochemistry, [ $^{18}\text{F}$ ]F-PEG<sub>6</sub>-IPQA, Epidermal growth factor receptor, Non-small cell lung carcinoma, Positron emission tomography

## Introduction

According to the American Cancer Society, 219,440 Americans were diagnosed with lung cancer in 2009; among which non-small cell lung carcinomas (NSCLC) represent the majority of lung cancer patients [1]. The outcome of conventional chemotherapy for advanced NSCLCs remains unsatisfactory, with low long-term survival rates. Molecular-targeted therapeutic agents that block pathways important for maintenance and progression of NSCLCs were expected to achieve a significant improvement in disease control and long-term survival. However, only marginal efficacy has been observed with epidermal growth factor receptor (EGFR) inhibitors, anti-EGFR monoclonal antibodies, and angiogenesis inhibitors in unselected populations of patients with advanced NSCLC. In contrast, patients with overexpression of EGFR and activating mutations in EGFR kinase domain demonstrate improved responses when treated with EGFR kinase inhibitors. Therefore, we and others have been developing radiotracers for positron emission tomography (PET) imaging of EGFR expression-activity in tumors and normal tissues at the EGFR kinase level derived from the 4-(anilino)quinazoline pharmacophore [2, 3], including: ML series of  $^{18}\text{F}$ -labeled five 4-(anilino)quinazoline derivatives ([ $^{18}\text{F}$ ]ML01) [4], N-{4-[(4,5-dichloro-2-fluorophenyl)-amino]quinazolin-6-yl}-acrylamide labeled with  $^{11}\text{C}$  ([ $^{11}\text{C}$ ]ML03) [5, 6], 4-dimethylamino-but-2-enoic acid [4-(phenylamino)-quinazoline-6-yl]-amides (ML04) labeled with  $^{11}\text{C}$  ([ $^{11}\text{C}$ ]ML04) [6], or with  $^{18}\text{F}$  ([ $^{18}\text{F}$ ]ML04) [7], [ $^{18}\text{F}$ ]F-PEG4-ML04 [7, 8], as well as [ $^{124}\text{I}$ ]IPQA [9], [ $^{18}\text{F}$ ]gefinitib [10], [ $^{11}\text{C}$ ]PD153035 [11], and [ $^{11}\text{C}$ ]erlotinib [12]. Recent studies by Pantaleo et al. (2010) using different PEG-ylated anilinoquinazoline derivatives labeled with  $^{124}\text{I}$ ,  $^{18}\text{F}$ , and  $^{11}\text{C}$ , failed to demonstrate the accumulation of these radiotracers in subcutaneous glioblastoma xenografts in mice [13]. Moreover, no differences in radiotracer accumulation levels were observed between U87MG. wtEGFR tumors overexpressing wild-type EGFR and U138MG tumors lacking EGFR expression [13]. In contrast, clinical studies with [ $^{11}\text{C}$ ]PD153035 have demonstrated some promise for imaging EGFR expression in NSCLC patients [14]. Thus, none of the imaging agents reported to date had demonstrated efficacy and/or selectivity for detection of activated EGFR or active mutant EGFR kinases

that confer sensitivity to small molecular EGFR inhibitors currently used in clinical practice [15].

Here, we describe radiosynthesis and initial *in vitro* evaluation of a novel radiotracer, 4-[(3-iodophenyl)amino]-7-{2-[2-{2-(2-[2-{2-([ $^{18}\text{F}$ ]fluoroethoxy)-ethoxy}-ethoxy)-ethoxy)-ethoxy}-ethoxy]-quinazoline-6-yl}-acrylamide ([ $^{18}\text{F}$ ]F-PEG<sub>6</sub>-IPQA) for PET imaging of EGFR expression-activity. We demonstrate that [ $^{18}\text{F}$ ]F-PEG<sub>6</sub>-IPQA accumulates *in vitro* significantly higher in H3255 lung carcinoma cells expressing the L858R active mutant EGFR, compared with H441 lung carcinoma cells overexpressing the wild-type EGFR. This is apparently due to an increased affinity and irreversible binding of [ $^{18}\text{F}$ ]F-PEG<sub>6</sub>-IPQA to the active mutant L858R EGFR kinase.

## Materials and Methods

### Reagents and Instrumentation

All reagents and solvents were purchased from Aldrich Chemical Co. (Milwaukee, WI) or Fisher Scientific (Pittsburgh, PA) and used without further purification. Silica gel solid-phase extraction cartridges (Sep-Pak, 900 mg) were purchased from Alltech Associates (Deerfield, IL). Reverse phase C<sub>18</sub> Sep-Pak® Plus Environmental cartridges were obtained from Waters (Milford, MA). Fluorine-18 was commercially supplied, as a solution of K[ $^{18}\text{F}$ ]Kryptofix<sub>222</sub>, by Cyclotope (Houston, TX). Thin layer chromatography (TLC) was performed on silica gel F-254 aluminum-backed plates (Merck, Darmstadt, Germany) with visualization under UV (254 nm) and by staining with potassium permanganate or ceric ammonium molybdate. Flash chromatography was performed using silica gel 60 mesh size 230–400 ASTM (Merck, Darmstadt, Germany) or CombiFlash Companion or SQ16× flash chromatography system (Isco, Lincoln, NE) with RediSep columns (normal phase silica gel; mesh size 230–400 ASTM) and Optima TM grade solvents (Fisher).

Melting points were recorded on a Buchi Melting Point B-545 apparatus and are uncorrected. Proton,  $^{19}\text{F}$ , and  $^{13}\text{C}$  NMR spectra were recorded on either a 300 or 600 MHz NMR spectrometers (Bruker, Germany) with tetramethylsilane used as an internal reference and hexafluorobenzene as an external reference at The University of Texas MD Anderson Cancer Center. Low resolution mass spectra (ion spray, a variation of electrospray) were acquired on a Perkin-Elmer Sciex API 100 spectrometer or Applied Biosystems Q-trap 2000 LC-MS-MS at

**Scheme 1.** Synthetic schemes for preparation of the non-radioactive compound 4-[[3-iodophenyl]amino]-7-[2-[2-(2-[2-(2-(2-fluoroethoxy)-ethoxy)-ethoxy]-ethoxy)-ethoxy]-ethoxy]-quinazoline-6-yl-acrylamide **1**. **a** Synthesis of **1**. **b** Preparation of **7**. **c** Preparation of precursor **9**.

24H), 0.87 (s, 9H), 0.04 (s, 6H); <sup>13</sup>C NMR δ—77.3, 77.1, 76.9, 72.6, 72.5, 70.7, 70.6, 70.6, 70.6, 70.6, 70.4, 62.7, 61.7, 60.4, 25.9, −5.3; MS (C<sub>18</sub>H<sub>40</sub>O<sub>7</sub>Si)—calculated 396.254, found 397.4 (M+H).

*Preparation of 2-(2-[2-{2-(2-[2-{4-(3-Iodophenylamino)-6-Nitro-Quinazoline-7-Yoloxyl}-Ethoxyl}-Ethoxyl)-Ethoxyl}-Ethoxyl)-Ethanol (8)*

A solution of **6** (596 mg, 1.6 mmol), **7** (957 mg, 2.4 mmol), and potassium trimethylsilanolate (621 g, 4.74 mmol) in DMSO (35 mL) was stirred together under N<sub>2</sub> for 5 h at room temperature. The deep crimson mixture was poured into stirred ice-water (40 mL), and then extracted with ethyl acetate (3×50 mL). The combined organic extracts were washed with aqueous 4% NaHCO<sub>3</sub> solution (2×50 mL) and water (2×25 mL), and then concentrated under vacuum. The resulting crude material was purified by flash chromatography eluting with 5% MeOH/CH<sub>2</sub>Cl<sub>2</sub> to obtain **8** [700 g, 71% yield; TLC: R<sub>f</sub>=0.45, MeOH/CH<sub>2</sub>Cl<sub>2</sub> (1:19)]. <sup>1</sup>H NMR (DMSO-d<sub>6</sub>) δ—10.08 (s, 1H), 9.25 (s, 1H), 8.69 (s, 1H), 8.29 (s, 1H), 7.94 (dd, J=1.2, 9.6 Hz, 1H), 7.52 (s, 1H), 7.51 (d, J=6.0 Hz, 1H), 7.22 (t, J=8.4 Hz, 1H), 5.77 (s, 1H), 4.59 (t, J=5.4 Hz, 1H), 4.44 (t, J=4.2 Hz, 1H), 3.84 (t, J=4.2 Hz, 2H), 3.62 (m, 2H), 3.54 (m, 2H), 3.49 (m, 14H); <sup>13</sup>C NMR δ—157.8, 157.4, 153.7, 153.2, 140.2, 139.0, 132.4, 130.5, 130.2, 121.7, 121.4, 110.5, 108.1, 94.2, 71.3, 68.4, 60.2; MS (C<sub>26</sub>H<sub>33</sub>IN<sub>4</sub>O<sub>9</sub>)—calculated 672.129, found 673.4 (M+H).

*Preparation of Methanesulfonic Acid 2-(2-[2-{2-(2-[2-{4-(3-Iodophenylamino)-6-Nitro-Quinazoline-7-Yoloxyl}-Ethoxyl}-Ethoxyl)-Ethoxyl}-Ethoxyl)-Ethyl Ester (9)*

Compound **8** (2 g, 3 mmol) was dissolved in CH<sub>2</sub>Cl<sub>2</sub> (50 mL) and Et<sub>3</sub>N (2.5 mL, 18 mmol) was added to the solution. Methanesulfonyl chloride (0.7 mL, 9.0 mmol) was added dropwise to the reaction mixture and stirred at room temperature for 3 h under argon. The reaction mixture was extracted with CH<sub>2</sub>Cl<sub>2</sub> (2×100 mL). The combined organic extracts were washed with brine (100 mL) and then dried over anhydrous Na<sub>2</sub>SO<sub>4</sub>. After filtration and evaporation of the organic solvent, the residue was purified by flash chromatography, eluting with 3% MeOH/CH<sub>2</sub>Cl<sub>2</sub> to afford **9** (1.5 g, 67% yield). <sup>1</sup>H NMR (DMSO-d<sub>6</sub>) δ—10.07 (s, 1H), 9.23 (s, 1H), 8.68 (s, 1H), 8.28 (s, 1H), 7.93 (dd, J=1.2, 7.8 Hz, 1H), 7.50 (d, J=10.2 Hz, 1H), 7.49 (s, 1H), 7.21 (t, J=7.8 Hz, 1H), 4.43 (t, J=3.6 Hz, 2H), 4.30 (m, 2H), 3.83 (t, J=4.2 Hz, 2H), 3.66 (m, 2H), 3.62 (m, 2H), 3.55 (m, 2H), 3.52 (m, 12H), 3.18 (s, 3H); <sup>13</sup>C NMR δ—157.8, 157.4, 153.7, 153.2, 140.1, 139.0, 132.4, 130.5, 130.2, 121.8, 121.4, 110.4, 108.1, 94.1, 70.1, 69.8, 69.7, 69.7, 69.7,

69.6, 68.4, 68.2, 36.8; MS (C<sub>27</sub>H<sub>35</sub>IN<sub>4</sub>O<sub>11</sub>S)—calculated 750.107, found 751.2 (M+H).

*Preparation of (3-Iodophenyl)-(7-[2-{2-(2-[2-{2-(2-Fluoroethoxy)-Ethoxyl}-Ethoxyl]-Ethoxyl)-Ethoxyl}-6-Nitro-Quinazolin-4-yl)-Amine (10)*

Compound **8** (350 mg, 0.52 mmol) was dissolved in dichloromethane (10 mL) and cooled to −78°C. A solution of diethylaminosulfur trifluoride (DAST, 0.681 mL, 5.2 mmol) in dichloromethane (5 mL) was added slowly to the cold solution while stirring. The stirred reaction mixture was allowed to warm to room temperature and stirring was continued for 12 h. The reaction mixture was poured into saturated sodium bicarbonate solution (25 mL), diluted with water (25 mL), and extracted with dichloromethane (3×50 mL). The combined organic extracts were washed with brine (50 mL), and then dried over anhydrous Na<sub>2</sub>SO<sub>4</sub>. After filtration and evaporation of the organic solvent, the residue was purified by flash chromatography, eluting with 3% MeOH/CH<sub>2</sub>Cl<sub>2</sub> to obtain **10** (150 mg, 42% yield). <sup>1</sup>H NMR (CDCl<sub>3</sub>) δ—9.17 (s, 1H), 8.71 (s, 1H), 8.33 (s, 1H), 7.88 (d, J=8.4 Hz, 1H), 7.47 (d, J=7.8 Hz, 1H), 7.20 (s, 1H), 7.10 (t, J=7.8 Hz, 1H), 4.52 (dm, J<sub>HF</sub>=48 Hz, J<sub>HH</sub>=4.2 Hz, 2H), 4.25 (t, J=4.2 Hz, 2H), 3.89 (t, J=4.8 Hz, 2H), 3.72 (m, 2H), 3.67 (m, 2H), 3.49 (m, 14H); <sup>13</sup>C NMR δ—158.3, 157.8, 154.4, 153.6, 139.6, 139.2, 133.4, 131.2, 130.2, 122.3, 121.8, 110.3, 108.6, 93.8, 83.6, 82.6, 71.1, 70.7, 70.6, 70.6, 70.5, 70.5, 70.4, 70.4, 70.3, 69.6, 69.1; <sup>19</sup>F NMR δ, −222.74 (tt, J<sub>HF</sub>=48 Hz, 28 Hz); MS (C<sub>26</sub>H<sub>32</sub>FIN<sub>4</sub>O<sub>8</sub>)—calculated 674.125, found 675.2 (M+H).

*Preparation of N<sup>4</sup>-(3-Iodophenyl)-7-[2-{2-(2-[2-{2-(2-Fluoroethoxy)-Ethoxyl}-Ethoxyl]-Ethoxyl)-Ethoxyl}-Quinazoline-4,6-Diamine (11)*

Compound **10** (200 mg, 0.3 mmol) was dissolved in tetrahydrofuran (3 mL). To this solution, stannous chloride (180 mg, 0.95 mmol) was added, and then heated to 60°C for 3 h under argon. The reaction mixture was cooled and water was added (25 mL), then saturated bicarbonate solution (10 mL) was added and extracted with ethyl acetate (3×75 mL). The combined organic extracts were concentrated, and the crude product was purified by flash chromatography, eluting with 3% MeOH/CH<sub>2</sub>Cl<sub>2</sub> to yield the amine **11** (150 mg, 43% yield). <sup>1</sup>H NMR (CDCl<sub>3</sub>) δ—8.54 (s, 1H), 8.16 (s, 1H), 7.74 (d, J=8.4 Hz, 1H), 7.66 (bs, 1H), 7.40 (d, J=7.8 Hz, 1H), 7.14 (s, 1H), 7.07 (m, 2H), 4.53 (dm, J<sub>HF</sub>=48 Hz, J<sub>HH</sub>=4.2 Hz, 2H), 4.21 (t, J=4.2 Hz, 2H), 3.88 (t, J=4.8 Hz, 2H), 3.72 (m, 2H), 3.69 (m, 2H), 3.49 (m, 14H); <sup>13</sup>C NMR δ—155.2, 152.4, 151.6, 145.4, 138.4, 132.2, 130.4, 129.7, 120.3, 110.6, 107.3, 101.0, 94.1, 83.8, 82.7, 70.9, 70.8, 70.7, 70.6, 70.6, 70.5, 70.5, 70.4, 70.3, 69.1, 68.1; <sup>19</sup>F NMR δ, −221.98 (tt, J<sub>HF</sub>=51, 28 Hz); MS (C<sub>26</sub>H<sub>34</sub>FIN<sub>4</sub>O<sub>6</sub>)—calculated 644.151, found 645.3 (M+H).

*Preparation of 4-[(3-Iodophenyl)Amino]-7-[2-{2-[2-{2-(2-Fluoroethoxy)-Ethoxy}-Ethoxy]-Ethoxy}-Ethoxy]-Quinazoline-6-Yl-Acrylamide (1)*

Acryloyl isobutyl carbonate was prepared *in situ* by adding isobutyl chloroformate (95  $\mu\text{L}$ , 0.72 mmol) dropwise to a stirred solution of acrylic acid (60  $\mu\text{L}$ , 0.86 mmol) and  $\text{Et}_3\text{N}$  (200  $\mu\text{L}$ , 1.44 mmol) in tetrahydrofuran (THF; 2.5 mL) at 0°C under  $\text{N}_2$ . Amine **11** (160 mg, 0.25 mmol) was added in one portion to the above solution of acryloyl isobutyl carbonate, and stirring was continued for 10 min. After another 30 min at 0°C, the reaction mixture was applied to a flash chromatography column and was eluted with 5%  $\text{MeOH}/\text{CH}_2\text{Cl}_2$  to give the desired product **1** (75 mg, 43% yield).  $^1\text{H}$  NMR ( $\text{CDCl}_3$ )  $\delta$ —9.12 (s, 1H), 8.96 (s, 1H), 8.67 (s, 1H), 8.22 (s, 1H), 7.76 (m, 2H), 7.47 (d,  $J$ =7.8 Hz, 1H), 7.25 (s, 1H), 7.11 (t,  $J$ =8.4 Hz, 1H), 6.51 (m, 2H), 5.84 (dd,  $J$ =3.6, 8.4 Hz, 1H), 4.55 (dm,  $J_{\text{HF}}$ =48 Hz,  $J$ =4.2 Hz, 2H), 4.38 (t,  $J$ =4.2 Hz, 2H), 3.98 (t,  $J$ =4.2 Hz, 2H), 3.75 (m, 2H), 3.70 (m, 2H), 3.65 (m, 14H);  $^{13}\text{C}$  NMR  $\delta$ —164.3, 156.7, 154.5, 152.3, 148.3, 139.8, 133.0, 131.3, 130.4, 130.3, 128.3, 128.3, 120.8, 110.2, 109.6, 108.0, 94.1, 83.7, 82.6, 70.8, 70.7, 70.6, 70.5, 70.5, 70.5, 70.5, 70.3, 69.0, 68.55;  $^{19}\text{F}$  NMR  $\delta$ , -222.81 (tt,  $J_{\text{HF}}$ =48 Hz, 28 Hz); MS ( $\text{C}_{29}\text{H}_{36}\text{FIN}_4\text{O}_7$ )—calculated 698.161, found 699.5 (M+H).

**Radiosynthesis of 4-[(3-iodophenyl)Amino]-7-[2-[2-{2-(2-[2-{2-([ $^{18}\text{F}$ ]Fluoroethoxy)-Ethoxy}-Ethoxy]-Ethoxy)-Ethoxy}-Ethoxy]-Quinazoline-6-Yl-Acrylamide (14)**

*Preparation of (3-Iodophenyl)-(7-[2-[2-{2-(2-[2-{2-([ $^{18}\text{F}$ ]Fluoroethoxy)-Ethoxy}-Ethoxy]-Ethoxy)-Ethoxy]-6-Nitro-Quinazolin-4-Yl)-Amine 12*

The aqueous [ $^{18}\text{F}$ ]fluoride ( $\text{K}^{18}\text{F}/\text{Kryptofix 2.2.2}$ ) was dried in a two-step evaporation process using the GE TRACERLab FX<sub>F-N</sub> synthesizer (GE Healthcare). A solution of methane-sulfonic acid 2-(2-[2-{2-(2-[2-{4-(3-iodophenylamino)-6-nitro-quinazoline-7-yloxy}-ethoxy]-ethoxy)-ethoxy}-ethoxy]-ethyl ester **9** (~10 mg) in anhydrous DMSO (0.4 mL) was added to the dried [ $^{18}\text{F}$ ]-complex. The reaction mixture was heated for 30 min at 120°C. After cooling to room temperature, the reaction mixture was passed through a silica gel cartridge, and the crude product **12** was eluted with 2.5 mL of  $\text{MeOH}/\text{CH}_2\text{Cl}_2$  (3:7).

*Preparation of  $\text{N}^4$ -(3-Iodophenyl)-(7-[2-[2-{2-(2-[2-{2-([ $^{18}\text{F}$ ]Fluoroethoxy)-Ethoxy}-Ethoxy]-Ethoxy)-Ethoxy]-Quinazoline-4,6-Diamine 13*

The solution of **12** was evaporated to dryness at 80°C under a stream of Ar, then  $\text{SnCl}_2$  (15 mg) in dry THF (0.4 mL) was added. The mixture was heated for 15 min at 60°C, cooled to

room temperature, then the mixture was passed through a silica gel cartridge (previously activated with 2 mL of n-hexane). The cartridge was eluted with dry THF (2 $\times$ 1 mL), and the solvent was evaporated at 60°C under a flow of Ar, down to about 200  $\mu\text{L}$ . The residue, crude  $\text{N}^4$ -(3-iodophenyl)-(7-[2-[2-{2-[2-[2-([ $^{18}\text{F}$ ]fluoroethoxy)-ethoxy]-ethoxy]-ethoxy)-ethoxy]-quinazoline-4,6-diamine **13** was cooled to 0°C for the next step.

*Preparation of 4-[(3-Iodophenyl)Amino]-7-[2-[2-{2-[2-{2-([ $^{18}\text{F}$ ]Fluoroethoxy)-Ethoxy}-Ethoxy]-Ethoxy)-Ethoxy]-Quinazoline-6-Yl-Acrylamide 14*

A mixture of acrylic acid (50  $\mu\text{L}$ ), isobutyl chloroformate (60  $\mu\text{L}$ ), and triethylamine (100  $\mu\text{L}$ ) in dry THF (0.2 mL) was prepared under Ar, which then formed a milky white suspension, that was cooled to 0°C. The solution of **13** in dry THF (0.2 mL) was also cooled to 0°C and transferred to the vial containing acryloyl isobutyl carbonate (milky suspension) under Ar. The vial containing **13** was rinsed with 0.1 mL of THF and transferred to the reaction vial containing acryloyl isobutyl carbonate. The reaction mixture was kept at 0°C for 10 min with occasional shaking. The solvent from the reaction mixture was evaporated at 70°C under Ar flow to near dryness and re-dissolved in prep-HPLC solvent (~1 mL) and passed through a 0.45- $\mu\text{m}$  filter (PTFE, 17 mm, Grace, Deerfield, IL). An additional membrane filter (Sartobind Q, 5  $\text{cm}^2$ , Sartorius AG, Goettingen, Germany) coupled with the PTFE filter was also employed in a few experiments. The filtered solution was injected onto a  $\text{C}_8$  preparative column (Zorbax CombiHT XDB, 21.2 $\times$ 100 mm) and eluted with acetonitrile/0.1% ammonium formate buffer (45:55) at a flow rate of 6 mL/min. The radioactive peak containing **14** was collected, diluted with 10 mL of water, then passed through a  $\text{C}_{18}$  Sep-Pak® (preconditioned with 10 mL of 95% ethanol, then 10 mL of water). The cartridge was washed with 10–15 mL of water and then eluted with 95% ethanol (2.5–3.0 mL) to isolate the product. For *in vivo* studies, ethanol was concentrated *in vacuo* to a small volume, and then diluted with saline for injection. The final product **14** was analyzed by radio-HPLC using a Zorbax Eclipse XDB- $\text{C}_8$  column (4.6 $\times$ 150 mm) with a mobile phase consisting of acetonitrile/0.1% ammonium formate buffer (47:53) at 1.0 mL/min flow rate. Radiochemical yield of **14** was in the range of 3.9–17.6% ( $n$ =11, d.c.) from the end of bombardment. The radiochemical purity was >97%, and specific activity was 34 GB/ $\mu\text{mol}$ . Total synthesis time was approximately 3 h.

**Tumor Cell Lines:** Four different NSCLC cell lines were used in this study, expressing different levels of wild-type and active mutant EGFRs and with different sensitivity to EGFR inhibitor Iressa: H441 (wild-type EGFR; resistant [16, 17]) and H3255 (mutant L858R EGFR; sensitive [16–18]). The cells were grown in flasks with D-MEM/F-12 medium supple-

mented with 10% FBS and antibiotics at 37°C in humidified atmosphere with 5% CO<sub>2</sub>. Cells were kept in the log phase of proliferative activity.

**Assessment of EGFR Expression by Western Blot** The H441 and H3255 NSCLC cell lines expressing wild-type and L858R mutant EGFR, respectively, were grown in 15-cm culture dish until 60–70% confluent. Then the cells were incubated for 30 min in fresh culture medium supplemented with 20% fetal calf serum (FCS) and [ $^{18}\text{F}$ ]F-PEG<sub>6</sub>-IPQA at 0.37 MBq/mL. Thereafter, the cells were washed with phosphate-buffered saline (PBS), harvested in PBS by scraping, pelleted by centrifugation at 1,500 rpm for 5 min, the supernatant was removed, and the cell pellet was frozen on dry ice. The cell pellet was thawed and lysed in appropriate volume of buffer (200  $\mu\text{L}$ /100 mg cells) containing 20 mM Tris–HCl pH 7.4, NaCl 150 mM, EDTA 1 mM, EGTA 1 mM, beta-glycerophosphate 1 mM, Na<sub>3</sub>VO<sub>4</sub> 1 mM, NaF 1 mM, Triton X-100 1%, and Protease Inhibitor Cocktail 10  $\mu\text{L}$ /mL (all reagents from Sigma-Aldrich, CA) for 1 h at 4°C. Then, the cell lysate was sonicated 3  $\times$  10 s on ice and cleared by 14,000 rpm centrifugation at 4°C for 10 min. The supernatant was denatured by heating at 70°C with LDS sample buffer (Invitrogen, Carlsbad, CA) and separated by SDS/polyacrylamide gel electrophoresis using precast 4–12% Tris–HCl gel cassettes (Invitrogen, Carlsbad, CA). After transferring proteins onto a nitrocellulose membrane using a semi-dry electroblotting device (Invitrogen, Carlsbad, CA), the membrane was immunostained with a goat polyclonal antibody against phospho-tyrosine 845 of EGFR (Santa Cruz, CA) and visualized using the ECL kit (Bio-Rad). For autoradiography, the membrane was exposed for 12 h to HyBlot CL film (Denville Scientific, Metuchen, NJ) to visualize the [ $^{18}\text{F}$ ]-labeled protein bands.

***In Vitro* Radiotracer Accumulation Assay:** Radiotracer uptake studies were performed in monolayer cultures of different NSCLC cell lines as previously described [9, 19]. Briefly, tumor cells were grown in 15-cm culture dishes until 60–70% confluent, at which time the culture medium was depleted of FCS to prevent EGFR activation. Then, the cell cultures were incubated with serum-free medium containing [ $^{18}\text{F}$ ]F-PEG<sub>6</sub>-IPQA (3.7 MBq/mL) for different time intervals (15, 30, 60, and 120 min). In the first part of the experiment, the cells were harvested by gentle scraping at different time intervals, transferred into 15-mL tubes, and centrifuged at 1,000 $\times g$  for 2 min. A 100  $\mu\text{L}$  aliquot of supernatant was transferred to a pre-weighed scintillation tube, and the rest of the supernatant was removed by aspiration. The cell pellet was snap-frozen on dry ice and transferred to another pre-weighed scintillation tube. The cell pellet and a sample of radioactive culture medium were weighed assessed for radioactivity concentration using a Packard Quantum gamma counter (Perkin-Elmer, Waltham, MA). The radioactivity concentration was expressed as cpm/g cells and cpm/mL

medium, respectively. Cells-to-medium radioactivity concentration ratios were calculated and plotted against time to evaluate the radiotracer accumulation and washout kinetics.

## Results and Discussion

### Chemistry

The scheme for synthesizing 4-[(3-iodophenyl)amino]-7-{2-[2-{2-(2-[2-{2-(fluoroethoxy)-ethoxy}-ethoxy)-ethoxy]-ethoxy}-ethoxy]-quinazoline-6-yl-acrylamide **1** is shown in Scheme 1a. Compounds **3**, **4**, and **6** were prepared according to literature methods [20, 22, 23] in 90%, 52%, and 84% yields, respectively. All compounds were fully characterized by spectroscopic methods; the  $^1\text{H}$  NMR spectra and mass spectra were consistent with those reported previously [20, 22, 23]. Compound **5** was prepared *in situ* and used without isolation toward the preparation of **6**.

Compound **7**, 2-[2-{2-(2-[2-{2-(tert-butyl-dimethyl-silyloxy)-ethoxy}-ethoxy)-ethoxy}-ethoxy)-ethoxy]-ethanol, was prepared according to a literature method [21] (Scheme 1b). Briefly, hexaethylene glycol was allowed to react with tert-butyldimethylsilyl chloride in the presence of imidazole in anhydrous DMF under inert atmosphere. After work-up and chromatographic purification, **7** was isolated in 50% yield. The  $^1\text{H}$  NMR spectrum was consistent with that reported in the literature [21].

Compound **8** was prepared from **6** by reaction with a mixture of **7** and potassium trimethylsilanolate in DMSO. The key intermediate compound **8** was obtained in 71% yield. The  $^1\text{H}$  NMR spectrum was consistent with that reported in the literature [22]. Compound **8** was reacted with DAST to get compound **10**, which was characterized by  $^1\text{H}$  and  $^{19}\text{F}$  NMR spectroscopy and mass spectrometry.  $^{19}\text{F}$  NMR spectrum (coupled) showed a peak at  $-222.74$  ppm as a triplet of triplets with geminal proton–fluorine coupling constant of 48 Hz and a vicinal proton–fluorine coupling constant of 28 Hz. The yield in this fluorination reaction was moderate at 42%. The nitro group of compound **10** was reduced by reaction with SnCl<sub>2</sub> to produce the amino-compound **11** in 43% yield. A reduction of such a nitro group was reported previously [22]; however, using that method would result in the iodine being lost, therefore, SnCl<sub>2</sub> was used as the reducing agent, which enabled reduction of the nitro group without any loss of iodine. Compound **11** was then reacted with acryloyl isobutyl carbonate, which was freshly prepared by reaction of acrylic acid with isobutyl chloroformate, to produce compound **1**. It should be noted that acryloyl isobutyl carbonate is not commercially available due to its high reactivity and instability, therefore, in every synthesis it was prepared and used immediately. Compound **1** was obtained in 43% yield, fully characterized by spectroscopic methods and used as a non-radioactive standard compound for HPLC analysis.

For radiosynthesis of [ $^{18}\text{F}$ ]F-PEG<sub>6</sub>-IPQA, a precursor compound **9** was prepared from **8** (Scheme 1c). The alcohol

**8** was treated with methanesulfonyl chloride in  $\text{CH}_2\text{Cl}_2$  in the presence of  $\text{Et}_3\text{N}$  at room temperature for 3 h. The mesylate precursor **9** was obtained in 67% yield and fully characterized by spectroscopic methods. Fluorination and radiofluorination reactions were performed on **9** with  $\text{KF/Kryptofix}_{222}$  or  $\text{K}^{18}\text{F/Kryptofix}_{222}$  in DMSO to obtain compound **10** and **12**, respectively. It was observed that the non-radioactive fluorination reaction gave a better chemical yield of **10** than the DAST reaction from **8**. The fluorination reaction afforded a 78% yield in comparison to 42% with the DAST reaction.

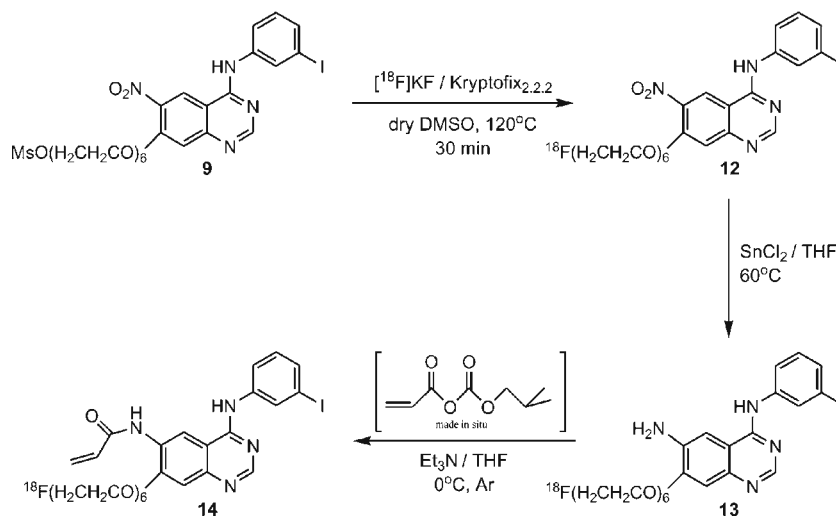
### Radiochemistry

Starting from the mesylate precursor **9**, the radiosynthesis of **14** consists of three steps as shown in Scheme 2. The initial step was accomplished using an automated synthesis module TRACERLab FX<sub>F-N</sub> (GE Healthcare), and the remaining steps were accomplished by manual operation. The radiofluorination of **9** with  $\text{K}^{18}\text{F/Kryptofix}_{222}$  in dry DMSO at  $120^\circ\text{C}$  (30 min) produced (3-iodophenyl)-(7-{2-[2-{2-(2-[2-{2-([ $^{18}\text{F}$ ]fluoroethoxy)-ethoxy}-ethoxy)-ethoxy}-ethoxy]-6-nitro-quinazolin-4-yl)-amine} **12** in an average radiochemical yield of 52% (d.c.) with a mean radiochemical purity of 72% ( $n=19$ ). The reduction of the 6-nitro group of **12** was achieved by using stannous chloride in THF at  $60^\circ\text{C}$  for 15 min.  $\text{N}^4$ -(3-iodophenyl)-(7-{2-[2-{2-(2-[2-{2-([ $^{18}\text{F}$ ]fluoroethoxy)-ethoxy}-ethoxy)-ethoxy}-ethoxy]-quinazoline-4,6-diamine} **13** was isolated after passing through a silica gel cartridge followed by elution with THF. Conversion of the amine function to an acrylamide group was accomplished by *in situ* production of acryloyl isobutyl carbonate from the reaction of isobutyl chloroformate, acrylic acid, and triethylamine in THF at  $0^\circ\text{C}$ , followed by addition of **13** within 10 min. The crude product, 4-[(3-iodophenyl)amino]-7-{2-[2-{2-(2-[2-{2-([ $^{18}\text{F}$ ]fluoroethoxy)-ethoxy}-ethoxy)-ethoxy)-ethoxy}-ethoxy]-quinazoline-6-yl)-acrylamide **14**, was then purified by

preparative HPLC. The synthesis time was about 3 h from the end of bombardment, including purification and formulation. The intermediate radiofluorinated compounds (**12**, **13**) and the final product (**14**) were all identified by analytical HPLC at each step of the radiosynthesis and were confirmed by co-elution with their respective non-radioactive standards. The radiochemical yields in labeling step were variable, ranging from 30% to 60%. The two other steps, such as reduction of compound **12** and coupling with acryloyl isobutyl carbonate, also gave variable yields; as a result, the overall yields were more variable than expected. Decay-corrected radiochemical yields ranged from 4% to 17%, with an average yield of 9.0% ( $n=11$ ). Radiochemical purity was found to be  $>97\%$ . A representative analytical radio-HPLC chromatogram of **14** is shown in Fig. 1. However, it must be noted that UV detector revealed presence of a double peak indicative of an unidentified impurity ( $\sim 60\%$ ). In contrast, only one peak was detectable by the radiation detector, which corresponded to [ $^{18}\text{F}$ ]F-PEG<sub>6</sub>-IPQA, based on the elution time of cold F-PEG<sub>6</sub>-IPQA standard. The average specific activity was determined to be  $34\text{ GBq}/\mu\text{mol}$  ( $n=10$ ), at the end of synthesis, considering only the amount of cold F-PEG<sub>6</sub>-IPQA without the impurity. Thus, further optimization of radiosynthetic and purification methods will be needed to eliminate or significantly reduce the impurity, which may potentially interfere with binding of [ $^{18}\text{F}$ ]F-PEG<sub>6</sub>-IPQA to EGFR kinase domain due to possible similarity of structure.

### Initial In Vitro Evaluation

*In vitro* radiotracer accumulation assay demonstrated a rapid uptake of [ $^{18}\text{F}$ ]F-PEG<sub>6</sub>-IPQA during the initial phase (first 20 min) in both H441 and H3255 cells. After the first 20 min, the accumulation of [ $^{18}\text{F}$ ]F-PEG<sub>6</sub>-IPQA has leveled in H441 at a cells/medium ratio of 30–40, while the accumulation in H3255 cell monolayers continued to increase up to 1 h and only thereafter leveled at cells/medium concentration ratio of



Scheme 2. Radiosynthesis scheme for the preparation of [ $^{18}\text{F}$ ]F-PEG<sub>6</sub>-IPQA **14**.

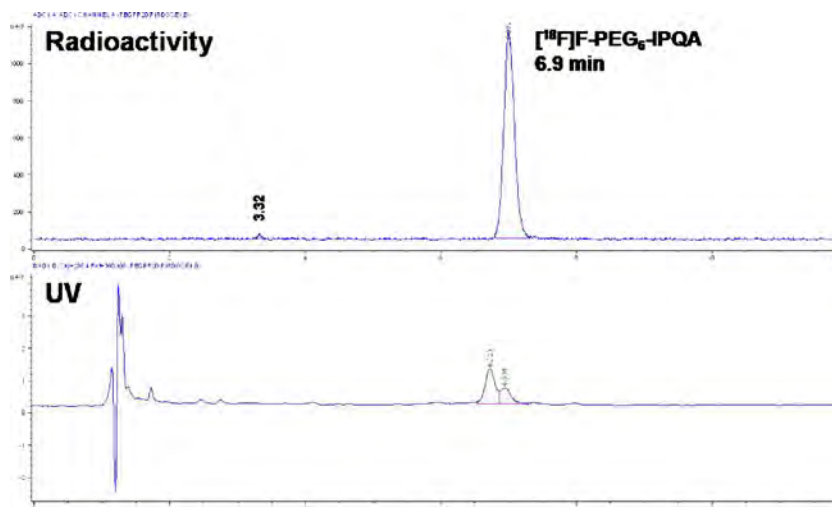


Fig. 1. Analytical radio-HPLC chromatogram of [ $^{18}\text{F}$ ]F-PEG<sub>6</sub>-IPQA **14** after formulation. The UV trace showed a small amount of unknown impurity.

400–600 (Fig. 2). The magnitude of [ $^{18}\text{F}$ ]F-PEG<sub>6</sub>-IPQA accumulation in H3255 cells was more than ten-fold higher than in H441 cells, despite a two-fold lower level of activated phospho-EGFR expression in H3255 cells compared with H441 cells (Fig. 3). Apparently, the presence of impurity in [ $^{18}\text{F}$ ]F-PEG<sub>6</sub>-IPQA preparation identified by HPLC with a UV detector (Fig. 1) did not interfere with [ $^{18}\text{F}$ ]F-PEG<sub>6</sub>-IPQA binding of to EGFR kinase and its accumulation in H3255 cells expressing L858R EGFR mutant. The magnitude of [ $^{18}\text{F}$ ]F-PEG<sub>6</sub>-IPQA accumulation in both cell lines was significantly decreased in presence of a small molecular EGFR kinase inhibitor Iressa at 100  $\mu\text{M}$  in culture medium (Fig. 2). Such significantly higher accumulation of [ $^{18}\text{F}$ ]F-PEG<sub>6</sub>-IPQA in H3255 tumors can be explained by the presence of L858R activating mutation in the EGFR kinase domain [16–18], and not by the difference in the level of EGFR expression, which was lower in H3255 cells, as compared to H441 cells. As

demonstrated by Western blot and autoradiographic analysis of electrophorograms of proteins extracted from H441 and H3255 cells exposed to [ $^{18}\text{F}$ ]F-PEG<sub>6</sub>-IPQA, the L858R activating mutation, apparently, increases irreversible covalent binding of [ $^{18}\text{F}$ ]F-PEG<sub>6</sub>-IPQA to the active mutant L858R EGFR kinase domain.

## Conclusions

We have successfully synthesized [ $^{18}\text{F}$ ]F-PEG<sub>6</sub>-IPQA with the  $^{18}\text{F}$  label attached at the end of the hexaethylene glycol side chain and demonstrated highly selective accumulation in active mutant L858R EGFR-expressing NSCLC cells *in vitro*. Further, *in vivo* studies are warranted to assess the ability of PET imaging with [ $^{18}\text{F}$ ]F-PEG<sub>6</sub>-IPQA to discriminate the active mutant L858R EGFR-expressing NSCLC

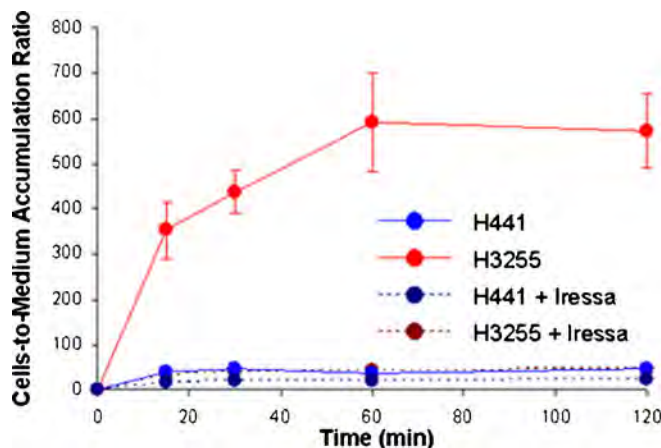


Fig. 2. Time-dependent accumulation of [ $^{18}\text{F}$ ]F-PEG<sub>6</sub>-IPQA **14** in H441 and H3255 tumor cells *in vitro*, before and after the addition of Iressa (100  $\mu\text{M}$ ) into the culture medium.

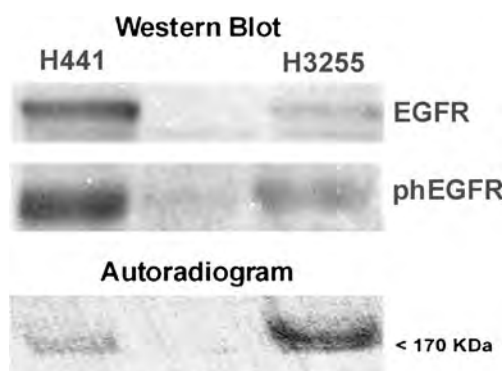


Fig. 3. Western blot analysis of total EGFR and phosphotyrosine 845 of EGFR expression in H441 and H3255 tumor cells. The autoradiogram of protein electrophoresis membrane demonstrates preferential irreversible and covalent binding of [ $^{18}\text{F}$ ]F-PEG<sub>6</sub>-IPQA to active mutant L858R EGFR kinase domain.

that are sensitive to therapy with EGFR kinase inhibitors vs NSCLC that express wild-type EGFR.

**Acknowledgments.** This work was supported by the following grants: W81XWH-05-2-0027 (J.G.—Project Leader; Imaging Core Leader) and U24CA126577 (J.G. co-PI). We thank Karen Yoas, M.S., for the excellent coordination of studies.

**Conflict of interest.** None of the authors of this manuscript has any conflict of interest in relation to studies and results presented herein.

## References

1. ACS (2009) Cancer Reference Information. [http://www.cancer.org/docroot/CRI/content/CRI\\_2\\_4\\_1x\\_What\\_Are\\_the\\_Key\\_Statistics\\_About\\_Lung\\_Cancer\\_15asp?sitearea=](http://www.cancer.org/docroot/CRI/content/CRI_2_4_1x_What_Are_the_Key_Statistics_About_Lung_Cancer_15asp?sitearea=)
2. Mishani E, Abourbeh G (2007) Cancer molecular imaging: radio-nuclide-based biomarkers of the epidermal growth factor receptor (EGFR). *Curr Top Med Chem* 7:1755–1772
3. Mishani E, Hagooley A (2009) Strategies for molecular imaging of epidermal growth factor receptor tyrosine kinase in cancer. *J Nucl Med* 50:1199–1202
4. Bonasera TA, Ortu G, Rozen Y, Kraiss R, Freedman NM, Chisin R, Gazit A, Levitzki A, Mishani E (2001) Potential (18)F-labeled biomarkers for epidermal growth factor receptor tyrosine kinase. *Nucl Med Biol* 28:359–374
5. Ortu G, Ben-David I, Rozen Y, Freedman NM, Chisin R, Levitzki A, Mishani E (2002) Labeled EGFR-TK irreversible inhibitor (ML03): *in vitro* and *in vivo* properties, potential as PET biomarker for cancer and feasibility as anticancer drug. *Int J Cancer* 101:360–370
6. Mishani E, Abourbeh G, Rozen Y, Jacobson O, Laky D, Ben David I, Levitzki A, Shaul M (2004) Novel carbon-11 labeled 4-dimethylamino-but-2-enoic acid [4-(phenylamino)-quinazoline-6-yl]-amides: potential PET bioprobes for molecular imaging of EGFR-positive tumors. *Nucl Med Biol* 31:469–476
7. Abourbeh G, Dissoki S, Jacobson O, Litchi A, Ben Daniel R, Laki D, Levitzki A, Mishani E (2007) Evaluation of radiolabeled ML04, a putative irreversible inhibitor of epidermal growth factor receptor, as a bioprobe for PET imaging of EGFR-overexpressing tumors. *Nucl Med Biol* 34:55–70
8. Dissoki S, Aviv Y, Laky D, Abourbeh G, Levitzki A, Mishani E (2007) The effect of the [18F]-PEG group on tracer qualification of [4-(phenylamino)-quinazoline-6-yl]-amide moiety—an EGFR putative irreversible inhibitor. *Appl Radiat Isot* 65:1140–1151
9. Pal A, Glekas A, Doubrovin M, Balatoni J, Namavari M, Beresten T, Maxwell D, Soghomonyan S, Shavrin A, Ageyeva L, Finn R, Larson SM, Bornmann W, Gelovani JG (2006) Molecular imaging of EGFR kinase activity in tumors with 124I-labeled small molecular tracer and positron emission tomography. *Mol Imaging Biol* 8:262–277
10. Su H, Seimbille Y, Ferl GZ, Bodenstern C, Fueger B, Kim KJ, Hsu YT, Dubinett SM, Phelps ME, Czernin J, Weber WA (2008) Evaluation of [(18)F]gefitinib as a molecular imaging probe for the assessment of the epidermal growth factor receptor status in malignant tumors. *Eur J Nucl Med Mol Imaging* 35:1089–1099
11. Wang H, Yu JM, Yang GR, Song XR, Sun XR, Zhao SQ, Wang XW, Zhao W (2007) Further characterization of the epidermal growth factor receptor ligand 11C-PD153035. *Chin Med J (Engl)* 120:960–964
12. Memon AA, Jakobsen S, Dagnaes-Hansen F, Sorensen BS, Keiding S, Nexø E (2009) Positron emission tomography (PET) imaging with [11C]-labeled erlotinib: a micro-PET study on mice with lung tumor xenografts. *Cancer Res* 69:873–878
13. Pantaleo MA, Mishani E, Nanni C, Landuzzi L, Boschi S, Nicoletti G, Dissoki S, Paterini P, Piccaluga PP, Lodi F, Lollini PL, Fanti S, Biasco G. (2010) Evaluation of modified PEG-anilinoquinazoline derivatives as potential agents for EGFR imaging in cancer by small animal PET. *Mol Imaging Biol*. doi:10.1007/s11307-010-0315-z
14. Liu N, Li M, Li X, Meng X, Yang G, Zhao S, Yang Y, Ma L, Fu Z, Yu J (2009) PET-based biodistribution and radiation dosimetry of epidermal growth factor receptor-selective tracer 11C-PD153035 in humans. *J Nucl Med* 50:303–308
15. Gelovani JG (2008) Molecular imaging of epidermal growth factor receptor expression-activity at the kinase level in tumors with positron emission tomography. *Cancer Metastasis Rev* 27:645–653
16. Paez JG, Janne PA, Lee JC, Tracy S, Greulich H, Gabriel S, Herman P, Kaye FJ, Lindeman N, Boggon TJ, Naoki K, Sasaki H, Fujii Y, Eck MJ, Sellers WR, Johnson BE, Meyerson M (2004) EGFR mutations in lung cancer: correlation with clinical response to gefitinib therapy. *Science (New York, NY)* 304:1497–1500
17. Mukohara T, Engelman JA, Hanna NH, Yeap BY, Kobayashi S, Lindeman N, Halmos B, Pearlberg J, Tsuchihashi Z, Cantley LC, Tenen DG, Johnson BE, Janne PA (2005) Differential effects of gefitinib and cetuximab on non-small-cell lung cancers bearing epidermal growth factor receptor mutations. *J Natl Cancer Inst* 97:1185–1194
18. Tracy S, Mukohara T, Hansen M, Meyerson M, Johnson BE, Janne PA (2004) Gefitinib induces apoptosis in the EGFR L858R non-small-cell lung cancer cell line H3255. *Cancer Res* 64:7241–7244
19. Najjar AM, Nishii R, Maxwell DS, Volgin A, Mukhopadhyay U, Bornmann WG, Tong W, Alauddin M, Gelovani JG (2009) Molecular-genetic PET imaging using an HSV1-tk mutant reporter gene with enhanced specificity to acycloguanosine nucleoside analogs. *J Nucl Med* 50:409–416
20. Wissner A, Fraser HL, Ingalls CL, Dushin RG, Floyd MB, Cheung K, Nittoli T, Ravi MR, Tan X, Loganzo F (2007) Dual irreversible kinase inhibitors: quinazoline-based inhibitors incorporating two independent reactive centers with each targeting different cysteine residues in the kinase domains of EGFR and VEGFR-2. *Bioorg Med Chem* 15:3635–3648
21. MacMahon S, Fong R 2nd, Baran PS, Safonov I, Wilson SR, Schuster DI (2001) Synthetic approaches to a variety of covalently linked porphyrin–fullerene hybrids. *J Org Chem* 66:5449–5455
22. Dissoki S, Eshet R, Billauer H, Mishani E (2009) Modified PEG-anilinoquinazoline derivatives as potential EGFR PET agents. *J Label Comp Radiopharm* 52:41–52
23. Iino T, Sasaki Y, Bamba M, Mitsuya M, Ohno A, Kamata K, Hosaka H, Maruki H, Futamura M, Yoshimoto R, Ohya S, Sasaki K, Chiba M, Ohtake N, Nagata Y, Eiki J, Nishimura T (2009) Discovery and structure-activity relationships of a novel class of quinazoline glucokinase activators. *Bioorganic & Medicinal Chemistry Letters* 19 (19):5531–5538



# Bayesian dose finding in oncology for drug combinations by copula regression

Guosheng Yin and Ying Yuan

*University of Texas M. D. Anderson Cancer Center, Houston, USA*

[Received September 2007. Final revision August 2008]

**Summary.** Treating patients with a combination of agents is becoming commonplace in cancer clinical trials, with biochemical synergism often the primary focus. In a typical drug combination trial, the toxicity profile of each individual drug has already been thoroughly studied in single-agent trials, which naturally offers rich prior information. We propose a Bayesian adaptive design for dose finding that is based on a copula-type model to account for the synergistic effect of two or more drugs in combination. To search for the maximum tolerated dose combination, we continuously update the posterior estimates for the toxicity probabilities of the combined doses. By reordering the dose toxicities in the two-dimensional probability space, we adaptively assign each new cohort of patients to the most appropriate dose. Dose escalation, de-escalation or staying at the same doses is determined by comparing the posterior estimates of the probabilities of toxicity of combined doses and the prespecified toxicity target. We conduct extensive simulation studies to examine the operating characteristics of the design and illustrate the proposed method under various practical scenarios.

**Keywords:** Adaptive design; Bayesian inference; Combining drugs; Continual reassessment method; Copula model; Maximum tolerated dose; Phase I trial; Toxicity probability

## 1. Introduction

In conventional phase I clinical trials, the primary objective is often to find the maximum tolerated dose (MTD) of the drug under study, i.e. the dose with a probability of toxicity that is closest to the physician's prespecified target. In such an early phase of a drug study, relatively little is known about the appropriate dose level; hence, a sequence of doses is screened to find the target dose that is associated with the maximum level of tolerable toxicity. Towards this goal, various statistical methods have been proposed for phase I clinical trial designs (see Storer (1989), O'Quigley *et al.* (1990, 2002), Korn *et al.* (1994), Møller (1995), Goodman *et al.* (1995), O'Quigley and Shen (1996) and Mukhopadhyay (2000), among others). The commonly used continual reassessment method (CRM) assumes a parametric link function, such as a hyperbolic tangent or a power function, between the true dose toxicity probabilities and the prespecified toxicity probabilities (O'Quigley *et al.*, 1990). The toxicity probability curve can be efficiently adjusted by updating the posterior estimate of a single unknown parameter (O'Quigley and Shen, 1996). Other methods include dose escalation with overdose control (Babb *et al.*, 1998), the curve-free dose finding procedure based on the product beta prior (Gasparini and Eisele, 2000) which can be exactly characterized by an equivalent CRM design, the decision theoretic approaches (Whitehead and Brunier, 1995; Leung and Wang, 2002) and the random-walk rule and the biased coin design under isotonic regression (Durham *et al.*, 1997; Stylianou and

*Address for correspondence:* Guosheng Yin, Department of Biostatistics, University of Texas M. D. Anderson Cancer Center, Houston, TX 77030, USA.  
E-mail: gsyin@mdanderson.org

Flournoy, 2002). Comprehensive reviews for phase I trial designs were given in Edler (2001) and Rosenberger and Haines (2002). More up-to-date and extensive discussions on statistical approaches for dose finding can be found in Chevret (2006).

However, all the aforementioned methods are developed for single-agent dose finding trials. Given the enormous advances in medicine and large numbers of new drugs to be tested, interest in finding combinations of drugs for patient treatment has grown. The goal of combination therapy is to achieve better patient response, particularly for cancer patients who are refractory to conventional therapies. In oncology, for example, combining agents can induce a synergistic treatment effect, allowing the clinician to target tumour cells with differing drug susceptibilities, and to achieve a higher intensity of dose with non-overlapping toxicities. Our research is motivated by many recent and more emerging dose finding drug combination clinical trials at the M. D. Anderson Cancer Center. One example is to find the MTD combination of a small molecule receptor (orally administered with four dose levels) and a mammalian target of rapamycin inhibitor (an intravenous drug with four dose levels) resulting in 16 combinations. The combined drugs are expected to induce a synergistic treatment effect by targeting different pathways.

The trend of drug combination trials poses a great challenge to finding the MTD combination with two or more drugs, particularly with small sample sizes in phase I studies. In a single-agent trial, we typically assume a monotonically increasing order of toxicity with respect to the dose. For any given dose, there are at most two adjacent doses and the order of toxicity is known. In contrast, for a two-drug combination dose space, there are up to eight adjacent doses, including diagonal and off-diagonal doses, as shown in Fig. 1. More importantly, complex drug–drug interactive effects often lead to unknown patterns of toxicity. Thus, the monotonic order of toxicity with respect to the dose level is lost, and it becomes unclear which dose combination should be assigned under a decision of dose escalation or de-escalation. Moreover, when two or more drugs are combined, the dimension of the dose space expands in a multiplicative fashion. This rapid increase in the dose dimension naturally requires a larger sample size, which can easily double or triple that of a single-agent trial.

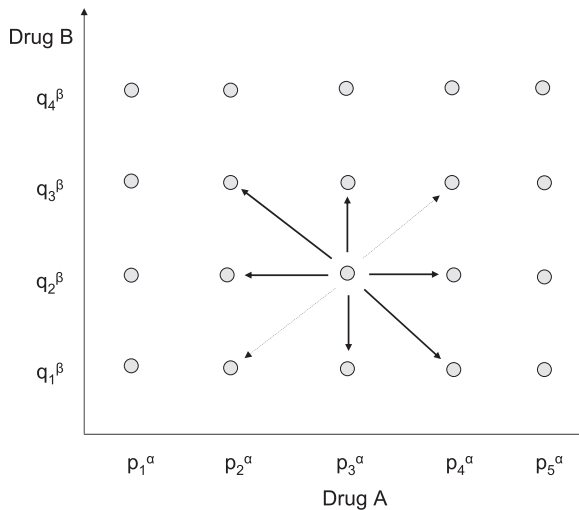


**Fig. 1.** Dose escalation and de-escalation diagram with  $5 \times 4$  combinations, while the dose change along the diagonal ( $\cdots$ ) is not allowed

A straightforward way to extend the traditional single-agent dose finding methods to drug combination trials is to conduct a series of one-dimensional dose finding trials: fixing one drug at each specified dose level and varying the other. This essentially transforms the two-dimensional dose finding space to a one-dimensional space. Korn and Simon (1993) introduced a graphical tolerable dose diagram to provide guidance in targeting specific MTD combinations. Kramar *et al.* (1999) proposed monotonically ordering a selected subset of drug combinations which reduced the dose finding to a one-dimensional space. Lokich (2001) presented a clinical trial that combined topotecan at four dose levels with irinotecan at two levels in the treatment of patients with advanced malignancy. Kuzuya *et al.* (2001) proposed combining paclitaxel and carboplatin to treat ovarian cancer, by alternately fixing one agent at a certain dose level and varying the other. Thall *et al.* (2003) proposed a six-parameter model to define the probability of toxicity with respect to the doses of gemcitabine and cyclophosphamide. The combined dose is first escalated along the diagonal line; then a toxicity equivalence contour is constructed for further investigation of proper dose combinations. Conaway *et al.* (2004) examined the simple and partial orders for drug combinations based on the pool adjacent violators algorithm. Wang and Ivanova (2005) proposed a two-dimensional dose finding design that was based on the logistic-type regression with standardized doses of the two drugs as the covariates. In this design, the interaction term can be included to capture the drug–drug interactive effects, which, however, might not be estimated reliably owing to a small variation in the covariate. Huang *et al.* (2007) extended the traditional ‘3 + 3’ design by classifying the two-dimensional dose space into zones. Yin and Yuan (2008) proposed a latent  $2 \times 2$  table approach to dose finding for drug combinations.

Trial designs involving drug combinations can be extended to a broader spectrum, for example, to search jointly for the optimal dose level and dose schedule for a single agent. As seen frequently in clinical trials, a single agent with a set of dose levels may be administered at several different dose schedules in a treatment cycle. To improve the treatment effect, the drug can be given at a more intense or frequent schedule instead of a regular schedule. More recently, Braun *et al.* (2007) proposed a Bayesian adaptive design that simultaneously optimizes both dose and schedule based on time-to-toxicity outcomes. Motivated by a phase I trial in allogeneic bone marrow transplantation at the M. D. Anderson Cancer Center, their design reflects the actual clinical practice and thus has potential of broad applications. Therefore, the drug combination can be formulated in a more general framework, that of a trial with several different drugs, each at a prespecified set of dose levels, or a study of a single agent at a set of dose levels, adding a change to different dose schedules. The terminology of ‘dose level’ or ‘dose schedule’ may be used exchangeably for our general purpose of describing statistical designs, as both would increase the probability of toxicity monotonically. Other work related to drug combination studies includes Plackett and Hewlett (1967), Ashford (1981), Abdelbasit and Plackett (1982), Simon and Korn (1990) and Korn and Simon (1992).

Before several drugs are combined, the toxicity profile of each individual drug needs to be thoroughly investigated. Hence, physicians usually have good prior knowledge of the probabilities of toxicity when each drug is administered alone. We propose to utilize this rich prior information and to develop a Bayesian adaptive dose finding procedure for combined agents. We model the rates of toxicity of the combined drugs via a copula-type regression. In particular, we first prespecify the underlying probabilities of toxicity for each drug on the basis of their individual toxicity information. To accommodate the uncertainty of this prespecification, we incorporate a power parameter to the probabilities of toxicity for each drug as in the CRM. We then link these probabilities of toxicity in a copula-type model to derive the joint toxicity probability of the combined drugs. Our method reduces to the CRM if only one drug is

tested. Patients are sequentially accrued in cohorts. Decisions on dose escalation, de-escalation or staying at the same dose are adaptively made as the data are coherently updated in the trial.

The rest of the paper is organized as follows. In Section 2, we propose the joint toxicity probability model for the binary outcomes through a copula-type regression. Moreover, we derive the likelihood function and the posterior distribution for the unknown parameters. We formulate the decision rules and the dose finding algorithm in Section 3. We conduct extensive simulation studies to examine the operating characteristics of the new design in Section 4, and we conclude with a brief discussion in Section 5.

The programs that were used to simulate the design can be obtained from

<http://www.blackwellpublishing.com/rss>.

The executable file can be downloaded from <http://odin.mdacc.tmc.edu/~gyin/software.htm>.

## 2. Probability model

### 2.1. Copula-type regression

For ease of exposition, we illustrate our design by using a drug combination trial with two agents, say A and B, though our approach can be easily generalized to the case of combining multiple agents. Let  $p_j$  be the prespecified probability of toxicity corresponding to  $A_j$ , the  $j$ th dose for drug A,  $p_1 < p_2 < \dots < p_J$ , and  $q_k$  be that of  $B_k$ , the  $k$ th dose for drug B,  $q_1 < q_2 < \dots < q_K$ . Typically, the maximum dose for each drug in the combination (i.e.  $A_J$  and  $B_K$ ) is the individual MTD that has already been determined in the single-agent trials. The remaining lower doses are some fractions of the MTD, specified by physicians. The probability of toxicity is monotonically increasing with the dose level when each drug is administered alone. However, the ordering of the probabilities of toxicity of the combined drugs and dose levels is less obvious. For example, it is not clear how to order the probabilities of toxicity  $\pi_{jk}$ ,  $\pi_{j-1,k+1}$  and  $\pi_{j+1,k-1}$ , where  $\pi_{jk}$  is the joint toxicity probability associated with the combined drug pair  $(A_j, B_k)$ .

In a drug combination study, the probability of toxicity corresponding to the MTD of each agent is known, i.e.  $p_J$  and  $q_K$  are known. Through further consultation with physicians, we can easily specify  $(p_1, \dots, p_{J-1})$  for drug A, and  $(q_1, \dots, q_{K-1})$  for drug B. To enhance the flexibility and to accommodate physicians' uncertainty, we take  $p_j^\alpha$  and  $q_k^\beta$  as the true probabilities of toxicity for drug A and drug B respectively, where  $\alpha > 0$  and  $\beta > 0$  are unknown parameters with prior means centred at 1. When two or more drugs are combined as a treatment, it would be unrealistic to assume that each drug acts independently on the patient, as the drug–drug interactive effects may have a strong influence on the joint toxicity profile. Therefore, it is critical to choose an appropriate model to link the joint toxicity probability  $\pi_{jk}$  with the  $p_j$ s and  $q_k$ s. A reasonable model for drug combinations needs to satisfy the following conditions: for  $j = 1, \dots, J$  and  $k = 1, \dots, K$ ,

- (a) if  $p_j^\alpha = 0$  and  $q_k^\beta = 0$ , then  $\pi_{jk} = 0$ ,
- (b) if  $p_j^\alpha = 0$ , then  $\pi_{jk} = q_k^\beta$ , and, if  $q_k^\beta = 0$ , then  $\pi_{jk} = p_j^\alpha$ , and
- (c) if either  $p_j^\alpha = 1$  or  $q_k^\beta = 1$ , then  $\pi_{jk} = 1$ .

These conditions are very intuitive for the joint model of drug combinations. The first condition requires that, if the probabilities of toxicity of both drugs are 0 (i.e. no drugs), the joint toxicity probability should also be 0. The second condition states that, if the probability of toxicity of one drug is 0 (i.e. a single-agent case), the joint toxicity probability should reduce to that of the other drug. Finally, the third condition asserts that, if the toxicity probability of either drug is 1, the joint toxicity probability should be 1 as well.

Although each drug has its own toxicity profile, the individual toxicity outcome cannot be observed in the trial. We typically can only observe a single toxicity binary outcome for the drug combination. For example, the outcome of a patient treated at  $(A_j, B_k)$  provides information on the joint toxicity probability  $\pi_{jk}$  that can be linked to the probabilities of toxicity  $(p_j^\alpha, q_k^\beta)$  through a copula-type regression model. There has been considerable interest in modelling the bivariate probability function through copula models (for example, see Clayton (1978), Hougaard (1986), Genest and Rivest (1993) and Nelsen (1999), among others). Copula models have an attractive structure by expressing the joint probability distribution through the marginal distributions and a dependence parameter. Suppose that  $C_\gamma$  is a distribution function on  $[0, 1]^2$  given an association parameter  $\gamma$ . The Archimedean copula family characterizes an important class of dependence functions, which has the representation

$$C_\gamma(u, v) = \psi_\gamma\{\psi_\gamma^{-1}(u) + \psi_\gamma^{-1}(v)\}, \quad 0 \leq u, v \leq 1,$$

where  $\psi_\gamma$  is the copula generator,  $\psi_\gamma^{-1}$  is its inverse function,  $0 \leq \psi_\gamma \leq 1$ ,  $\psi_\gamma(0) = 1$  and first and second derivatives  $\psi'_\gamma < 0$  and  $\psi''_\gamma > 0$ . It encompasses many well-known bivariate parametric distributions, such as the Clayton, Gumbel–Hougaard and Frank copula models (see Nelsen (1999)).

Motivated by the Clayton copula, we propose a copula-type regression model to link the joint toxicity probability  $\pi_{jk}$  with  $(p_j^\alpha, q_k^\beta)$  in the form of

$$\pi_{jk} = 1 - \{(1 - p_j^\alpha)^{-\gamma} + (1 - q_k^\beta)^{-\gamma} - 1\}^{-1/\gamma}, \quad (1)$$

where  $\gamma > 0$  characterizes the drug–drug interactive effect.  $\lim_{p_j \rightarrow 1} \{(1 - p_j^\alpha)^{-\gamma}\} = \infty$  and  $\lim_{q_k \rightarrow 1} \{(1 - q_k^\beta)^{-\gamma}\} = \infty$ , and thus  $\pi_{jk} = 1$  as  $p_j$  or  $q_k$  goes to 1. Moreover, if only one drug is tested, say  $p_j > 0$  and  $q_k = 0$  ( $k = 1, \dots, K$ ), model (1) reduces to the CRM, with  $\pi_j = p_j^\alpha$  ( $j = 1, \dots, J$ ). Our approach can be regarded as a multivariate generalization of the CRM which enables internal learning from other dose level combinations. As a result, this model satisfies the three model conditions. In Fig. 2, we illustrate the joint toxicity probability surface based on model (1) with  $\alpha = \beta = 2$  and  $\gamma = 1.5$  in the two-dimensional probability space. Depending on the three parameters  $(\alpha, \beta, \gamma)$ , the toxicity probability surface may have various shapes. If the target toxicity probability is 40%, as shown by the horizontal plane in Fig. 2, there is an intersection curve representing the MTD contour for the two drugs. Therefore, depending on the physician-specified doses, there could be more than one MTD combination in the discrete dose space. We focus on selecting one MTD combination, whereas, if multiple MTDs are found, physicians can determine the one for further investigation on the basis of disease and subject-matters. Other copula models can be used as well, depending on mathematical convenience and computational simplicity. For example, on the basis of the Gumbel–Hougaard copula, we can model the joint toxicity probability by

$$\pi_{jk} = 1 - \exp(-[\{-\log(1 - p_j^\alpha)\}^{1/\gamma} + \{-\log(1 - q_k^\beta)\}^{1/\gamma}]^\gamma),$$

which clearly also satisfies the three model conditions.

## 2.2. Likelihood and prior specification

We can construct the likelihood function on the basis of the binomial distribution with the probabilities  $\pi_{jk}$ . Suppose that, at the current stage of the trial, among  $n_{jk}$  patients treated at the paired dose level  $(j, k)$ ,  $x_{jk}$  patients have experienced toxicity. The likelihood is then given by

$$\text{lik}(\alpha, \beta, \gamma | \text{data}) \propto \prod_{j=1}^J \prod_{k=1}^K \pi_{jk}^{x_{jk}} (1 - \pi_{jk})^{n_{jk} - x_{jk}}.$$

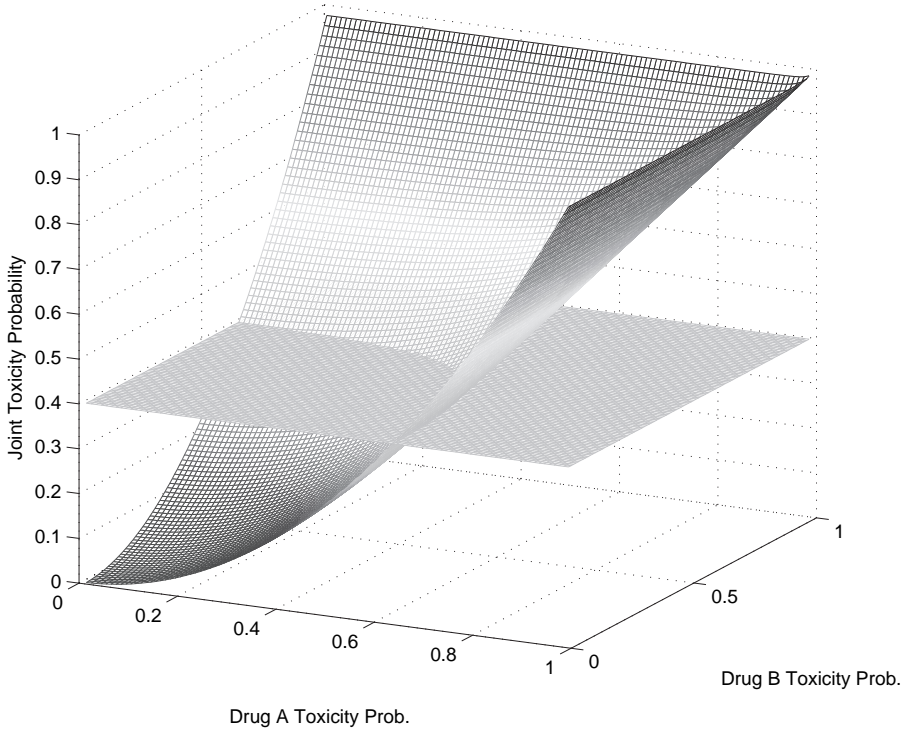


**Fig. 2.** Toxicity probability surface and MTD contour for the two-drug combination

For ease of computation, we take the prior distributions of the model parameters to be independent, i.e.  $f(\alpha, \beta, \gamma) = f(\alpha) f(\beta) f(\gamma)$ . Since the drugs in the combination have already been studied in single-agent trials, physicians often have some prior information of the probabilities of toxicity for each individual drug. We assign intermediate informative prior distributions to  $\alpha$  and  $\beta$  by centring the prior mean at 1 with a relatively small variance, e.g.  $\text{gamma}(2, 2)$ , a gamma distribution with mean 1 and variance 0.5. Essentially, these priors centre  $(p_j^\alpha, q_k^\beta)$  at the probabilities of toxicity when each drug is administered alone. The drug–drug interactive effect is mainly determined by  $\gamma$ , for which much less information can be elicited from physicians. Hence, we take a non-informative prior for  $\gamma$ , a gamma distribution with a large variance, so that the data will dominate the posterior estimation of  $\gamma$ . The joint posterior distribution is given by

$$f(\alpha, \beta, \gamma | \text{data}) \propto \text{lik}(\alpha, \beta, \gamma | \text{data}) f(\alpha) f(\beta) f(\gamma),$$

from which the full conditional distributions of the model parameters can be easily obtained. After the outcomes of each cohort of patients have been observed, we use the Gibbs sampling algorithm to sample from the posterior distributions of the unknown parameters. Thus, we can easily obtain the posterior estimates for  $\pi_{jk}$ , on which the next stage of the trial design will be based.

### 2.3. Multiple drugs in combination

In practice, drug combination trials often involve a pair of drugs, each with several prespecified doses. However, clinicians may find it beneficial to combine more than two drugs to treat

a patient. When the dimension of the drug combination space is higher than 2, dose finding becomes a much more complicated process, for which most of the currently available methods might not work well. Our method, however, can be easily generalized to such a high dimensional dose combination problem. For example, if three drugs are combined in a trial, we denote  $p_j$  to be the physician-specified probability of toxicity for the  $j$ th dose of drug A,  $j = 1, \dots, J$ ,  $q_k$  to be that for the  $k$ th dose of drug B,  $k = 1, \dots, K$ , and  $s_l$  to be that for the  $l$ th dose of drug C,  $l = 1, \dots, L$ , i.e. the triplet  $(p_j, q_k, s_l)$  represents the prespecified probabilities of toxicity that are associated with the combined drug doses  $(A_j, B_k, C_l)$ . By incorporating a power parameter for each prior probability of toxicity, the true probabilities of toxicity are  $(p_j^\alpha, q_k^\beta, s_l^\zeta)$ , where  $\alpha, \beta$  and  $\zeta$  have gamma distributions with prior means centred at 1. The dose combination searching space grows multiplicatively into a three-dimensional cube of dimension  $J \times K \times L$ .

In this three-dimensional toxicity probability space, we can still quantify the joint toxicity probabilities through a copula-type model. Under the Clayton copula, we define

$$\pi_{jkl} = 1 - \{(1 - p_j^\alpha)^{-\gamma} + (1 - q_k^\beta)^{-\gamma} + (1 - s_l^\zeta)^{-\gamma} - 2\}^{-1/\gamma}$$

and, under the Gumbel–Hougaard copula, we have

$$\pi_{jkl} = 1 - \exp(-[\{-\log(1 - p_j^\alpha)\}^{1/\gamma} + \{-\log(1 - q_k^\beta)\}^{1/\gamma} + \{-\log(1 - s_l^\zeta)\}^{1/\gamma}]^\gamma),$$

where  $\alpha, \beta$  and  $\zeta$  are the unknown parameters for each individual drug and  $\gamma$  is the association parameter for synergism. The corresponding likelihood based on the binomial distribution is given by

$$\text{lik}(\alpha, \beta, \zeta, \gamma | \text{data}) \propto \prod_{j=1}^J \prod_{k=1}^K \prod_{l=1}^L \pi_{jkl}^{x_{jkl}} (1 - \pi_{jkl})^{n_{jkl} - x_{jkl}},$$

where, among  $n_{jkl}$  patients treated at  $(A_j, B_k, C_l)$ ,  $x_{jkl}$  patients have experienced toxicity. The rest of the prior specifications and posterior derivations can be carried forward similarly.

### 3. Dose finding algorithm

Let  $\phi$  be the physician-specified targeting toxicity limit, and  $c_e$  and  $c_d$  be the fixed probability cut-offs for dose escalation and de-escalation respectively.  $c_e$  and  $c_d$  can be calibrated through simulation studies such that the trial has desirable operating characteristics, and  $c_e + c_d > 1$ . Patients are treated in cohorts, for example, with a cohort size of 3. To be conservative, we restrict dose escalation or de-escalation to one dose level of change only, while also not allowing a move along the diagonal direction (corresponding to simultaneous escalation or de-escalation of both agents), as shown in Fig. 1. For a trial involving two drugs, the dose finding algorithm works as follows.

- (a) Patients in the first cohort are treated at the lowest dose combination  $(A_1, B_1)$ .
- (b) If, at the current dose combination  $(j, k)$ ,

$$\Pr(\pi_{jk} < \phi) > c_e,$$

the dose is escalated to an adjacent dose combination with the probability of toxicity higher than the current value and closest to  $\phi$ . If the current dose combination is  $(A_j, B_k)$ , the doses stay at the same levels.

- (c) If, at the current dose combination  $(j, k)$ ,

$$\Pr(\pi_{jk} > \phi) > c_d,$$

the dose is de-escalated to an adjacent dose combination with the probability of toxicity lower than the current value and closest to  $\phi$ . If the current dose combination is  $(A_1, B_1)$ , the trial is terminated.

- (d) Otherwise, the next cohort of patients continues to be treated at the current dose combination (doses staying at the same levels).
- (e) Once the maximum sample size has been reached, the dose combination that has the probability of toxicity that is closest to  $\phi$  is selected as the MTD combination.

As is common to model-based clinical trial designs, the dose finding algorithm is difficult to apply at the beginning of the trial, because very limited information except for the prior knowledge is available. Thus, the posterior estimates of the probabilities of toxicity for dose combinations may not be reliable. To circumvent this difficulty, we use the following start-up rule: we first treat patients along the vertical dose escalation in the order of  $\{(A_1, B_1), (A_1, B_2), \dots\}$  until the first toxicity is observed; we then continue to treat patients by escalating doses in the horizontal direction  $\{(A_2, B_1), (A_3, B_1), \dots\}$  until the first toxicity occurs. As long as one toxicity is observed in both the vertical and the horizontal directions, e.g., if one patient experiences toxicity at  $(A_1, B_k)$  and  $(A_j, B_1)$  for some values of  $j$  and  $k$ , the Bayesian dose finding algorithm will be in effect seamless for the rest of the trial.

#### 4. Simulation study

We investigated the operating characteristics of our two-dimensional Bayesian copula dose finding method through simulation studies under 12 different toxicity scenarios, as listed in Table 1. In our simulation, the target probability of toxicity was  $\phi = 40\%$ , and the sample size of each trial was 60, with a cohort size of 3. We set  $c_e = 0.8$  and  $c_d = 0.45$  to direct dose escalation and de-escalation. The dose assignment decision was made after observing the outcomes of every cohort of patients. In the Clayton copula, we took  $\text{gamma}(2, 2)$  as the prior distribution for  $\alpha$  and  $\beta$ , and  $\text{gamma}(0.1, 0.1)$  for  $\gamma$ . In the Markov chain Monte Carlo procedure, we recorded 2000 posterior samples of the model parameters after 100 burn-in iterations. We simulated 2000 trials under each scenario. The first six scenarios represent drug combinations with five dose levels of drug A and four dose levels of drug B, but with different numbers and different locations of the MTD combinations. The toxicity rates of the MTDs for drug A and drug B were 0.4 and 0.3 respectively, when administered alone. For drug A, we specified the prior marginal toxicity probabilities  $p_j$  as (0.08, 0.16, 0.24, 0.32, 0.4); and, for drug B, we specified  $q_k$  as (0.075, 0.15, 0.225, 0.3). In scenarios 7–10, we examined a different dose configuration with a  $4 \times 4$  grid. The prior toxicity probabilities were (0.07, 0.15, 0.22, 0.3) for drug A, and (0.12, 0.18, 0.24, 0.3) for drug B. As a part of the sensitivity analysis, scenarios 11 and 12 were designed to examine the robustness of the Bayesian copula design to model misspecifications. Under these two scenarios the probabilities of toxicity were generated according to the Frank and Gumbel copulas (Nelsen, 1999). We compared the performance of our method with the CRM and non-parametric optimal design (O'Quigley *et al.*, 1990, 2002). We applied the CRM in a series of one-dimensional dose finding trials by fixing drug B at each given dose and searching over the doses of drug A (referred to as the restricted CRM). The total 60 patients were equally allocated to the four independent trials, 15 patients for each trial. We adopted a stopping rule: if  $\Pr\{\text{toxicity rate at } (A_1, B_1) > \phi\} > 0.9$ , the trial is terminated for safety (Goodman *et al.*, 1995; Möller, 1995). The non-parametric optimal design offers a theoretical bound as a benchmark for numerical comparisons.

In Table 2, we report the selection probabilities of dose combinations based on the restricted CRM, the non-parametric optimal design and the Bayesian copula method proposed. Scenar-

**Table 1.** 12 toxicity scenarios for the two-drug combinations with the target toxicity probability 0.4†

Dose level of drug B	Toxicity probabilities for the following levels of drug A:									
	1	2	3	4	5	1	2	3	4	5
	<i>Scenario 1</i>					<i>Scenario 2</i>				
4	0.54	0.67	0.75	0.81	0.86	0.49	0.58	0.68	0.75	0.81
3	0.48	0.59	0.68	0.75	0.81	0.40	0.49	0.59	0.68	0.75
2	0.40	0.45	0.59	0.67	0.74	0.27	0.40	0.45	0.59	0.67
1	0.24	0.40	0.47	0.56	0.64	0.18	0.29	0.40	0.47	0.56
	<i>Scenario 3</i>					<i>Scenario 4</i>				
4	0.31	0.40	0.50	0.61	0.75	0.40	0.52	0.72	0.75	0.84
3	0.23	0.34	0.40	0.53	0.67	0.29	0.40	0.51	0.60	0.68
2	0.16	0.25	0.34	0.40	0.52	0.20	0.31	0.40	0.50	0.59
1	0.09	0.16	0.18	0.22	0.40	0.12	0.21	0.30	0.40	0.47
	<i>Scenario 5</i>					<i>Scenario 6</i>				
4	0.11	0.16	0.23	0.31	0.40	0.79	0.85	0.89	0.92	0.94
3	0.06	0.11	0.17	0.24	0.32	0.74	0.81	0.86	0.89	0.92
2	0.03	0.07	0.11	0.17	0.24	0.67	0.76	0.81	0.86	0.89
1	0.01	0.03	0.07	0.11	0.18	0.57	0.67	0.74	0.79	0.84
	<i>Scenario 7</i>					<i>Scenario 8</i>				
4	0.28	0.30	0.32	0.40		0.52	0.69	0.70	0.75	
3	0.22	0.24	0.27	0.39		0.30	0.62	0.68	0.71	
2	0.20	0.22	0.26	0.28		0.20	0.40	0.50	0.66	
1	0.14	0.20	0.21	0.24		0.15	0.30	0.40	0.55	
	<i>Scenario 9</i>					<i>Scenario 10</i>				
4	0.50	0.66	0.67	0.73		0.50	0.52	0.57	0.63	
3	0.40	0.54	0.62	0.68		0.28	0.40	0.55	0.59	
2	0.21	0.40	0.50	0.60		0.26	0.30	0.40	0.50	
1	0.15	0.25	0.40	0.56		0.20	0.23	0.24	0.40	
	<i>Scenario 11</i>					<i>Scenario 12</i>				
4	0.46	0.53	0.58	0.61	0.64	0.46	0.53	0.60	0.65	0.70
3	0.45	0.50	0.55	0.58	0.61	0.39	0.47	0.54	0.60	0.66
2	0.40	0.44	0.50	0.53	0.56	0.31	0.40	0.47	0.54	0.61
1	0.20	0.40	0.47	0.48	0.50	0.23	0.32	0.40	0.47	0.54

†The MTD combinations are in italics.

ios 1, 2 and 3 describe situations in which there are two, three and four MTD combinations respectively. Under the first three scenarios, our method selected the MTD combinations with higher probabilities than the restricted CRM which tended to select over-MTD combinations in scenarios 1 and 2, and under-MTD combinations in scenario 3. Under the restricted CRM design, the trials corresponding to each dose level of drug B were completely independent of each other and no information or strength was borrowed across them. In contrast, the Bayesian copula dose finding method continuously updated the posterior estimates of probabilities of toxicity for all dose combinations on the basis of the available data and efficiently searched for the target across the whole drug combination space. Even in the cases where the set of doses of drug A contained the MTD for each fixed dose level of drug B, as illustrated by scenarios 3 and 4, our method performed slightly better than the restricted CRM, and comparably with the non-parametric optimal design. When the MTD is in the upper right-hand corner of the grid as in scenario 5, the Bayesian copula design proposed significantly outperformed the restricted

**Table 2.** Selection probabilities of the restricted CRM, non-parametric optimal design and Bayesian copula design under the first 10 scenarios

Scenario	Results for the restricted CRM					Results for the non-parametric optimal design					Results for the Bayesian copula design				
1	15.5	2.0	0.0	0.0	0.0	3.2	0.0	0.0	0.0	0.0	0.9	0.1	0.0	0.0	0.0
	15.5	4.8	0.5	0.0	0.0	6.9	0.1	0.0	0.0	0.0	10.2	1.7	0.1	0.0	0.0
	11.8	8.8	2.3	0.3	0.0	29.1	17.2	0.1	0.0	0.0	24.9	11.6	1.7	0.1	0.0
2	5.0	12.3	6.0	1.5	0.3	6.0	29.0	7.6	0.7	0.0	3.1	19.1	6.2	0.3	0.0
	15.3	4.5	0.3	0.0	0.0	3.8	0.5	0.0	0.0	0.0	5.0	1.5	0.0	0.0	0.0
	12.8	8.3	2.0	0.3	0.0	16.0	4.1	0.2	0.0	0.0	17.6	11.6	1.4	0.1	0.0
3	5.8	11.8	6.0	1.3	0.3	2.9	16.3	17.1	0.1	0.0	7.3	19.2	9.3	1.7	0.1
	1.5	9.0	9.8	3.5	1.3	0.1	11.2	16.8	8.7	2.1	0.1	5.1	11.2	5.0	0.3
	7.0	11.3	5.3	1.0	0.0	8.4	12.3	15.8	0.5	0.0	3.8	11.7	8.5	1.3	0.1
4	3.3	10.5	7.8	2.8	0.8	0.3	9.2	11.7	2.5	0.0	0.7	5.9	12.7	8.0	1.2
	0.8	6.8	10.0	5.0	2.5	0.0	1.5	9.2	12.1	3.7	0.0	0.7	3.5	12.0	10.3
	0.0	1.8	5.0	7.3	11.0	0.0	0.0	0.0	0.1	12.7	0.0	0.0	0.3	3.5	15.8
5	13.3	9.0	0.8	0.0	0.0	12.6	2.2	0.0	0.0	0.0	10.2	8.7	0.9	0.0	0.0
	6.0	12.3	5.5	1.0	0.3	3.6	13.1	2.1	0.3	0.0	5.3	16.7	5.9	0.5	0.0
	2.0	10.0	8.8	3.5	1.0	0.0	11.0	12.9	4.9	0.5	0.4	4.7	14.1	8.3	1.0
6	0.3	4.3	9.5	7.0	4.0	0.0	0.2	5.0	12.6	19.0	0.1	0.2	5.8	11.5	5.3
	0.3	3.0	7.3	7.3	7.8	0.0	0.0	0.1	8.1	77.2	0.0	0.0	0.4	3.2	87.6
	0.0	0.8	4.3	7.0	13.0	0.0	0.0	0.0	0.4	13.5	0.0	0.0	0.0	0.4	7.5
7	0.0	0.3	1.5	4.8	18.8	0.0	0.0	0.0	0.0	0.5	0.0	0.0	0.0	0.0	0.7
	0.0	0.0	0.3	1.8	23.0	0.0	0.0	0.0	0.0	0.0	0.0	0.0	0.0	0.0	0.1
	2.8	0.0	0.0	0.0	0.0	0.0	0.0	0.0	0.0	0.0	0.0	0.0	0.0	0.0	0.0
8	4.8	0.0	0.0	0.0	0.0	0.0	0.0	0.0	0.0	0.0	0.0	0.0	0.0	0.0	0.0
	8.8	0.3	0.0	0.0	0.0	0.1	0.0	0.0	0.0	0.0	0.0	0.0	0.0	0.0	0.0
	14.0	1.8	0.3	0.0	0.0	99.9	0.1	0.0	0.0	0.0	0.1	0.0	0.0	0.0	0.0
9	4.3	8.3	7.0	5.3		0.9	4.6	13.7	44.7		0.4	4.3	7.0	45.9	
	2.0	6.5	8.0	8.5		0.0	0.3	0.6	33.7		0.2	1.8	3.0	24.0	
	1.3	6.0	7.5	10.3		0.0	0.0	0.7	0.6		0.0	0.3	1.1	9.0	
10	0.5	3.8	6.3	14.5		0.0	0.0	0.0	0.1		0.0	0.1	0.2	1.8	
	16.0	2.5	0.3	0.0		4.2	0.0	0.0	0.0		11.8	0.2	0.0	0.0	
	12.8	10.8	0.8	0.0		8.7	0.2	0.0	0.0		10.9	12.2	0.3	0.0	
9	3.3	13.3	6.8	1.5		0.1	30.1	15.5	0.0		1.4	26.2	9.2	0.4	
	1.0	9.0	10.0	5.0		0.0	8.6	30.7	1.8		0.0	7.0	15.0	3.4	
	16.5	3.0	0.3	0.0		9.4	0.0	0.0	0.0		5.1	0.7	0.1	0.0	
10	13.5	8.3	1.3	0.3		21.9	2.4	0.0	0.0		15.7	10.2	1.0	0.1	
	3.5	13.3	6.5	1.8		0.2	23.9	9.9	0.2		1.9	24.1	10.7	0.5	
	0.8	7.5	11.0	5.8		0.0	7.5	23.9	0.7		0.0	5.9	17.7	4.2	
10	14.0	5.0	1.0	0.3		9.2	3.3	0.4	0.0		6.9	5.9	0.9	0.1	
	5.8	13.3	4.8	1.0		2.7	20.9	0.8	0.3		4.9	16.9	6.7	2.4	
	3.5	9.8	8.0	3.5		0.9	13.0	20.4	8.7		0.7	6.8	14.3	10.1	
10	1.5	5.8	8.0	9.8		0.0	0.2	0.3	19.0		0.1	1.5	4.5	13.3	

CRM. Scenario 6 examines the situation that all drug combinations are over toxic. Our method successfully early terminated 99.9% of the simulated trials without any selection. This scenario again demonstrates the enormous advantage of jointly modelling the probabilities of toxicity across the two-dimensional space. Note that the non-parametric optimal design does not have a stopping rule. Scenarios 7–10 investigate the performance of our method under a smaller drug combination space with four dose levels for each drug. The main differences between the scenarios are the numbers of MTD combinations and their locations in the  $4 \times 4$  grid. When two MTD combinations lie together in the upper right-hand corner as in scenario 7, both can be selected with a high percentage. Scenarios 8 and 10 are more difficult situations, in which the MTD contour is not complete, as the MTD is skipped in the first column (fixing drug A

at dose level 1) owing to the discreteness of the dose space. Yet, our method still selected the MTD combinations with high percentages. In scenario 9, three MTD combinations exist, and our method correctly selected them almost up to 60%. The overall performance of the Bayesian copula design is satisfactory and is better than the restricted CRM. In many cases, the performance of the Bayesian copula design is also comparable with the non-parametric optimal design.

Table 3 displays the average number of patients treated at each dose combination across 2000 simulations. Our method generally performed better than the restricted CRM in the sense that a higher percentage of patients were treated at the MTD or the dose combinations nearby. This advantage is especially prominent in scenarios 1, 5, 7 and 8, where the set of prespecified doses of drug A may not contain the MTD for a fixed level of drug B. For example, in scenario

**Table 3.** Number of patients treated at each dose combination for the restricted CRM and Bayesian copula design under the first 10 scenarios

Scenario	Results for the restricted CRM					Results for the Bayesian copula design				
1	10.5	2.4	0.2	0.0	0.0	0.8	0.1	0.0	0.0	0.0
	10.1	3.4	0.4	0.0	0.0	4.7	1.0	0.1	0.0	0.0
	8.5	4.7	1.2	0.1	0.0	14.2	5.2	1.0	0.1	0.0
	5.7	6.3	2.5	0.4	0.1	14.5	9.2	2.9	0.6	0.1
2	10.1	3.2	0.4	0.0	0.0	2.7	0.8	0.1	0.0	0.0
	8.6	4.7	1.1	0.1	0.0	8.4	3.6	0.6	0.1	0.0
	6.2	6.0	2.3	0.4	0.1	9.4	7.9	3.5	0.7	0.1
	4.3	5.7	3.7	1.1	0.2	8.5	6.0	5.7	2.5	0.7
3	6.6	5.8	2.2	0.3	0.0	3.7	3.9	2.8	0.9	0.3
	5.2	5.9	3.1	0.7	0.1	3.7	3.1	4.1	2.3	1.3
	4.0	5.3	4.1	1.4	0.3	3.7	1.3	2.3	4.1	4.0
	3.2	3.9	4.1	2.6	1.2	6.2	2.8	2.8	3.7	6.0
4	8.7	4.9	0.8	0.0	0.0	4.9	2.8	0.6	0.1	0.0
	6.2	6.2	2.2	0.3	0.0	5.9	5.7	2.5	0.3	0.2
	4.7	5.8	3.5	0.9	0.2	4.7	3.9	5.0	2.4	0.8
	3.5	4.7	4.4	1.9	0.5	6.6	3.3	4.8	5.1	3.1
5	3.4	4.1	4.2	2.4	0.9	2.8	0.6	0.7	2.2	22.7
	3.1	3.6	4.0	2.8	1.5	2.8	0.0	0.1	0.3	5.2
	3.0	3.2	3.6	3.1	2.1	3.0	0.0	0.0	0.0	3.1
	3.0	3.0	3.2	3.2	2.6	6.0	2.9	3.0	3.2	4.3
6	7.7	0.4	0.0	0.0	0.0	0.0	0.0	0.0	0.0	0.0
	8.5	0.6	0.0	0.0	0.0	0.2	0.0	0.0	0.0	0.0
	9.4	1.2	0.0	0.0	0.0	3.6	0.0	0.0	0.0	0.0
	10.3	2.1	0.2	0.0	0.0	12.3	0.4	0.0	0.0	0.0
7	5.7	5.2	3.0	1.0		1.8	2.7	3.1	12.1	
	4.6	5.1	3.6	1.7		2.8	2.3	2.4	7.5	
	4.3	5.0	3.8	2.0		3.8	1.5	1.4	4.9	
	3.6	4.6	4.0	2.8		7.0	3.3	2.8	3.4	
8	10.6	2.4	0.2	0.0		3.6	0.6	0.1	0.0	
	8.1	5.9	0.8	0.0		9.8	4.5	0.5	0.1	
	5.1	6.6	2.8	0.5		6.9	8.7	3.5	0.7	
	3.9	5.9	3.9	1.3		7.5	7.3	5.9	2.4	
9	10.6	2.7	0.3	0.0		2.2	0.6	0.2	0.0	
	8.9	4.7	0.8	0.1		8.4	4.2	0.6	0.2	
	5.3	6.5	2.7	0.5		7.6	8.9	3.9	0.9	
	3.8	5.4	4.3	1.5		7.5	6.6	7.2	2.9	
10	9.8	3.2	0.5	0.1		2.6	1.8	0.6	0.4	
	6.2	6.2	2.2	0.3		5.1	6.5	2.2	1.3	
	5.5	5.5	3.1	0.9		5.3	4.7	4.9	3.6	
	4.4	4.9	3.8	1.9		8.3	4.3	3.9	5.4	

**Table 4.** Total number of observed toxicities for the restricted CRM and Bayesian copula design under the first 10 scenarios

<i>Scenario</i>	<i>Results for the restricted CRM</i>	<i>Results for the Bayesian copula design</i>
1	26.2	20.3
2	23.5	21.8
3	17.3	20.4
4	20.5	21.3
5	8.4	14.5
6	27.8	8.2
7	14.8	17.5
8	24.0	22.2
9	23.7	22.3
10	20.9	20.7

1, the restricted CRM treated the majority of patients at dose combinations above the MTD, whereas in scenario 5 most of the patients were treated at doses below the MTD. In addition to the benefit of treating more patients at desirable doses, our method is safer than the restricted CRM in terms of the average number of patients experiencing toxicity in six of the 10 cases, as shown in Table 4. In scenario 5, on average, six more patients experienced toxicity under our design than under the restricted CRM, as most of the patients were treated at the under-MTD combinations in the restricted CRM design. Under scenario 6, in which all doses were overly toxic, the restricted CRM had to be implemented independently for each of the four rows as it

**Table 5.** Sensitivity analysis of the Bayesian copula design, including model misspecifications and alternative prior specifications

Results for selection probability					Results for numbers of patients treated				
Scenario 11 (Frank copula)									
1.9	0.5	0.0	0.0	0.0	1.1	0.3	0.1	0.0	0.0
8.7	3.0	0.7	0.2	0.1	5.1	1.4	0.3	0.1	0.0
24.1	12.6	3.7	0.5	0.3	14.0	5.2	1.2	0.2	0.1
2.5	20.4	6.9	1.1	0.4	13.6	9.9	3.7	1.1	0.3
Scenario 12 (Gumbel copula)									
5.6	1.7	0.2	0.0	0.0	2.3	0.9	0.1	0.0	0.0
14.2	9.5	1.6	0.2	0.0	7.3	3.1	0.7	0.1	0.0
9.3	18.8	8.5	1.4	0.1	10.9	6.8	2.8	0.6	0.1
0.7	6.7	8.6	3.5	0.3	9.8	6.1	4.6	1.9	0.6
Scenario 3 with prior $\alpha, \beta \sim \text{gamma}(1, 1)$									
3.4	11.2	9.5	1.2	0.2	3.3	4.1	2.7	0.9	0.4
1.1	7.6	12.7	7.6	1.8	3.9	4.0	4.2	2.2	1.5
0.0	0.7	4.2	12.7	9.8	4.1	1.3	2.5	4.0	3.7
0.0	0.1	0.2	3.6	12.2	6.4	2.9	2.7	3.3	4.9
Scenario 3 with prior $\alpha, \beta \sim \text{gamma}(0.5, 0.5)$									
3.6	11.4	10.7	2.0	0.1	3.3	4.0	3.2	1.1	0.4
1.0	7.5	12.4	7.6	1.9	3.6	3.9	4.6	2.4	1.3
0.0	0.8	6.2	11.6	8.5	4.2	1.6	3.2	3.9	3.2
0.0	0.0	0.5	2.9	10.8	6.3	2.9	2.7	2.9	4.2

could not borrow information across the rows. As a result, the restricted CRM allocated at least a few patients to the first column and more patients experienced toxicity than in our design, which stopped the trial earlier. As to other scenarios, the method proposed performed comparably with the restricted CRM. Across the 10 scenarios, on average 207.1 patients experienced toxicity by using the restricted CRM as opposed to 189.2 patients by using our method.

We conducted two types of sensitivity analysis, which are summarized in Table 5. To examine the robustness of our method to model misspecifications, the probabilities of toxicity in scenarios 11 and 12 were simulated from the Frank and Gumbel copula models (comparing with scenarios 1 and 2) respectively. Under these two scenarios, our method performed very well with high selection percentages of the MTD combinations. Moreover, to evaluate the effect of the prior specifications, we investigated the performance of our design under two more diffusive prior distributions for  $\alpha$  and  $\beta$  under scenario 3. The Bayesian copula design appeared not to be sensitive to the prior specification and yielded very similar results on the basis of different hyperparameters.

## 5. Concluding remarks

To accommodate the enormous need for designing clinical trials with drug combinations, we have developed a copula-type model to link the joint toxicity probability with the probabilities of toxicity of each drug. The method proposed can fully evaluate the joint toxicity profiles of the combined drugs, as well as preserve their single-agent properties. The drug–drug interactive effects are naturally modelled through a copula-type model, which reduces to the CRM design if only one drug is considered. The attractive feature of this design is that it efficiently reorders the probabilities of toxicity of the dose combinations on the basis of the accrued data, so that the next cohort of patients to be treated will receive the most appropriate dose. The toxicity surface for the combined drugs can be adequately captured and reshaped by the three unknown parameters. In a typical drug combination trial, the doses of each drug are often bounded by the corresponding single-agent MTDs for which the toxicity probabilities are known from previous studies. Therefore, the prior specification for the probabilities of toxicity of each drug are much more accurate than the usual CRM for single-agent cases. The start-up rule was introduced for safety and did not affect the performance of the trial. We also implemented the design proposed by using the Gumbel copula in the simulation study, and we obtained similar results to those in the Clayton copula. The Bayesian Markov chain Monte Carlo algorithm can coherently update the posterior estimates for the model parameters as more patients enter the trial and more outcomes are observed. It achieves the goal of designing a Bayesian dose finding clinical trial by borrowing strength from all the available data.

## Acknowledgements

We thank the referees, Associate Editor and Joint Editor for helpful comments that substantially improved the paper. The research was partially supported by funds from the Physician Referral Service at the M. D. Anderson Cancer Center, 5 P50 CA116199-03 breast cancer ‘Specialized program of research excellence’ and US Department of Defense grant W81XWH-05-2-0027.

## References

- Abdelbasit, K. M. and Plackett, R. L. (1982) Experimental design for joint action. *Biometrics*, **38**, 171–179.
- Ashford, J. R. (1981) General models for the joint action of mixtures of drugs. *Biometrics*, **37**, 457–474.
- Babb, J., Rogatko, A. and Zacks, S. (1998) Cancer phase I clinical trials: efficient dose escalation with overdose control. *Statist. Med.*, **17**, 1103–1120.

- Braun, T. M., Thall, P. F., Nguyen, H. and de Lima, M. (2007) Simultaneously optimizing dose and schedule of a new cytotoxic agent. *Clin. Trials*, **4**, 113–124.
- Chevret, S. (2006) *Statistical Methods for Dose-finding Experiments*. Chichester: Wiley.
- Clayton, D. G. (1978) A model for association in bivariate life tables and its application in epidemiological studies of familial tendency in chronic disease incidence. *Biometrika*, **65**, 141–152.
- Conaway, M. R., Dunbar, S. and Peddada, S. D. (2004) Designs for single- or multiple-agent phase I trials. *Biometrics*, **60**, 661–669.
- Durham, S. D., Flournoy, N. and Rosenberger, W. F. (1997) A random walk rule for phase I clinical trials. *Biometrics*, **53**, 745–760.
- Edler, L. (2001) Overview of phase I trials. In *Handbook of Statistics in Clinical Oncology* (ed. J. Crowley), pp. 1–34. New York: Dekker.
- Gasparini, M. and Eisele, J. (2000) A curve-free method for phase I clinical trials. *Biometrics*, **56**, 609–615.
- Genest, C. and Rivest, L.-P. (1993) Statistical inference procedures for bivariate Archimedean copulas. *J. Am. Statist. Ass.*, **88**, 1034–1043.
- Goodman, S. N., Zahurak, M. L. and Piantadosi, S. (1995) Some practical improvements in the continual reassessment method for phase I studies. *Statist. Med.*, **14**, 1149–1161.
- Hougaard, P. (1986) A class of multivariate failure time distributions. *Biometrika*, **73**, 671–678.
- Huang, X., Biswas, S., Oki, Y., Issa, J. P. and Berry, D. A. (2007) A parallel phase I/II clinical trial design for combination therapies. *Biometrics*, **63**, 429–436.
- Korn, E. L., Midthune, D., Chen, T. T., Rubinstein, L. V., Christian, M. C. and Simon, R. M. (1994) A comparison of two phase I trial designs. *Statist. Med.*, **13**, 1799–1806.
- Korn, E. L. and Simon, R. (1992) Selecting dose-intense drug combinations: metastatic breast cancer. *Breast Cancer Res. Trtmnt*, **20**, 155–166.
- Korn, E. L. and Simon, R. (1993) Using the tolerable-dose diagram in the design of Phase I combination chemotherapy trials. *J. Clin. Oncol.*, **11**, 794–801.
- Kramar, A., Lebecq, A. and Candalh, E. (1999) Continual reassessment methods in phase I trials of the combination of two drugs in oncology. *Statist. Med.*, **18**, 1849–1864.
- Kuzuya, K., Ishikawa, H., Nakanishi, T., Kikkawa, F., Nawa, A., Fujimura, H., Iwase, A., Arii, Y., Kawai, M., Hattori, S., Sakakibara, K., Sasayama, E., Furuhashi, Y., Suzuki, T. and Mizutani, S. (2001) Optimal doses of paclitaxel and carboplatin combination chemotherapy for ovarian cancer: a phase I modified continual reassessment method study. *Int. J. Clin. Oncol.*, **6**, 271–278.
- Leung, D. H.-Y. and Wang, Y.-G. (2002) An extension of the continual reassessment method using decision theory. *Statist. Med.*, **21**, 51–63.
- Lokich, J. (2001) Phase I clinical trial of weekly combined topotecan and irinotecan. *Am. J. Clin. Oncol.*, **24**, 336–340.
- Møller, S. (1995) An extension of the continual reassessment methods using a preliminary up-and-down design in a dose finding study in cancer patients, in order to investigate a greater range of doses. *Statist. Med.*, **14**, 911–922.
- Mukhopadhyay, S. (2000) Bayesian nonparametric inference on the dose level with specified response rate. *Biometrics*, **56**, 220–226.
- Nelsen, R. B. (1999) *An Introduction to Copulas*. New York: Springer.
- O'Quigley, J., Paoletti, X. and Maccario, J. (2002) Non-parametric optimal design in dose finding studies. *Bio-statistics*, **3**, 51–56.
- O'Quigley, J., Pepe, M. and Fisher, L. (1990) Continual reassessment method: a practical design for Phase I clinical trials in cancer. *Biometrics*, **46**, 33–48.
- O'Quigley, J. and Shen, L. Z. (1996) Continual reassessment method: a likelihood approach. *Biometrics*, **52**, 673–684.
- Plackett, R. L. and Hewlett, P. S. (1967) A comparison of two approaches to the construction of models for quantal responses to mixtures of drugs. *Biometrics*, **23**, 27–44.
- Rosenberger, W. F. and Haines, L. M. (2002) Competing designs for phase I clinical trials: a review. *Statist. Med.*, **21**, 2757–2770.
- Simon, R. and Korn, E. (1990) Selecting drug combinations based on total equivalent dose (dose intensity). *J. Natn. Cancer Inst.*, **82**, 1469–1476.
- Storer, B. E. (1989) Design and analysis of Phase I clinical trials. *Biometrics*, **45**, 925–937.
- Stylianou, M. and Flournoy, N. (2002) Dose finding using the biased coin up-and-down design and isotonic regression. *Biometrics*, **58**, 171–177.
- Thall, P. F., Millikan, R. E., Müller, P. and Lee, S.-J. (2003) Dose-finding with two agents in phase I oncology trials. *Biometrics*, **59**, 487–496.
- Wang, K. and Ivanova, A. (2005) Two-dimensional dose finding in discrete dose space. *Biometrics*, **61**, 217–222.
- Whitehead, J. and Brunier, H. (1995) Bayesian decision procedures for dose determining experiments. *Statist. Med.*, **14**, 885–893.
- Yin, G. and Yuan, Y. (2008) A latent contingency table approach to dose finding for combinations of two agents. *Biometrics*, to be published.

The phase II trial of erlotinib and radiotherapy following chemoradiotherapy for patients with stage III Non-Small Cell Lung Cancer has shown a favorable response profile

Ritsuko Komaki, M. D., George Blumenschein, M.D., Ignacio Wistuba, M. D., J. Jack Lee, Ph.D., Pamela Allen, Ph.D. Xiong Wei, M.D., Xi Ming Tang, M.D., Raymond E. Meyn, Ph.D. Diane Liu, MS, Wuan Ki Hong, M.D.

#### Background

Majority of Non-Small Cell Lung Cancer (NSCLC) overexpress EGFR. Our prospective phase II trial investigated EGFR-TKI (erlotinib) as a radiosensitizer for inoperable stage III NSCLC patients (pts) who also received standard chemoradiotherapy (ChT/RT).

#### Patients and Methods:

48 stage III NSCLC pts were enrolled from 3/2008 through 6/2010. ChT/RT was given every Monday followed by erlotinib/RT on Tuesday-Friday and erlotinib alone over the weekend. RT (63 Gy in 35 fractions) with weekly paclitaxel (45mg/m<sup>2</sup>) / carboplatin (AUC=2) and erlotinib (150 mg p.o. daily except on the day of chemotherapy) were given for 7 weeks. After one month break, pts received two cycles consolidation of paclitaxel (AUC=6) and carboplatin (200mg/m<sup>2</sup>). EGFR mutation analysis was performed for 41 pts. The response was evaluated by CT scan three months after completion of ChT/RT based on RECIST criteria. Fisher's exact and Kaplan-Meier's tests were used for the statistical analysis.

#### Results:

46 pts completed the entire treatment are evaluable for response. All had PS KPS $\geq$ 8 0, 17 (37%) were female, 23 adenocarcinoma, and 87% former or current smokers, with median age 63 year-old (range: 46-81). Responses showed 14 (30%) CR, 23 (50%) PR and 9 (20%) stable or progressive disease. Five in 41 pts (12%) had EGFR mutation (EGFR-M), all adenocarcinoma with 2 females, compared to none of squamous histology (p=0.05). CR and non-CR were 3 and 2 in the EGFR-M group compared to 11 and 25 in the EGFR-wild group (p=0.32), respectively. The median OS and PFS were 25.8 mons & 13.6 mons, respectively. 1-year & 2-year OS were 84% & 75% and PFS 54% & 32%, respectively. Toxicity showed 2 grade 3 acne, 1 Grade 3 esophagitis, 3 Grade 3 pneumonitis and no Grade 4-5.

#### Conclusions:

This prospective phase II clinical study demonstrated an excellent 1-year OS 84 % and median OS 25.8 mons. All EGFR-M were seen in adenocarcinomas. Erlotinib demonstrated a radiosensitization effect. .

## IPQA Manufacturing Process

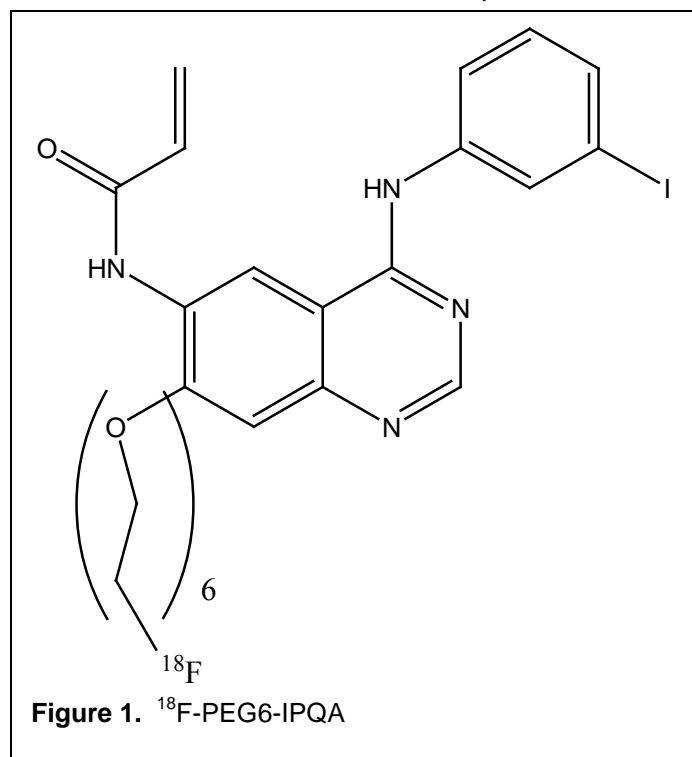
### Chemistry, Manufacturing, and Control (CMC)

The product,  $^{18}\text{F}$ -fluoro-PEG6-IPQA injection, to be used in the phase I clinical trial will be manufactured by Cyclotope (Houston, TX). An automated radio synthesis using customized GE box has been developed and validated. The same synthesis route and precursors for clinical production have been used in part for the preclinical studies.

### Drug substance

#### Physical and chemical characteristics

Fluoro-PEG6-IPQA is an anilinoquinazoline compound with the chemical name: 4-[(3-



iodophenyl)amino]-7-{2-[2-{2-(2-[2-(2-(fluoroethoxy)-ethoxy)-ethoxy]-ethoxy)-ethoxy]-quinazoline-6-yl-acrylamide. The structure formula is represented in Figure 1. F-PEG6-IPQA has the molecular formula  $\text{C}_{29}\text{H}_{36}\text{FIN}_4\text{O}_7$  and molecular weight of 698.52. It is a yellowish solid. It is relatively insoluble in water, but soluble in organic solvents including acetone, chloroform, and DMSO.

The 18-fluorine labeled fluoro-PEG6-IPQA as a PET imaging agent is synthesized through a no-carrier added process. The drug substance is isolated and purified using a preparative liquid chromatography. The collected fraction passes through a Supelco HiTrap SP ion exchange cartridge and is subsequently eluted with ethanol/saline solution to form the final product. Drug substance is therefore not separately obtained nor

characterized. The characterization is performed at the stage when the final product is made.

### Drug Product

#### Drug product composition

The final product of  $^{18}\text{F}$ -fluoro-PEG6-IPQA injection consists of  $^{18}\text{F}$ -fluoro-PEG6-IPQA in 6% ethanol of saline solution. The targeted radiation dose of  $^{18}\text{F}$ -fluoro-PEG6-IPQA for the first cohort is at 70 MBq or approximately 2 mCi.

### Manufacturing process

An automated and no carrier added procedure using two GE TracerLab FX<sub>F-N</sub> synthesizers is developed and validated to produce  $^{18}\text{F}$ -PEG6-IPQA. The precursor (compound 1 in figure 2), methanesulfonic acid 2-(2-[2-(2-{2-[4-(3-iodophenylamino)-6-nitro-quinazolin-7-yloxy]-ethoxy]-ethoxy]-ethoxy)-ethyl ester, is purchased from manufacturer: ABX Advanced Biochemical Compounds. The purity of the precursor is > 98% determined by NMR. The

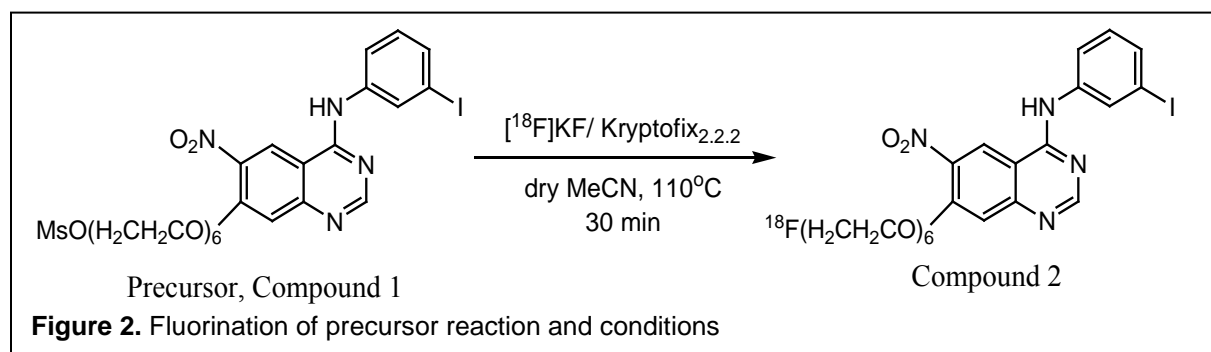
certificate of analysis is supplied with the precursor by ABX (see appendix 1 for a copy of Certificate of Analysis).

$^{18}\text{F}$  is produced on site by irradiating highly enriched  $^{18}\text{O}\text{-H}_2\text{O}$  with 18 MeV protons from a TR19/9 cyclotron (EBCO/ACS, Vancouver, Canada).  $^{18}\text{F}$  is trapped with a Chromafix PS- $\text{HCO}_3$  resin and then eluted using standard  $\text{K}_2\text{CO}_3$ /Kryptofix in acetonitrile/water solution. This  $^{18}\text{F}\text{-KF/Kryptofix222}$  solution is transferred to the first GE TracerLab  $\text{FX}_{\text{F-N}}$  synthesizer. Solvents are removed during the two-step evaporation processes and render dried  $^{18}\text{F}$ .

All materials used in the manufacturing of the final product are summarized in Table 1. Radiochemistry synthesis schemes are illustrated in figure 2.

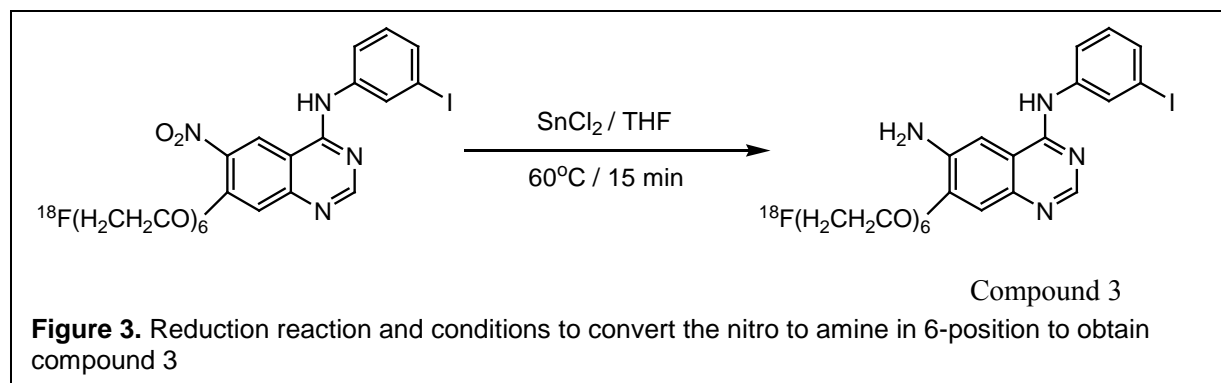
**Step 1: Fluorination of Precursor (in the first GE TracerLab  $\text{FX}_{\text{F-N}}$  synthesizer)**

In the first GE TracerLab  $\text{FX}_{\text{F-N}}$  synthesizer, a solution of precursor (10 mg, Compound 1 in Figure 2) dissolved in anhydrous acetonitrile (0.6 mL) is added to the dried  $^{18}\text{F}\text{-KF/Kryptofix}_{222}$  complex. This reactor is heated for 30 minutes at  $110^\circ\text{C}$ . After cooling the reaction mixture to room temperature, this mixture is passed through a silica gel cartridge (900 mg) which is pre-conditioned with 2 mL of hexane. This cartridge is then eluted with 2.5 mL of dichloromethane/methanol (3/7, v/v) solvent mixture. The eluent is transferred to reactor #1 of the second GE TracerLab  $\text{FX}_{\text{F-N}}$  synthesizer. The precursor is now labeled with  $^{18}\text{F}$  to yield 4-[(3-iodophenyl)amino]-7-{2-[2-{2-(2-[2-{2-([ $^{18}\text{F}$ ]fluoroethoxy)-ethoxy)-ethoxy]-ethoxy)-ethoxy]-ethoxy}-6-nitro-quinazoline (compound 2 in Figure 2). The compound 2 containing residual is used for second step reaction without further purification.



**Step 2: Reduction of 6-nitro to 6-amine (in the second GE synthesizer, reactor #1)**

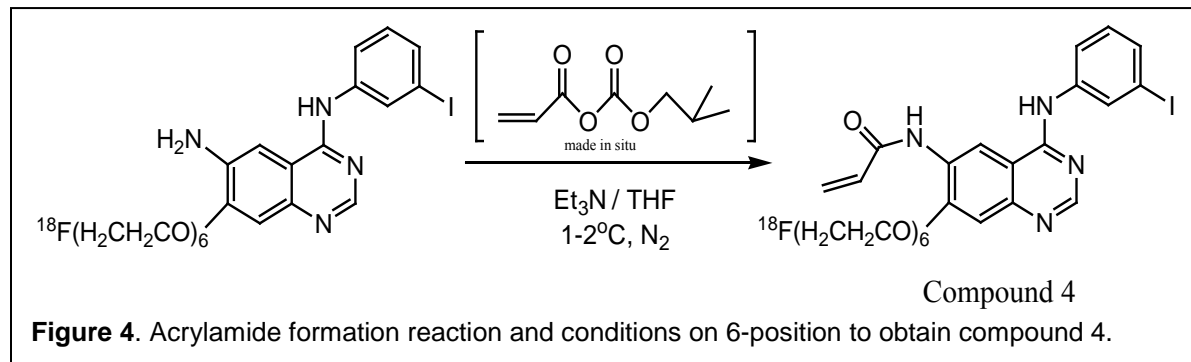
The solvent is evaporated to dryness at  $80^\circ\text{C}$  under nitrogen flow and vacuum. The dried mixture is cooled to about  $50^\circ\text{C}$  when a solution of  $\text{SnCl}_2$  (15 mg) in 0.45 mL of dry THF is added into the compound 2 containing residual in reactor #1. The resulting mixture is heated for 15 minutes at  $60^\circ\text{C}$  to allow optimal reaction. The mixture is cooled to about  $40^\circ\text{C}$  before passing it through a silica gel cartridge (900 mg) which is pre-conditioned with 2mL hexane. The cartridge is eluted with 2 mL of dichloromethane/methanol solvent mixture (3/7, v/v) into



reactor #2 to obtain compound 3 (Figure 3). The solvent is evaporated to dryness at 80°C under nitrogen flow and vacuum. Cool the dried mixture containing compound 3 to about 1 – 2 °C or lower for next step.

*Step 3: Acrylamide formation (in the second GE synthesizer, reactor #2)*

A solution of acrylic acid (0.05 mL), triethylamine (0.1 mL) and dry THF (0.2 mL) is added to the dried mixture in reactor #2. Stir the solution. Another 0.3 mL of THF is added to the stirred reaction mixture. Add isobutyl chloroformate (0.07 mL) to the cooled, stirring reaction mixture in reactor #2. Continue to stir the mixture for 9 min while maintaining a low temperature of 1 – 2°C to allow acrylamidation at the 6-position to yield the final compound (compound 4) in Figure 4.



While the solution in reactor #2 is still cold (1 – 2°C) and stirred, add 2.5 mL of HPLC mobile phase to the mixture. This mixture is then warmed to about 25°C before passing it through a nylon membrane (National Scientific, 30 mm diameter and 0.45 µm pore size) filter which has a glass pre-filter of 1 µm pore size. The filtrate is received in an intermediate vial.

*Step 4. Purification using Prep-HPLC to obtain final product*

This filtrate is transferred to the prep-HPLC injector and is injected onto a C8 preparative column (Zorbax CombiHT XDB, 21.2 x 100 mm with a matching guard column). The mobile phase to separate and elute the final compound (compound #4) from the mixture consists of acetonitrile/0.1% aqueous ammonium formate (46/54, v/v) and is operated at a flow rate of 6.0 mL/min. Duo detectors of the prep-HPLC having UV-vis (set at λ=254 nm) and the built-in PIN diode radiodetector are used to monitor the components in the final synthesis mixture in order to collect compound 4.

*Step 5. Formulation of the final dosage*

The radiochromatogram is monitored and the product fraction is collected using operator control. The product fraction is transferred to an intermediate flask containing about 8 mL of sterile water. Stir the diluted production fraction and transfer it to a C18 solid phase extraction cartridge (Waters or equivalent) which is pre-conditioned with 10 mL 95% ethanol in sterile water and followed it by 10 mL sterile water to trap the compound 4 free of solvent. Thereafter, the C18 cartridge is first washed with sterile water discarding the eluent of the wash and the trapped compound 4, <sup>18</sup>F-PEG6-IPQA is then eluted with 2 mL of 95% ethanol through a 0.22 µm, vented, sterile Millipore filter into a sterile, apyrogen, vial (Hospira or equivalent) which contains about 29 mL of injectable saline solution to form the final formulated dosage.

**Table 1.** Components (with quality and supplier) used in the manufacturing of  $^{18}\text{F}$ -PEG6- IPQA injection

REAGENT	DESCRIPTION	SUPPLIER
Sterile Water for Injection, SWFI	USP	Hospira, Austin TX
Cryptand 222	$\geq 97.5\%$ Purity, off-white to white crystals or powder	ABX - Germany $15 \pm 2$ mg
$\text{K}_2\text{CO}_3$	White granular powder	Sigma-Aldrich
Acetonitrile	HPLC gradient grade, $\geq 99.9\%$	Sigma-Aldrich
$^{18}\text{F}$ -PEG6-IPQA Precursor, Compound 1	Packed under argon atmosphere in dark glass vials which are sealed with Teflon-faced rubber stoppers and tear-off crimp caps; store at $-20^\circ\text{C}$ , protected from light until use	ABX - Germany
Saline for Injection	0.9%, USP	B. Braun Medical
Acrylic acid	99%	Sigma-Aldrich
Acetonitrile	Anhydrous	Sigma-Aldrich
$\text{H}_2^{18}\text{O}$ , Target material	$\geq 80\%$ $^{18}\text{O}$ enrichment	Cambridge, Isotec, others
Ammonium Formate	Certified	Fisher
Dichloromethane	HPLC grade, 99.9%	Acros Organics
Ethanol	190 Proof, ACS Spectrophotometric grade	Sigma-Aldrich
Haxane	Anhydrous, 95%	Sigma-Aldrich
Isobutyl Chloroformate	98%	Sigma-Aldrich
Methanol	99.9%	Sigma-Aldrich
Tetrahydrofuran	Anhydrous, $\geq 99.9\%$	Sigma-Aldrich
Tin (II) Chloride	98%	Sigma-Aldrich
Triethylamine	$\geq 99.5\%$	Sigma-Aldrich

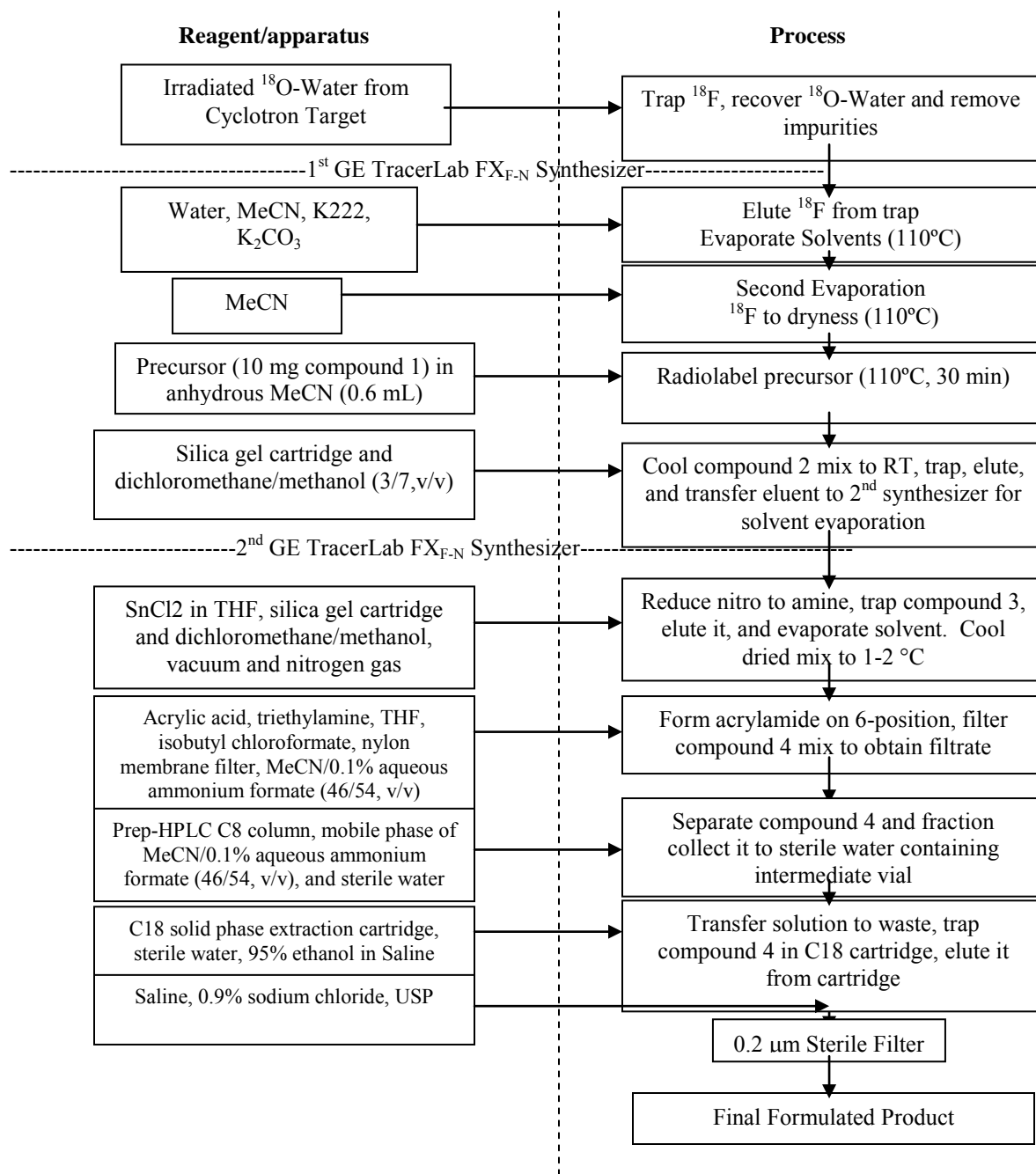


**Figure 5.** Flow Diagram of Manufacturing Process for  $^{18}\text{F}$ -PEG6-IPQA on Automated Synthesis Unit

### **Release tests**

The following QC tests are performed on each batch prior to product release except the Sterility test. Sterility test is performed within 24 hours of product manufacturing or the next business day.

<b>Test description</b>
Appearance
Filter Integrity
pH measurement
Radionuclide purity
Residual solvent (GC)
Chemical & Radiochemical ID, purity, and impurity (HPLC)
Bacterial Endotoxin (LAL)
Half-life determination
Sterility Test

### **Specifications**

Specifications for each test method are listed in Table 3. Each production batch will be tested and results meet the pre-set specifications before it can be released for clinical phase I use.

**Table 3.** Specifications

<b>Test description</b>	<b>Specification</b>
Appearance	Clear, colorless, no particulates
Filter Integrity	≥ 56 psi
pH	5 – 8
Radionuclide purity	≥ 99.5% gamma emissions at 511KeV, 1022KeV or comppton scatter peaks
Residual solvent	Acetonitrile <0.04%
Chemical & Radiochemical Purity (HPLC)	Radiochemical Purity >90%
Bacterial Endotoxin (LAL)	<175 EU per dose
Half-life determination	105 – 115 minutes 1 <sup>st</sup> activity/time 2 <sup>nd</sup> activity/time
Sterility Test	Negative/No Growth

### **Stability**

The short and long term chemical stability of the product has not been evaluated. Due to the nature of auto decay of <sup>18</sup>fluorine, the product is only intended to be used within 8 hours after manufacturing. In addition, we plan to conduct chemical stability study of the product to support the claimed shelf life/expiration period.

### **Environmental Analysis**

The institution requests a claim of categorical exclusion under 21 CFR 25.31. MD Anderson is currently in compliance with the provisions of 21 CFR 25.31 as it relates to IND's and that to our knowledge there are no extraordinary circumstances that would significantly affect the quality of the human environment.

# 1. Introduction and general investigational plan

Epidermal growth factor receptor, EGFR, signaling pathway has created tremendous interest within oncology research over the past decades. EGFR is a transmembrane protein comprised of an extracellular ligand-binding domain, a lipophilic transmembrane domain, and an intracellular tyrosine kinase domain. EGFR can be activated by a variety of ligands including epidermal growth factor (EGF), transforming growth factor- $\alpha$  (TGF- $\alpha$ ), and etc. After binding of activating ligand to the extracellular domain of the receptor, EGFR dimerizes and consequently leads to tyrosine kinase activation and tyrosine autophosphorylation. The EGFR can also be activated by EFG/ligand-independent mechanisms. EGFR is expressed, overexpressed, or dysregulated in many human solid tumors, including breast, ovarian, non-small-cell lung cancer (NSCLC), colorectal and head and neck cancers. Activation of the EGFR TK has been linked to oncogenesis and maintenance of different types of tumors, making it an attractive target for antitumor therapies.

Targeted therapies toward EGFR receptors and tyrosine kinase have been widely studied and developed. Monoclonal antibodies (mAbs) that bind specifically to the receptors have shown efficacy in tumor treatment. Cetuximab (C225 or Erbitux™) is an FDA approved mAb of this class (1) used for treating colorectal cancer. More efforts, in the meantime, have been focused on the discovery of small molecules for the inhibition of EGFR tyrosine kinase (EGFR-TK). These molecules are aimed at binding to the Mg-adenosine triphosphate (ATP) binding sites to inhibit EGFR phosphorylation which, in turn, blocks the downstream signal transduction it could otherwise initiate. The initial success of and enthusiasm for this strategy is exemplified by reversible inhibitors such as gefitinib (Iressa®) and erlotinib (Tarceva®) as well as some irreversible inhibitors including HKI-272 and GW572010. These have shown efficacy treating non-small cell lung cancer (NSCLC) and other EGFR-overexpressing cancers (1).

It has soon become clear that these reversible small molecule inhibitors are only effective in 10-15% NSCLC patients. Gefitinib showed no added benefit in survival compared with standard chemotherapy alone in a phase III trial in advanced NSCLC (2). Later findings demonstrated that only patients who have specific EGFR mutations are responsive to gefitinib or erlotinib (3). Stratifying patients for effective trials and monitoring their early response after treatment become critical to the success of EGFR inhibitor drug development.

Currently, there is a lack of a way to accurately measure EGFR expression. Tissue biopsy with immunohistochemistry testing provides spatially limited and temporally static information. Furthermore, this invasive procedure may be performed only infrequently for many obvious reasons, which limits its feasibility as a tool in the required repeated assessments of treatment response. A noninvasive procedure, e.g. employing positron emission tomography (PET) and CT (PET/CT) with an appropriate agent for quantitative imaging of tumor's EGFR-TK activity, might be an ideal approach. Repeated use of the agent for multiple assessments by PET imaging is feasible. In

addition, tumors with locations difficult for biopsy, such as those in the brain, may be easily imaged using PET.

Great effort has been devoted to the discovery and optimization of EGFR-TK selective PET imaging agents. Most candidates for PET imaging agents have been centered on various modifications of the well recognized anilinoquinazoline pharmacophore which is believed to be responsible for their fitting into the ATP pocket of tyrosine kinase domain. Both gefitinib and erlotinib, for instance, possess this pharmacophore. Radio-labeling of these candidates for PET imaging have included 11-Carbon, 124-Iodine, and 18-Fluorine. Preclinical characterizations of a number of agents in cell lines, mice and rats with tumor xenografts, and/or nonhuman primates have been conducted(4-6). Among these, a compound from our group labeled with 124-iodine, (E)-but-2-enedioic acid [4-(3-[<sup>124</sup>I]iodoanilino)-quinazolin-6-yl]-amide-(3-morpholin-4-yl-propyl)-amide, has demonstrated effectiveness of detecting tumors with high EGFR kinase signaling activity, including brain tumors expressing EGFRvIII mutants and NSCLC expressing gain-of-function EGFR kinase mutants(6). The main drawback of this agent, however, includes significant hepatobiliary clearance rendering imaging tumors of abdomen not feasible. Also, this agent has a short half-life in the circulation resulting in reduced availability for tumor uptake. Further, the long half-life of 124-iodine isotope can be a safety and logistic concern in clinical practice.

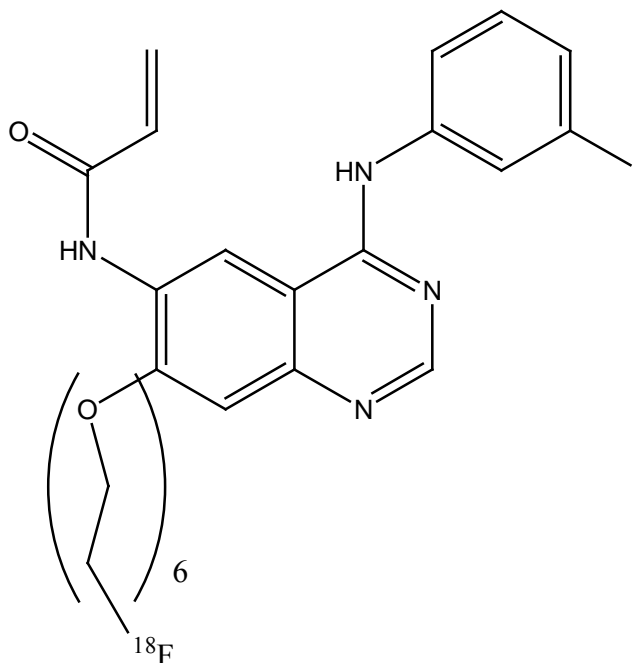
Modifications of imaging agents to overcome these shortcomings included changes made mainly to the 6-and 7-positions of the quinazoline moiety. It has been found that attaching a reactive acrylamide group to the 6-position gives rise to irreversible binding of the agent with Cys-773 residue in the EGFR kinase domain. The strong driving force due to the irreversible targeted binding should enhance this agent's tumor uptake. Also, adding a polyethylene glycol (PEG) chain of 4 – 6 units to the 7-position has been shown to render an increased solubility of the compound, hence, an expected longer residence time in the blood circulation (7). Based on the structure-property relationships and preclinical results on many analogs from us and others, we finally selected the novel PET imaging agent, <sup>18</sup>Fluoro-PEG6-IPQA (4-[3-Iodophenyl]amino]-7-{2-[2-{2-(2-[2-(<sup>18</sup>F-fluoroethoxy)-ethoxy]-ethoxy)-ethoxy]-ethoxy}-ethoxy]-quinazoline-6-yl-acrylamide) for further development (figure 1).

This EGFR-TK selective PET imaging agent is formulated as an intravenous injection in 6% ethanol containing saline. Although structurally similar agents (i.e., Irressa® and Tarceva®) have been used in humans for therapeutic purpose, this particular agent has not been introduced to human. We've conducted a GLP single dose toxicity study (by Charles River Laboratories) of Fluoro-PEG6-IPQA administered by intravenous (bolus) injection to rats with a 14-day recovery period. The following parameters and end points were evaluated in this study: clinical signs, body weights, body weight changes, food consumption, clinical pathology parameters (hematology, coagulation, clinical chemistry, and urinalysis), gross necropsy findings, organ weights, and histopathologic examinations. The results from this study revealed that administration of Fluoro-PEG6-IPQA to rats as a single intravenous (bolus) injection was well tolerated at a dose level of

136.245  $\mu\text{g/kg}$  (more than 100 times the intended dose). No systemic toxicity was observed and no target organs were identified.

The acute toxicity induced by single intravenous injection of  $^{18}\text{F}$ -PEG6-IPQA with a mean dose of 3.8 mCi (3.47  $\mu\text{g}$ ) was determined in 3 male and 3 female monkeys. Electrocardiogram during PET study, hematology, and chemistry before and after injection of this radiotracer were obtained. The electrocardiograms were monitored for significant changes from baseline. None of these non-human primates injected with  $^{18}\text{F}$ -PEG6-IPQA manifested any alternations in cardiac rhythm or wave patterns from the point of administration to 180 minutes post injection. Hematology and chemistry data revealed that there were no significant changes induced by  $^{18}\text{F}$ -PEG6-IPQA on blood chemistry, liver enzyme and renal function after 14 days post  $^{18}\text{F}$ -PEG6-IPQA PET study. Mild elevated levels of liver enzymes as represented by AST and ALT together with LDH on day 3 indicated a transient impact on liver function potentially due to the imaging agent or other factors such as anesthetic agents administered during the process. These levels resumed normal in 14 days without any intervention. Minor albumin elevation tested on day-14 may reflect the status of dehydration of the animal. An average increase of platelet count on the six monkeys over the 14 day period after  $^{18}\text{F}$ -PEG6-IPQA administration was observed and the significance of which has yet to be determined.

Based on the encouraging results from preclinical studies, we file this IND to gain permission to conduct a clinical phase I study using this novel PET imaging agent.



Chemical Formula: C<sub>29</sub>H<sub>36</sub>FIN<sub>4</sub>O<sub>7</sub>  
Molecular Weight: 698.52

Figure 1. Molecular structure of <sup>18</sup>F-fluoro-PEG6-IPQA, 4-[3-Iodophenylamino]-7-{2-[2-{2-(2-[2-{2-(<sup>18</sup>F-fluoroethoxy)-ethoxy}-ethoxy)-ethoxy}-ethoxy)-ethoxy]-ethoxy}-quinazoline-6-yl-acrylamide

In the phase I study, PET imaging with <sup>18</sup>F-PEG6-IPQA in NSCLC patients will be carried out at the University of Texas M. D. Anderson Cancer Center. The primary goals of the phase I trial include evaluating this new agent's biodistribution, dosimetry, pharmacokinetics, metabolites, and safety. The secondary goals are to assess the new agent's tumor detectability and its correlation with tumor's sensitivity to treatment with EGFR tyrosine kinase inhibitors.

Based on biodistribution and dosimetry results obtained from our nonhuman primate study, the initial administered dose/activity for the first cohort of three female patients will be approximately 2 mCi. Dynamic whole-body PET/CT imaging along with blood and urine sample analysis will be performed. Dosimetry will be calculated after the first cohort is completed and a new administered dose will be determined using only the human data for the subsequent cohorts. Fifteen (15) patients will be accrued for this phase I study.

## References

1. JG. G. Molecular imaging of epidermal growth factor receptor expression-activity at the kinase level in tumors with positron emission tomography. *Cancer Metastasis Review*. 2008 2008;27(4):645-653.
2. Herbst RS GG, Schiller JH, Natale RB, Miller V, Manegold C, Scagliotti G, Rosell R, Oliff I, Reeves JA, Wolf MK, Krebs AD, Averbuch SD, Ochs JS, Grous J, Fandi A, Johnson DH. Gefitinib in combination with paclitaxel and carboplatin in advanced non-small-cell lung cancer: a phase III trial--INTACT 2. *J Clin Oncol*. Mar 1 2004;22(5): .
3. Paez JG JP, Lee JC, Tracy S, Greulich H, Gabriel S, Herman P, Kaye FJ, Lindeman N, Boggon TJ, Naoki K, Sasaki H, Fujii Y, Eck MJ, Sellers WR, Johnson BE, Meyerson M. EGFR mutations in lung cancer: correlation with clinical response to gefitinib therapy. *Science*. Jun 4 2004;304(5676).
4. Mishani E AG, Jacobson O, Dissoki S, Ben Daniel R, Rozen Y, Shaul M, Levitzki A. High-affinity epidermal growth factor receptor (EGFR) irreversible inhibitors with diminished chemical reactivities as positron emission tomography (PET)-imaging agent candidates of EGFR overexpressing tumors. *J Med Chem*. Aug 11 2005;48(16).

5. Bonasera TA OG, Rozen Y, Kraiss R, Freedman NM, Chisin R, Gazit A, Levitzki A, Mishani E. Potential (18)F-labeled biomarkers for epidermal growth factor receptor tyrosine kinase. *Nucl Med Biol.* 2001;28(4).
6. Pal A GA, Doubrovin M, Balatoni J, Namavari M, Beresten T, Maxwell D, Soghomonyan S, Shavrin A, Ageyeva L, Finn R, Larson SM, Bornmann W, Gelovani JG. Molecular imaging of EGFR kinase activity in tumors with 124I-labeled small molecular tracer and positron emission tomography. *Mol Imaging Biol.* Pet-Oct 2006;5(5).
7. Dissoki S AY, Laky D, Abourbeh G, Levitzki A, Mishani E. The effect of the [18F]-PEG group on tracer qualification of [4-(phenylamino)-quinazoline-6-YL]-amide moiety--an EGFR putative irreversible inhibitor. *Appl Radiat Isot.* October 2007;65(10).

## Table of Contents

- 3. Protocol
  - 3.1 Study Objectives and Rationale
  - 3.2 Study Population
    - 3.2.1 Eligibility Criteria
    - 3.2.2 Subject Recruitment
  - 3.3 Study Plan
    - 3.3.1 Study Design
    - 3.3.2 Investigational Center
  - 3.4 Method of dose determination
  - 3.5 Study Procedures and Evaluations
    - 3.5.1 Pre-dose administration Period
    - 3.5.2 Radiopharmaceutical administration period
    - 3.5.3 Imaging Period
    - 3.5.4 Blood Sample Acquisition Period
    - 3.5.5 Urine Sample Acquisition Period
    - 3.5.6 Post administration/imaging period
  - 3.6 Efficacy and Safety Endpoints
    - 3.6.1 Primary endpoint
    - 3.6.2 Secondary Endpoints
    - 3.6.3 Efficacy Assessments
    - 3.6.4 Safety Assessments
  - 3.7 Statistical Methods of Analysis
    - 3.7.1 General Statistical Considerations
    - 3.7.2 Subject Characteristics
    - 3.7.3 Efficacy analysis
    - 3.7.4 Safety Analysis
    - 3.7.5 Procedures for missing, unused and spurious data
    - 3.7.6 Rules for excluding subjects from analysis
    - 3.7.7 Procedures for reporting deviations from original statistical plan
  - 3.8 Study Administration and Investigator Obligations
    - 3.8.1 Institutional Review Board
    - 3.8.2 Informed Consent
    - 3.8.3 Modification of the Protocol
    - 3.8.4 Protocol Deviations
    - 3.8.5 Concomitant Medications
    - 3.8.6 Biosafety Procedures
    - 3.8.7 Pregnancy
    - 3.8.8 Case Report Forms
    - 3.8.9 Termination of the Study
    - 3.8.10 Records Retention
    - 3.8.11 Study Monitoring
    - 3.8.12 Medical Monitoring
    - 3.8.13 Ethical and Legal Considerations
    - 3.8.14 Risks/Benefits
    - 3.8.15 Gender and Minority Inclusion

### 3.8.16 Subject Records

### **3. Protocol**

#### **3.1 Study Objectives and Rationale**

The primary and secondary objectives of the study are as follows:

Primary Objectives:

- To determine the optimum dosimetry of  $^{18}\text{F}$ -PEG6-IPQA injection based on critical organ safety.
- To obtain data on  $^{18}\text{F}$ -PEG6-IPQA distribution, pharmacokinetics and metabolites.
- To assess the safety of a single intravenous administration of  $^{18}\text{F}$ -PEG6-IPQA in subjects with solid tumors.

Secondary Objectives:

- To determine the optimum dosimetry of  $^{18}\text{F}$ -PEG6-IPQA injection based on detection sensitivity.
- To obtain preliminary data on the feasibility of detection of both primary and metastatic tumor lesions using  $^{18}\text{F}$ -PEG6-IPQA PET as compared to standard of care modalities (e.g.  $^{18}\text{F}$ -fluorodeoxyglucose PET, contrast enhanced static computed tomography (CECT), magnetic resonance imaging (MRI), bone scintigraphy and/or US).
- To correlate the magnitude of tumor uptake and retention of  $^{18}\text{F}$ -PEG6-IPQA with tumor EGFR expression and/or therapeutic drug response for patients in whom tumor tissue EGFR expression has already been obtained and for those patients who do subsequently undergo therapy with an agent targeting EGFR.

The rationale of the current study will be to determine the optimum dosimetry of this novel PET imaging agent in patients with non-small cell lung cancer; and to demonstrate that it is feasible and safe to be employed in routine PET imaging use based on characteristics of its biodistribution, pharmacokinetics, and metabolites. It is also aimed to assess the detectability of this agent for NSCLC and to evaluate the correlation of magnitude of  $^{18}\text{F}$ -PEG6-IPQA retention in tumor with EGFR expression and/or drug response.

#### **3.2 Study Population**

Eligibility criteria for this study have been carefully considered to ensure the safety of the study subjects and to ensure that the results of the study can be used. It is imperative that subjects fully meet all eligibility criteria. For entry into the study, the following criteria must be met.

### **3.2.1 Eligibility Criteria**

#### **3.2.1.1 Inclusion Criteria**

1. All patients must give written informed consent.
2. Subjects must be at least 18 years of age.
3. Patients should have pathologically or cytologically confirmed non-small cell lung cancer with clinical or radiological evidence that it is not amenable to therapy with curative intent
4. Patients should be potential candidates for therapy with an EGFR tyrosine kinase inhibitor or with an anti-EGFR monoclonal antibody by clinical criteria.
5. Patients should have clinical characteristics that would suggest an increased probability of benefit from an EGFR inhibitor. Specifically, they should have either:
  - Less than a 10 pack-year smoking history AND a latency period from last tobacco use to diagnosis of longer than 10 years AND either lung adenocarcinoma or NSCLC not otherwise specified, OR
  - Known EGFR mutations OR high EGFR gene copy number
6. Patients should have at least one tumor deposit that is > 1.0 cm in diameter, and that is amenable to imaging
7. Patients should be ECOG performance status 0-2
8. Patients with brain metastases are eligible provided they meet all other eligibility criteria and do not require corticosteroids or enzyme-inducing anticonvulsants and provided it is felt clinically that they will not require radiotherapy in the three (3) weeks subsequent to their participation in the study.
9. Women of childbearing potential must agree to use adequate contraception (hormonal or barrier method of birth control; abstinence) prior to study entry and for the duration of study participation. Childbearing potential will be defined as women who have had menses within the past 12 months, who have not had tubal ligation or bilateral oophorectomy. Should a woman become pregnant or suspect that she is pregnant while participating in this study, she should inform her treating physician immediately. The patient, if a man, agrees to use effective contraception or abstinence

10. The patient must be considered legally capable of providing his or her own consent for participation in this study

### **3.2.1.2 Exclusion Criteria**

1. Prior therapy with an EGFR inhibitor or an anti-EGFR monoclonal antibody
2. Radiotherapy, chemotherapy or any investigational agent within the previous 4 weeks of administering  $^{18}\text{F}$ -PEG6-IPQA for PET/CT imaging.
3. A non-investigational targeted agent within the previous 2 weeks of  $^{18}\text{F}$ -PEG6-IPQA for PET/CT imaging.
4. Thoracic or abdominal surgery within the previous 2 weeks of  $^{18}\text{F}$ -PEG6-IPQA for PET/CT imaging.
5. A tumor that is known to have a K-ras mutation
6. Squamous cell, large cell undifferentiated, neuroendocrine or small cell undifferentiated carcinoma of the lung
7. A known other currently active malignancy. (Benign tumors and benign polyps, basal cell carcinomas of skin, superficial papillary bladder tumors, and pre-invasive carcinoma of the cervix are permitted)
8. Physical inability to undergo a scanning procedure (e.g., inability to lie flat for the required period of time – three sessions of roughly an hour each with ten minutes' rest in between)
9. Serum creatinine  $>1.5 \times \text{ULN}$ , bilirubin  $>1.5 \times \text{ULN}$ , AST  $> 3 \times \text{ULN}$
10. Hemoglobin  $< 8 \text{ g/dL}$ , absolute neutrophil count  $< 1,500/\text{mm}^3$ , platelet count  $< 100,000/\text{mm}^3$
11. Potentially life-threatening arrhythmia; myocardial infarct within the previous 3 months; unstable angina, or angina at rest; congestive heart failure (New York Heart Association Functional Classification class II or worse), uncontrolled hypertension (systolic BP  $> 160$  or diastolic BP  $> 100$ ).
12. Active acute infection (i.e. currently treated with antibiotics). Patients with chronic infections such as hepatitis B or C, mycobacterium avium or similar infections will be eligible provided they meet all other eligibility criteria.
13. Oxygen saturation  $< 90\%$  on room air

14. Clinical requirement for systemic corticosteroids for control of cerebral edema or for enzyme-inducing anticonvulsants. (Inhaled steroids and systemic steroids for COPD are permitted).
15. Pregnant or nursing
16. Any condition that is unstable or could jeopardize the safety of the patient and his or her compliance in the study, in the investigator's judgment.

### **3.2.2 Subject Recruitment**

MD Anderson Cancer Center (MDACC): Representatives from Thoracic/Head & Neck Medical Oncology (i.e., the principal investigator, the co-principal investigator, sub-investigators, and the research nurse) will screen and evaluate patients seen in the M.D. Anderson Thoracic Center to identify potential subjects.

## **3.3 Study Plan**

### **3.3.1 Study Design**

This will be a phase 1, open-label, proof-of-concept study to assess the dosimetry, distribution, pharmacokinetics, metabolism, and excretion of  $^{18}\text{F}$ -PEG6-IPQA PET imaging agent. Also, it is designed to assess the ability of  $^{18}\text{F}$ -PEG6-IPQA PET imaging to detect tumors. The safety of  $^{18}\text{F}$ -PEG6-IPQA will be monitored and evaluated in the study.

Up to 15 evaluable subjects are planned to be included at a single study center, M. D. Anderson Cancer Center. Subjects are considered evaluable if they undergo administration of  $^{18}\text{F}$ -PEG6-IPQA injection, PET imaging procedure, and follow up visits.

After enrollment, the subject will be scheduled for PET imaging using  $^{18}\text{F}$ -PEG6-IPQA injection. Each subject in the first cohort will receive  $^{18}\text{F}$ -PEG6-IPQA injection with a maximum total activity of approximately 2 mCi (70 Mbq). The  $^{18}\text{F}$ -PEG6-IPQA injection will be administered by intravenous injection and that will be followed by a saline flush.

PET imaging will comprise 3 sessions of imaging periods. The total imaging time is approximately 3 hours. Within 3 weeks prior to the PET imaging day, the subject will undergo imaging procedures as required for standard of care, e.g. CT, MRI, bone scintigraphy, X-ray,  $^{18}\text{F}$ -FDG PET, or ultrasound. The diagnosis obtained from these examinations will be an imaging reference standard for part of the secondary efficacy evaluation.

Subjects will be included in the study for approximately 6 weeks: from signing the informed consent until 2 weeks after PET imaging visit.

The images obtained from all sessions will be used for the dosimetry and distribution analysis of the  $^{18}\text{F}$ -PEG6-IPQA PET imaging agent. Estimates of uptake and retention in tumors will be made and compared to those in normal tissue using data from the multiple PET acquisitions. Tumors identified with  $^{18}\text{F}$ -PEG6-IPQA PET imaging will be correlated to the tumors identified with standard of care imaging examinations. Comparisons will be made on an overall (i.e., all tumor lesions) and tumor type basis. Only tumors (or metastases) identified with standard of care imaging will be used for the secondary endpoint efficacy/delectability analysis.

Safety will be assessed from the rates of adverse events (AEs), changes in vital signs, changes in ECG parameters, and changes in physical examination findings. Safety assessments will be performed at various pre- and post-treatment time points (see Table 3).

### **3.3.2 Investigational Center**

This single-site phase I trial will be conducted at M. D. Anderson Cancer Center under the principle investigator Donald A. Podoloff, MD and the co-principle investigator Davis J. Stewart, MD. Their contact information is in the following:

#### **Principal Investigator (MDACC):**

Donald A. Podoloff, MD  
University of Texas M.D. Anderson Cancer Center  
1515 Holcombe Blvd., Unit 0057  
Houston, TX 77030  
Phone: 713-745-1160  
Fax: 713-745-1155  
e-mail: dpodoloff@mdanderson.org

#### **Co-Principal Investigator (MDACC):**

David J. Stewart, MD  
University of Texas M.D. Anderson Cancer Center  
1515 Holcombe Blvd., Unit 432  
Houston, TX 77030  
Phone: 713-792-6363  
Fax: 713-792-1220  
e-mail: dstewart@mdanderson.org

### **3.4 Method of dose determination**

## Radiation dose based on Statistical Considerations

Up to 15 patients will be imaged in this study using  $^{18}\text{F}$ -PEG6-IPQA as a PET imaging agent. The maximum allowed single absorbed radiation doses for sensitive organs (whole body, gonads and red marrow) and non-sensitive organs are 3 and 5 rems, respectively. Absorbed dose estimates for 25 organs must be monitored. The study is designed with the intent to limit the probability that a patient exceeds the target dose (e.g., 3 or 5 rems depending on the organ) in any organ to be less than 0.10.

We propose a three-stage design in which three female patients in the first stage and six patients (three females and three males) in each of the 2<sup>nd</sup> and 3<sup>rd</sup> stages are imaged, for a total of 15 patients. Since imaging quality is usually better in smaller patients, we want the first three patients to be female, and small in size, to maximize the likelihood of achieving useful data with the starting level of administered dose/activity. A cohort summary will need to be completed and submitted to the Clinical Research Monitor in the IND Office prior to moving to cohort 2 and 3. Prior to advancing cohorts, all subjects in the cohort should be observed for at least 1 week. The result of the 1 week follow up examination, the dosimetry result of the cohort, and the statistical evaluation method stated below will be the bases for determining the activity level for the next cohort.

Following the completion of each stage, the 90<sup>th</sup> percentile for the distribution of equivalent dose per unit administered activity (1 rem/MBq = 10 mSv/MBq) for the highest radiation dose administered will be estimated and used to determine the acceptable administered dose levels (or activities) for the next cohort. The initial administered dose level, determined as described below based on primate experiments, will be 70 MBq. Radiation absorbed dose will be estimated and monitored after each patient study and the administered dose will be recomputed if any patient exceeds the allowed single-dose limit in any organ (ref: RDRC (21CFR361.1)). For purposes of experimental design, we assume that the radiation absorbed dose in each organ follows a Gaussian distribution. Preliminary data from 6 primates imaged with  $^{18}\text{F}$ -PEG6-IPQA were collected for the purpose of obtaining initial estimates of average organ doses per MBq, as well as between subject variations. Radiation absorbed doses in 25 different organ systems were estimated for 3 female and 3 male primates, from which humanized organ doses were constructed. These data are used to estimate the two quantities relevant for the estimation of radiation dose experienced by patients included in this study: the population mean and the standard deviation of radiation exposure between patients for each organ. Because large differences were observed between the radiation doses absorbed in different organs during the primate study, hierarchical modeling of these parameters across organs was not performed.

Based on these assumptions, we estimate radiation absorbed doses associated with an imaging study to be approximately independently distributed within each organ with mean  $\mu_{organ}$  and inter-subject standard deviation  $\sigma_{organ}$ . Upon completion of this study, the 90<sup>th</sup> percentile of each organ's radiation dose within a randomly selected patient will be

$$\bar{x}_{organ} + t_{1-\alpha, n-1} \cdot s_{organ}, \quad (1)$$

where  $n$  denotes the number of patients imaged at certain dose level,  $\bar{x}_{organ}$  denotes the sample mean of exposure for the given organ, and  $s_{organ}$  denotes the sample standard deviation of measurements for that organ. Because of the imbalance of exposure found among primate organs and the fact that the primary risk of high exposure occurs primarily in the gallbladder wall, we do not propose standard Bonferroni-type adjustments to the probability of exposure, which would distribute the probability that exposure would exceed specified limits evenly across all organs. Instead, we propose a 0.09, 0.002, and 0.003 probability limit that the 5 rems will be exceeded in an individual patient's gallbladder wall, small intestine and kidney, respectively, and  $0.005/22=0.0002$  probability limit that radiation dose will be exceeded in each remaining organ. This results in a total probability that the target radiation dose exceeding the specified limit in any organ is less than 0.10.

The variance of the estimate of the bound (1) is

$$Var(\bar{x}_{organ} + t_{1-\alpha, n-1} \cdot s_{organ}) = Var(\bar{x}_{organ}) + t_{1-\alpha, n-1}^2 Var(s_{organ}) \quad (2)$$

where  $Var(\bar{x}_{organ}) = \frac{\sigma_{organ}^2}{n}$ , and

$$Var(s) = \frac{\sigma_{organ}^2}{n-1} \left[ (n-1) - \left( \sqrt{2} \frac{\Gamma\left(\frac{n}{2}\right)}{\Gamma\left(\frac{n-1}{2}\right)} \right)^2 \right]. \quad (3)$$

Based on these expressions and the humanized primate data, we estimate the expected 90<sup>th</sup> percentile on total equivalent dose for each organ system. These values, along with the standard error of the joint 90<sup>th</sup> percentiles for sample sizes of  $N=3, 9$ , and  $15$  are displayed in Table 1, assuming a total radiation dose of 70MBq for all cohorts. Note that effective samples sizes for gender-specific organs will differ from non-gender specific organs and is accounted for in the table for the 2<sup>nd</sup> and 3<sup>rd</sup> cohorts by assuming that half of each sample will be of each gender. Based on Table 1, a total sample size of 15 is proposed. With 15 patients at one administered dose, we will achieve a precision measured by coefficient of variation (CV) of  $0.10 \pm 0.04$  (range 0.05 ~ 0.20) in estimating the radiation exposure for each organ. With 12 patients from the last two cohorts, we will achieve a CV of  $0.12 \pm 0.05$  (range 0.06 ~ 0.23). We recommend an initial administered dose of 70MBq to ensure that no organ is exposed to excessive radiation.

Table 1 is based on humanized data from the primate experiments, and estimates in this table will be updated after data from the initial cohort of three human patients are obtained. Specifically, only human data will be used to calculate recommended

administered doses for the 2<sup>nd</sup> and 3<sup>rd</sup> patient cohorts, and standard  $t$  prediction interval distributions will be used to calculate these intervals. Procedures similar to those described for the first cohort will be used to distribute the probability that maximum doses are exceeded to those organs most at risk. Linearity of exposure/dose assumptions will be verified using data collected upon completion of the Phase 1 study, where it is expected that modified administered doses/activity will be assigned to each cohort.

Table 1. Anticipated 90<sup>th</sup> percentile of radiation exposure required to guarantee that the probability of exceeding the dose limits is less than 10% as a function of sample size. Columns 2 and 3 provide estimated mean and SD of absorbed dose in human organs (mSv/MBq) based on primate data. Columns 4-7 are family-wise 90<sup>th</sup> percentile for each organ's dose (rem) with their corresponding SD, assuming a total administered dose of 70MBq for all cohorts. Column 8 is the posterior probability of exceeding exposure limit for each organ.

	Mean	SD	90 <sup>th</sup> percentile (SD) for each organ's radiation dose (rem) with total administered dose of 70MBq				Pr (Exceeding Limit)
			N=3	N=9	N=15	N=12**	
Adrenals	0.0152	0.0017	0.66(0.25)	0.17(0.02)	0.16(0.01)	0.16(0.01)	0.0002
Brain	0.0055	0.0009	0.33(0.14)	0.07(0.01)	0.07(0.01)	0.07(0.01)	0.0002
Breasts	0.0071	0.0010	0.38(0.15)	0.09(0.01)	0.08(0.01)	0.08(0.01)	0.0002
Gallbladder Wall	0.3871	0.2518	6.28(1.94)	5.30(0.87)	5.20(0.65)	5.23(0.74)	0.09
LLI Wall	0.0133	0.0043	1.50(0.65)	0.26(0.04)	0.23(0.03)	0.24(0.03)	0.0002
Small Intestine	0.0589	0.0389	4.71(2.00)	1.50(0.28)	1.35(0.19)	1.40(0.22)	0.002
Stomach Wall	0.0129	0.0009	0.39(0.14)	0.13(0.01)	0.12(0.01)	0.12(0.01)	0.0002
ULI Wall	0.0308	0.0121	4.17(1.83)	0.70(0.12)	0.60(0.08)	0.63(0.09)	0.0002
Heart Wall	0.0132	0.0012	0.49(0.19)	0.14(0.01)	0.13(0.01)	0.13(0.01)	0.0002
Kidneys	0.0802	0.0669	6.58(2.80)	2.30(0.45)	2.08(0.31)	2.15(0.36)	0.003
Liver	0.0422	0.0169	5.84(2.57)	0.97(0.17)	0.83(0.11)	0.88(0.13)	0.0002
Lungs	0.0127	0.0031	1.11(0.47)	0.21(0.03)	0.19(0.02)	0.20(0.02)	0.0002
Muscle	0.0095	0.0012	0.46(0.18)	0.11(0.01)	0.10(0.01)	0.11(0.01)	0.0002
Ovaries	0.0159	0.0054	1.88(0.82)	0.42(0.10)	0.33(0.05)	0.42(0.10)	0.0002
Pancreas	0.0173	0.0021	0.82(0.32)	0.21(0.02)	0.19(0.01)	0.19(0.02)	0.0002
Red Marrow	0.0107	0.0014	0.55(0.22)	0.13(0.01)	0.12(0.01)	0.12(0.01)	0.0002
Osteogenic Cells	0.0131	0.0022	0.82(0.34)	0.18(0.02)	0.16(0.01)	0.17(0.02)	0.0002
Skin	0.0066	0.0010	0.39(0.16)	0.09(0.01)	0.08(0.01)	0.08(0.01)	0.0002
Spleen	0.0117	0.0012	0.48(0.18)	0.13(0.01)	0.12(0.01)	0.12(0.01)	0.0002
Testes	0.0079	0.0017		0.63(0.26)	0.15(0.03)	0.15(0.03)	0.0002
Thymus	0.0083	0.0014	0.52(0.21)	0.11(0.01)	0.10(0.01)	0.11(0.01)	0.0002
Thyroid	0.0076	0.0016	0.56(0.23)	0.11(0.02)	0.10(0.01)	0.11(0.01)	0.0002
Urinary Bladder Wall	0.0356	0.0225	7.65(3.43)	1.15(0.23)	0.97(0.14)	1.03(0.17)	0.0002
Uterus	0.0161	0.0052	1.83(0.80)	0.41(0.09)	0.32(0.05)	0.41(0.09)	0.0002
Total Body	0.0113	0.0011	0.43(0.16)	0.12(0.01)	0.11(0.01)	0.12(0.01)	0.0002

\*\* If only the last two cohorts are combined.

The 90th percentile of each organ's exposure per unit (mSv/MBq) and its standard deviation will be updated after observing data from each stage using the following formula:

$$UB_{ij} = \bar{x}_{ij} + t_{1-\alpha_i, n-1} \cdot s_{ij}, i = 1, 2, \dots, 25, j = 1, 2 \quad (4)$$

Where  $i$  denotes organ,  $j$  denotes dose level,  $\bar{x}_{ij}$  is the observed mean exposure/dose (mSv/MBq) of the  $i^{\text{th}}$  organ at  $j^{\text{th}}$  dose,  $s_{ij}$  is the observed standard deviation of the  $i^{\text{th}}$  organ at  $j^{\text{th}}$  dose,  $n$  equals the number of patients treated at each dose level,  $\alpha_i$  is the one-

sided type I error rate spent on the  $i^{\text{th}}$  organ. The family-wise alpha level will be maintained at 0.10 level,

$$\alpha = \sum_{i=1}^{25} \alpha_i = 0.10, \quad (5)$$

but it will be distributed unevenly among organs based on how close the organ dose is to its limit.

The 90th percentile of each organ's dose (rems) is calculated as  $UB_{ij} \times \text{Dose}_j / 10$  ( $\text{Dose}_1 = 70$  MBq). If for any organ, the 90th percentile of dose exceeds its limit, then dose escalation will not occur and the trial will stop. If the 90th percentile of dose in each organ does not exceed its dose limit, then the next cohort of patients can be administered the same or a higher activity. The next administered dose will be determined such that the upper bound of absorbed dose to any given organ will not exceed its limit, i.e.

$$\text{Dose}_{j+1} = \min \{ \text{Limit}_i / UB_{ij} * 10, \text{MAX} \}, i = 1, 2, \dots, 25, j = 1, 2 \quad (6)$$

where  $\text{Limit}_i$  is the exposure limit (3 or 5 rems) for the  $i^{\text{th}}$  organ and MAX is the pre-specified maximum administered dose level, 370 MBq.

Based on three female patients' data from the 1<sup>st</sup> cohort, four scenarios have been evaluated for optimized administered dose decision using formula (6). The results are shown in Table 2.

Scenario 1: The average radiation absorbed dose for the 1<sup>st</sup> cohort is the same as that expected from the humanized primate data, however the standard deviation for each organ is 30% of the sample mean. The recommended administered dose level for cohort 2 will be 79 MBq.

Scenario 2: The average radiation absorbed dose for the 1<sup>st</sup> cohort is the same as that expected from the humanized primate data, however the standard deviation for each organ is 15% of the sample mean. The recommended administered dosage level for cohort 2 will be 99 MBq.

Scenario 3: The average radiation absorbed doses for some of the 1<sup>st</sup> cohort's organs are lower than expected from the humanized primate data, e.g., the average doses for gallbladder wall, small intestine, kidney, liver, and urinary bladder wall are 50% lower than expected and the standard deviation for each organ is 30% of the mean. The recommended administered dose level for cohort 2 will be 108 MBq.

Scenario 4: The average radiation absorbed dose for some of the 1<sup>st</sup> cohort's organs are lower than expected from the humanized primate data, e.g., the average radiation exposures for gallbladder wall, small intestine, kidney, liver, and urinary bladder wall are

50% lower than expected and the standard deviation for each organ is 15% of the mean. The recommended administered dose level for cohort 2 will be 198 MBq.

Table 2. Radiation dose for each organ of the 1<sup>st</sup> cohort in four scenarios

	Scenario 1		Scenario 2		Scenario 3		Scenario 4	
	Mean	SD	Mean	SD	Mean	SD	Mean	SD
	(mSv/MBq)		(mSv/MBq)		(mSv/MBq)		(mSv/MBq)	
Adrenals	0.0152	0.0046	0.0152	0.0023	0.0152	0.0046	0.0152	0.0023
Brain	0.0055	0.0017	0.0055	0.0008	0.0055	0.0017	0.0055	0.0008
Breasts	0.0071	0.0021	0.0071	0.0011	0.0071	0.0021	0.0071	0.0011
Gallbladder Wall	0.3871	0.1161	0.3871	0.0581	0.1936	0.0581	0.1936	0.0290
LLI Wall	0.0133	0.0040	0.0133	0.0020	0.0133	0.0040	0.0133	0.0020
Small Intestine	0.0589	0.0177	0.0589	0.0088	0.0295	0.0088	0.0295	0.0044
Stomach Wall	0.0129	0.0039	0.0129	0.0019	0.0129	0.0039	0.0129	0.0019
ULI Wall	0.0308	0.0092	0.0308	0.0046	0.0308	0.0092	0.0308	0.0046
Heart Wall	0.0132	0.0040	0.0132	0.0020	0.0132	0.0040	0.0132	0.0020
Kidneys	0.0802	0.0241	0.0802	0.0120	0.0401	0.0120	0.0401	0.0060
Liver	0.0422	0.0127	0.0422	0.0063	0.0211	0.0063	0.0211	0.0032
Lungs	0.0127	0.0038	0.0127	0.0019	0.0127	0.0038	0.0127	0.0019
Muscle	0.0095	0.0029	0.0095	0.0014	0.0095	0.0029	0.0095	0.0014
Ovaries	0.0159	0.0048	0.0159	0.0024	0.0159	0.0048	0.0159	0.0024
Pancreas	0.0173	0.0052	0.0173	0.0026	0.0173	0.0052	0.0173	0.0026
Red Marrow	0.0107	0.0032	0.0107	0.0016	0.0107	0.0032	0.0107	0.0016
Osteogenic Cells	0.0132	0.0040	0.0132	0.0020	0.0132	0.0040	0.0132	0.0020
Skin	0.0066	0.0020	0.0066	0.0010	0.0066	0.0020	0.0066	0.0010
Spleen	0.0117	0.0035	0.0117	0.0018	0.0117	0.0035	0.0117	0.0018
Testes	0.0079	0.0024	0.0079	0.0012	0.0079	0.0024	0.0079	0.0012
Thymus	0.0083	0.0025	0.0083	0.0012	0.0083	0.0025	0.0083	0.0012
Thyroid	0.0077	0.0023	0.0077	0.0012	0.0077	0.0023	0.0077	0.0012
Urinary Bladder Wall	0.0356	0.0107	0.0356	0.0053	0.0178	0.0053	0.0178	0.0027
Uterus	0.0161	0.0048	0.0161	0.0024	0.0161	0.0048	0.0161	0.0024
Total Body	0.0113	0.0034	0.0113	0.0017	0.0113	0.0034	0.0113	0.0017

### 3.5 Study Procedures and Evaluations

All efficacy and safety measurements obtained during the course of the study are summarized in the study schedule of events (Table 3).

Table 3. Study Schedule of Events

	Baseline	- 72 hours	Imaging day prior to dosing	Dose	+1, 3, 8, and 16 min	+ 30 min	+45, 60, 90, & 150 min	+ 3 hour or end of imaging procedure	+ 24 hours	+ 1 week	+ 2 weeks
Informed consent	●										
Study entry criteria	●										
Demographic information	●										
Medical history	●										
Prior/concomitant medication	●										
<sup>1</sup> Physical examination	●										●
Injection site monitoring			●			●		●	●	●	●
<sup>2</sup> Pregnancy test females of childbearing potential)		●									
<sup>A</sup> Vital signs	●		●			●		●	●	●	●
<sup>3</sup> Standard of care Diagnostic Imaging	●										
<sup>A,4</sup> Electrocardiogram	●		●					●			●
<sup>A,5</sup> Blood samples (serum biochemistry, haematology)	●								●	●	●
Adverse events (post –treatment )				●				●	●	●	●
<sup>18</sup> F-PEG6-IPQA injection				●							
<sup>A</sup> Blood sample acquisition					●	●	●				
<sup>A,6</sup> Urine sample acquisition											
<sup>718</sup> F-PEG6-IPQA PET imaging											

<sup>1</sup> Physical exam includes vital signs, exam of heart, lungs, mental status, motor strength, sensory perception, pertinent organ systems and anatomic sites as medically necessary.

<sup>2</sup> Subjects not surgically sterile by tubal ligation or hysterectomy or amenorrheic for less than 12 months will be considered "of childbearing potential".

<sup>3</sup>Standard of care imaging for all tumor types must be within 21 days of protocol PET imaging

<sup>4</sup> Lead II ECGs will be obtained on the study day prior to <sup>18</sup>F-PEG6-IPQA administration and at 3 hours after administration or at the end of the imaging procedure. Regular 12 lead ECG will be obtained at baseline and 2 weeks post imaging.

<sup>5</sup> Serum biochemistry: BUN, creatinine, total bilirubin, AST and ALT, alkaline phosphatase; albumin, total protein, and serum glucose. Hematology will be CBC.

<sup>6</sup> Urine sample acquisition: Urine will be collected when the patient has to void or at the end of imaging. Shaded area indicates continuous assessment.

<sup>7</sup> Imaging timeline and manual are in Appendices E and F. 3 imaging sessions per study are performed. Each imaging session is composed of two PET/CT scans for a total of 6 scans in total per the Timelines.

<sup>A</sup> All will be performed by the research staff

The following time windows will be allowed:

Table 4. Time Window for Blood Sampling and Safety Assessments

Time Point	Variation Around Time Point
Baseline	28 days +/- 3 days of <sup>18</sup> F-PEG6-IPQA PET/CT imaging day
+ 1 and 3 minutes after administration	+ 3 minutes, record actual time
+ 8 and 16 minutes after administration	± 4 minutes, record actual time
+ 30, 45, and 60 minutes after administration	± 10 minutes, record actual time
+ 90 and 150 minutes after administration	± 15 minutes, record actual time
+ 24 hours after administration	± 8 hours
+ 1 and 2 weeks after administration	± 3 days

### 3.5.1 Pre-dose administration Period

The pre-treatment period combines subject screening and baseline safety examinations, within 28 days prior to <sup>18</sup>F-PEG6-IPQA administration.

The investigator identifies a suitable subject and invites the subject to participate in this study. The subject must satisfy the inclusion/exclusion criteria requirements, which are listed in Sections 3.2. A signed written informed consent must be obtained from each subject prior to entering the study or performing any study specific procedures. A notation will be made in the subject's medical chart that he/she is participating in a clinical study and has provided signed and dated informed consent.

The following subject demographic and other covariate data will be recorded:

- Age
- Gender
- Childbearing potential (Subjects not surgically sterile by tubal ligation or hysterectomy or amenorrheic for less than 12 months, will be considered "of childbearing potential".)
- Race/Ethnicity identifications
- Weight
- Height
- Main diagnosis or reason for referral
- Concurrent illnesses (medical history)
- Concurrent medications
- Other therapies
- Vital signs
- ECG
- Serum Biochemistry and hematology
- Subject meets all inclusion and exclusion criteria

All pre-treatment events will be recorded in the medical history. Blood samples for serum biochemistry will be drawn. All female subjects of childbearing potential will undergo a serum pregnancy test within 72 hours prior to administration. Vital signs will be measured. A limited physical examination will be performed (Table 3).

Prior to  $^{18}\text{F}$ -PEG6-IPQA administration, vital signs will be measured again and lead II ECG will be recorded. The injection site will be examined for any abnormal findings.

Prior to  $^{18}\text{F}$ -PEG6-IPQA injection and with the subject lying supine on the scanner bed, the subject will undergo a whole body CT scout view for selection of the field of view for PET.

### **3.5.2 Radiopharmaceutical administration period**

ECG monitoring will occur before administration of  $^{18}\text{F}$ -PEG6-IPQA injection and again at the end of imaging procedures, approximately 3 hours.

$^{18}\text{F}$ -PEG6-IPQA injection will be administered as a single intravenous injection. Each individual dose will be administered only to the subject assigned to it. However, the preloaded syringe containing  $^{18}\text{F}$ -PEG6-IPQA could contain more radioactivity than is required for a 1-subject dose at the time of administration, so the correct volume needs to be calculated before administration. The volume to be injected must be calculated from the required dose and documented.

The subject will receive the  $^{18}\text{F}$ -PEG6-IPQA injection under the direct supervision of study personnel. The  $^{18}\text{F}$ -PEG6-IPQA will be injected intravenously with the subject lying in a supine position. Each subject will receive a single intravenous bolus of  $^{18}\text{F}$ -PEG6-IPQA injection with an approximate volume of 2-4 mL over a time period of up to approximately 10 seconds followed by a saline flush of 20 to 50 mL. The administration site will be evaluated pre- and post administration for any reaction (e.g. bleeding, hematoma, redness, or infection).

The maximum administered activity for the first cohort (3 patients) will be 70 MBq.

Documentation of the  $^{18}\text{F}$ -PEG6-IPQA injection administered to a subject will be recorded on the appropriate Nuclear Medicine radiopharmacy documentation form, including date, total volume, total radioactivity, start/stop time of administration, and injection site. After the dose has been given any remaining  $^{18}\text{F}$ -PEG6-IPQA may not be used.

### **3.5.3 Imaging Period**

After  $^{18}\text{F}$ -PEG6-IPQA administration, PET imaging data will be acquired for 3 sessions up to 3 hours. Each imaging session is composed of two PET/CT scans for a total of 6 scans per the imaging manual.

#### **3.5.4 Blood Sample Acquisition Period**

After  $^{18}\text{F}$ -PEG6-IPQA administration and saline flushing, 3 mL of blood samples will be drawn from a second indwelling catheter (different from the catheter through which  $^{18}\text{F}$ -PEG6-IPQA was injected) according to the time schedule listed as follows: 1, 3, 8, 16, 30, 45, 60, 90, 150 minutes.

The samples will be prepared and analyzed for  $^{18}\text{F}$ -PEG6-IPQA and its metabolites.

#### **3.5.5 Urine Sample Acquisition Period**

Urine sample(s) will be collected for analysis of  $^{18}\text{F}$ -PEG6-IPQA and its metabolites at the end of PET imaging sessions or the end of the entire imaging procedure.

#### **3.5.6 Post administration/imaging period**

Safety measurements will be performed from administration of  $^{18}\text{F}$ -PEG6-IPQA injection until 2 weeks after administration. These include injection site monitoring, vital signs, ECG recordings, limited physical examination, and laboratory evaluation done at the times specified in Table 3.

### **3.6 Efficacy and Safety Endpoints**

#### **3.6.1 Primary endpoint**

- Determine biodistribution and optimum dosimetry of  $^{18}\text{F}$ -PEG6-IPQA injection for the next cohorts from previous cohort based on statistical evaluation of critical organ exposure and safety limitations.
- Obtain pharmacokinetic data of  $^{18}\text{F}$ -PEG6-IPQA and establish pharmacokinetic model from blood sample analysis.
- Identify and measure metabolites from blood and urine samples.
- Assess safety profiles of subjects based on results from all safety monitoring procedures required in the protocol. The baseline data sets are the control for comparison.

### **3.6.2 Secondary Endpoints**

- Obtain preliminary data on the feasibility of detection of both primary and metastatic tumor lesions in particular tumor types using  $^{18}\text{F}$ -PEG6-IPQA PET and comparing them to standard of care modalities (e.g.  $^{18}\text{F}$ -fluorodeoxyglucose PET), contrast enhanced static computed tomography (CECT), magnetic resonance imaging (MRI), and bone scintigraphy.
- To correlate the magnitude of tumor uptake and retention of  $^{18}\text{F}$ -PEG6-IPQA with tumor EGFR expression and/or therapeutic drug response for patients in whom tumor tissue EGFR expression has already been obtained and for those patients who do subsequently undergo therapy with an agent targeting EGFR.

### **3.6.3 Efficacy Assessments**

#### **3.6.3.1 Biodistribution and dosimetry determination**

The biodistribution of  $^{18}\text{F}$ -PEG6-IPQA will be measured during the PET scans. The percent injected dose (%ID) obtained in different organs will be derived from the PET data.

The initial dose for the first three patients is proposed to be 70 MBq to ensure no organ is exposed to excessive radiation based on a careful statistical evaluation of data obtained from the six nonhuman primate studies.

The administered dose for the second cohort (six patients) will be updated after data from the initial cohort of three human patients is obtained. Specifically, only human data will be used to calculate acceptable doses for the second and the rest of the cohorts (see section 3.4 for details). We have employed OLINDA software for the dosimetry study of the primates and will use the same software for dosimetry determination in this trial.

#### **3.6.3.2 PK and metabolite data acquisition**

The total radioactivity in the blood and plasma compartments and urine samples of radiotracer will be assayed for radioactivity concentration using a gamma counter. A portion of each plasma sample, extracted with methanol and water, and the urine sample will be analyzed using an HPLC system coupled with a radiation detector. The method employs a Zorbax Eclipse XDB-C8 (4.6 x 150 mm, 5 $\mu\text{m}$ ) and a mobile phase of Acetonitrile/0.1% ammonium formate aqueous solution (47/53, v/v). Pharmacokinetic rate of accumulation or clearance will be determined.

### **3.6.3.3 Image acquisition**

Detailed information on the technology aspects of the trial is specified in a separate Imaging Manual (Appendix F).

The  $^{18}\text{F}$ -PEG6-IPQA PET images will be acquired by means of a PET/CT scanner. Three imaging sessions per study will be performed after administration of  $^{18}\text{F}$ -PEG6-IPQA. Each imaging session is composed of two PET/CT scans for a total of 6 scans.

Preparation for the PET scanning procedure prior to  $^{18}\text{F}$ -PEG6-IPQA administration will take approximately 10-15 minutes. Between each PET session, patient will have a 10 minute rest where he/she is encouraged to urinate and the urine sample will be collected. Patient will then be repositioned for the next PET session. The total imaging time including rest and repositioning will be approximately 180 minutes (3 hours).

### **3.6.3.4 Image data quality control**

The images data will be considered evaluable if they have been acquired according to this protocol and the procedures described in the Imaging Manual for the minimum of 2 complete sessions. Reference standard images are considered evaluable if clinical diagnosis is made based on those.

### **3.6.3.5 Reference standards**

In this study, the standard of care imaging modalities (i.e. the imaging reference standard) will be used as reference standard.

### **3.6.3.6 Standard of care imaging modalities**

For each subject, diagnostic standard of care examinations, e.g. CT, MRI, FDG PET, bone scintigraphy or X-ray, will be performed to detect or further evaluate the tumor lesions (primary tumor and/or metastases). All imaging procedures have to be performed prior to any major invasive diagnostic or therapeutic procedure related to the malignancy.

Technical details for the standard of care examinations will not be provided, since they will follow the clinical routine and standard of the respective care provider. To enable a comparison of  $^{18}\text{F}$ -PEG6-IPQA PET images to images obtained from standard of care imaging examinations, both imaging examinations should cover the same tumor lesion in a given subject.

The examinations will be scheduled according to the clinical needs of the subject within 3 weeks prior to  $^{18}\text{F}$ -PEG6-IPQA PET imaging, if the results of these evaluations are planned to be included in the study.

### **3.6.3.7 Image interpretation and correlation with reference standard**

All image data will be evaluated and compared to the reference standard in an unblinded fashion by one or more specialists in the area of the respective diagnostic procedure (e.g. radiology, ultrasound, nuclear medicine).

### **3.6.3.8 Quantitative assessment of $^{18}\text{F}$ -PEG6-IPQA dosimetry**

The dosimetry assessment of  $^{18}\text{F}$ -PEG6-IPQA will be derived from all data acquired during the imaging sessions. All data will be decay corrected to the time of administration. Whole organ activities will be determined and the time-activity curve analyzed for the area under the curve. The resident times and absorbed dose will then be calculated using the MIRD methodology.

### **3.6.3.9 Correlation of whole-body $^{18}\text{F}$ -PEG6-IPQA PET to standard of care imaging**

$^{18}\text{F}$ -PEG6-IPQA PET data will be correlated with standard of care imaging data described in section 3.6.3.4. If several diagnostic standard of care imaging examinations are available per study subject, the subject's clinician should combine the information resulting from these examinations into a single dataset consisting of location and number of lesions.

If a tumor lesion (primary tumor or metastasis) is identified in both examinations, this lesion will be regarded as a "match". If a tumor lesion is not identified in  $^{18}\text{F}$ -PEG6-IPQA PET, but is by a different diagnostic imaging procedure, this lesion will be regarded as a "mismatch". If a focal uptake is detected in  $^{18}\text{F}$ -PEG6-IPQA PET but cannot be verified by a different diagnostic imaging examination(s), this lesion will be regarded as a "mismatch".

The number of "matches" and "mismatches" will be evaluated by the following:

- Lesion (total lesions) level (i.e. total number of lesions correctly identified).
- Tumor type level (i.e. total number of tumors in a tumor type group correctly identified).

## **3.6.4 Safety Assessments**

The investigator(s) will review the safety data. All AEs and SAEs will be graded using NCI V3 Toxicity Criteria.

### **3.6.4.1 Clinical laboratory evaluation**

A local (M. D. Anderson) laboratory will perform clinical laboratory evaluation. Blood samples collected at 24 hour post  $^{18}\text{F}$ -PEG6-IPQA administration will be radioactive and will be labeled appropriately. The receiving laboratory will be informed about the sample status in advance. The blood sample obtained at the 1 and 2 week time points are fully decayed and are handled as regular non-radioactive samples.

Blood samples will be obtained and analyzed for serum biochemistry at the various pre- and post-  $^{18}\text{F}$ -PEG6-IPQA administration time point ranges described in Table 3. Any abnormal laboratory findings that constitute an AE that occurs during the study period (up through 14 days after  $^{18}\text{F}$ -PEG6-IPQA injection is administered) must be followed until clinical recovery is complete and laboratory tests have returned to baseline, or until progression of the event has been stabilized, or until the PI determines there has been acceptable resolution of the event. Also, additional diagnostic tests may be indicated to determine a more precise diagnosis of the subject's condition (e.g. ordering a white blood cell differential to help characterize a high or low WBC count, or ordering a determination of red blood cell indices to help characterize a low hematocrit).

#### **3.6.4.2 Vital signs**

Vital signs will be measured at the various pre- and post-  $^{18}\text{F}$ -PEG6-IPQA administration time point ranges described in Table 3. Vital sign parameters include measurements of heart rate, systolic and diastolic blood pressures, respiration rate, and body temperature. Before vital signs are measured, the subject should be resting for at least 5 minutes (if possible). The same position will be used each time vital signs are measured for a given subject and blood pressure will be measured from the arm contra-lateral to the site of  $^{18}\text{F}$ -PEG6-IPQA administration as possible.

Interpretation and follow-up of vital signs results that are outside the normal limits should be conducted in conjunction with the clinical situation of the subject.

#### **3.6.4.3 Electrocardiograms**

ECGs (12 lead) will be obtained at baseline and 2 weeks post imaging. Lead II ECGs will be obtained on the study day prior to  $^{18}\text{F}$ -PEG6-IPQA administration and at 3 hours after administration or at the end of the imaging procedure. All ECG recordings will be read per Cardiology standard of care. Lead II strips will be read and QTc intervals will be calculated by a board-certified cardiologist. The physician reading ECGs may make clinical management decisions as needed. However, the hardcopy ECG strips will be read on the same day or day after the ECG examination by a board-certified cardiologist.

Subject management decisions may be based on the lead II ECG findings. Each lead II ECG tracing must be signed, dated, and assessed. The assessment results will be entered into PDMS and the signed strips will be scanned into the patient's EMR. During the ECG monitoring, the investigator will observe the real-time ECG findings and take note of any changes in intervals and/or waveforms. The investigator will not be expected to calculate QTc intervals. Abnormalities will be graded using CTC Version 3 Toxicity Criteria.

#### **3.6.4.4 Physical examination**

A qualified physician or a non-physician medically-certified individual will conduct limited physical examinations at the following time points range specified in Table 3. Information about the physical examination must be present in the source documentation at the study site. PDMS entry as the CRF will be in the AE section for both existing at baseline and new AEs.

In the event that new and worsening abnormal physical examination findings are encountered during the study, these terms are defined as follows: a new abnormal physical examination finding is defined as one that occurs when a subject's normal baseline physical examination becomes abnormal post baseline, based on clinical grounds. A worsening abnormal physical examination finding is defined as one that occurs when a subject's abnormal baseline physical examination becomes worse post baseline, also based on clinical grounds.

#### **3.6.4.5 Injection site monitoring**

The injection site will be monitored periodically from the time of the injection up to 24 hours after injection and at the following discrete time points: 30 minutes, 3 hours, and 24 hours after administration, and at the 1 week and 2 weeks post dose time points.

Abnormal injection site findings include radiopharmaceutical extravasation, bleeding, hematoma, redness, and infection.

#### **3.6.4.6 Pre-treatment events**

Pre-treatment events (i.e. signs and symptoms occurring prior to  $^{18}\text{F}$ -PEG6-IPQA administration) will be recorded during the screening/pre-treatment period (i.e. within 3 weeks before  $^{18}\text{F}$ -PEG6-IPQA administration and on the study day prior to administration) in the adverse event section of the CRF. These events should not be pre-existing conditions that are reflected in the medical history.

The following information on pre-treatment events will also be recorded in the CRF:

- The onset date and time
- The resolution date and time
- Intensity (mild, moderate, or severe)
- Severity
- Action taken
- Outcome

Only pre-treatment events that increase in intensity after administration of  $^{18}\text{F}$ -PEG6-IPQA injection will be recorded as an AE.

#### **3.6.4.7 Adverse events**

Subjects will be assessed for the occurrence of AEs from administration of  $^{18}\text{F}$ -PEG6-IPQA injection until 3 hours after administration. Thereafter, subjects will be asked to report any AEs up to 2 weeks after  $^{18}\text{F}$ -PEG6-IPQA PET imaging.

The Investigator or physician designee is responsible for verifying and providing source documentation for all adverse events and assigning the attribution for each event for all subjects enrolled on the protocol. An AE is defined as any untoward medical occurrence in a patient or clinical investigation subject administered a pharmaceutical product and which does not necessarily have to have a causal relationship with this treatment. An AE can therefore be any unfavorable and unintended sign (including an abnormal laboratory finding), symptom, or disease temporally associated with the use of an  $^{18}\text{F}$ -PEG6-IPQA, whether or not considered related to that product. AEs (including event name, grade, start/stop date, and attribution) will be documented in the medical record and then entered into PDMS. All AEs will be recorded using NCI Common Toxicity Criteria, Version 3. If an AE has already been reported it is not necessary to report each individual sign and symptom of that AE as a separate AE.

The subject will be closely observed and questioned for any kind of AE during the study procedures and at follow-up appointments throughout the study period with non-leading questioning (e.g. “how do you feel?”). The subjects will be instructed to report any symptoms and signs to the study staff in a timely manner (i.e. between formal observations).

A large number of AEs not related to the  $^{18}\text{F}$ -PEG6-IPQA are expected due to the subjects’ underlying disease.

#### **3.6.4.8 Other significant adverse events**

Clinical laboratory abnormalities that qualify as AEs (other than those meeting the definition for serious) and any events that lead to an intervention (including premature discontinuation of  $^{18}\text{F}$ -PEG6-IPQA, dose reduction or significant additional concomitant therapy), other than those reported as SAEs, will be reported and evaluated as other significant AEs.

#### **3.6.4.9 Serous adverse events**

A serious adverse event is – any adverse drug experience occurring at any dose that results in any of the following outcomes:

- Death
- A life-threatening adverse drug experience – any adverse experience that places the patient, in the view of the initial reporter, at immediate risk of death from the

- adverse experience as it occurred. It does not include an adverse experience that, had it occurred in a more severe form, might have caused death.
- Inpatient hospitalization or prolongation of existing hospitalization
- A persistent or significant disability/incapacity – a substantial disruption of a person’s ability to conduct normal life functions.
- A congenital anomaly/birth defect.

Important medical events that may not result in death, be life-threatening, or require hospitalization may be considered a serious adverse drug experience when, based upon appropriate medical judgment, they may jeopardize the patient or subject and may require medical or surgical intervention to prevent one of the outcomes listed in this definition. Examples of such medical events include allergic bronchospasm requiring intensive treatment in an emergency room or at home, blood dyscrasias or convulsions that do not result in inpatient hospitalization, or the development of drug dependency or drug abuse (21 CFR 312.32).

- Important medical events as defined above, may also be considered serious adverse events. Any important medical event can and should be reported as an SAE if deemed appropriate by the Principal Investigator or the IND Sponsor-IND Office.).
- SAE must be reported to the IRB in accordance with the timeframes and procedures outlined in “University of Texas M. D. Anderson Cancer Center Institutional Review Board Policy on Reporting Serious Adverse Events”. Unless stated otherwise in the protocol, all SAEs, expected or unexpected, must be reported to the IND Office, regardless of attribution (within 5 working days of knowledge of the event).
- All life-threatening or fatal events, expected or unexpected, and regardless of attribution to the study drug, must have a written report submitted within 24 hours (next working day) of knowledge of the event to the Safety Project Manager in the IND Office.
- The MDACC “Internal SAE Report Form for Prompt Reporting” will be used for reporting to the IND Office.
- Serious adverse events will be captured from the time the patient signs consent until 30 days after the last dose of drug. Serious adverse events must be followed until clinical recovery is complete and laboratory tests have returned to baseline, progression of the event has stabilized, or there has been acceptable resolution of the event.
- Additionally, any serious adverse events that occur after the 30 day time period that are related to the study treatment must be reported to the IND Office. This may include the development of a secondary malignancy.

#### Reporting to FDA:

Serious adverse events will be forwarded to FDA by the IND Sponsor (Safety Project Manager/IND Office ) according to 21 CFR 312.32.

## Reporting to USAMRMC:

All serious adverse events (defined below), whether or not deemed study-related or expected, must be reported by the Principal Investigator or designee to the HSRRB (Human Subjects Research Review Board) and/or USAMRMC Human Research Protection Office within 24 hours (one working day) by telephone. A written report must follow as soon as possible, which includes a full description of the event and any sequelae. This includes serious adverse events that occur any time after the inclusion of the subject in the study (defined as the time when the subject signs the informed consent) up to 30 days after the subject completed or discontinued the study. The subject is considered completed either after the completion of the last visit or contact (e.g., phone contact with the Investigator or designee). Discontinuation is the date a subject and/or Investigator determines that the subject can no longer comply with the requirements for any further study visits or evaluations (e.g., the subject is prematurely discontinued from the study). An adverse event temporarily related to participation in the study should be documented whether or not considered to be related to the test article. This definition includes intercurrent illnesses and injuries and exacerbations of preexisting conditions. Include the following in all IND safety reports: Subject identification number and initials; associate investigator's name and name of MTF; subject's date of birth, gender, and ethnicity; test article and dates of administration; signs/symptoms and severity; date of onset; date of resolution or death; relationship to the study drug; action taken; concomitant medication(s) including dose, route, and duration of treatment, and date of last dose.

Reports of all serious adverse events must be communicated to the appropriate Institutional Review Board (IRB) or ethical review committee and/or reported in accordance with local laws and regulations. Unanticipated problems involving risk to subjects or others, serious adverse events related to participation in the study and all subject deaths should be promptly reported by phone (301-619-2165), by email (hsrrb@det.amedd.army.mil), or by facsimile (301-619-7803) to the U.S. Army Medical Research and Materiel Command, Human Subjects Research Review Board (HSRRB). A complete written report should follow the initial notification. In addition to the methods above, the complete report can be sent to the U.S. Army Medical Research and Materiel Command, ATTN: MCMR-ZB-QH, 504 Scott Street, Fort Detrick, Maryland 21702-5012.

For all protocols conducted at M.D. Anderson Cancer Center, the Principal Investigator is responsible for submitting adverse event reports to the Institutional IRB and the HSRRB and/or USAMRMC Human Research Protection Office on an ongoing basis.

## Reporting of Subject Death

The death of any subject during the study or within 30 days of study completion (as

defined above), regardless of the cause, must be reported within 24 hours by telephone, to the principal investigator and/or study coordinator and the HSRRB and/or USAMRMC Human Research Protection Office. A full written report must follow as soon as possible. If an autopsy is performed, the report must be provided to the Sponsor. Reports of all **serious adverse events, including deaths**, must be communicated to the appropriate Institutional Review Board or ethical review committee and/or reported in accordance with local law and regulations.

**It is the responsibility of the PI and the research team to ensure serious adverse events are reported according to the Code of Federal Regulations, Good Clinical Practices, the protocol guidelines, the sponsor's guidelines, and Institutional Review Board policy.**

### **3.7 Statistical Methods of Analysis**

#### **3.7.1 General Statistical Considerations**

Tabulations of summary statistics, graphical presentations, and statistical analysis will be performed. All summary tables and data listings will also be separated by tumor type. The last pre-treatment observation will be used as the baseline value for calculating post-treatment changes from baseline. All data obtained on the CRF and entered into the database will be provided in separate data listings showing individual subject values. All subject data will be presented in separate data listings. All subjects who are enrolled in the study and receive  $^{18}\text{F}$ -PEG6-IPQA injection will be included in the safety analysis. All subjects with tumor lesions who have received  $^{18}\text{F}$ -PEG6-IPQA injection and undergone PET imaging will be included in the efficacy analysis.

#### **3.7.2 Subject Characteristics**

A table will be provided with the following information:

- Number of subjects enrolled
- Number of subjects included in the efficacy analysis
- Number of subjects included in the safety analysis
- Number of subjects withdrawn from the study and the reason for withdrawal

Demographic information (age, height, weight, and body mass index) will be summarized using descriptive statistics. Gender and race will be summarized by counts and percents. Medical history findings will be summarized by counts and percents. Concurrent medications will be recorded and coded using a standard classification system and grouped by primary and secondary classes, if applicable.

#### **3.7.3 Efficacy analysis**

Statistical evaluation and dosimetry calculation is detailed in section 3.4. PK and metabolites data from each evaluable subject will be tabulated and graphed to illustrate the results and conclusions.

### **3.7.4 Safety Analysis**

The safety population will include all subjects who received the  $^{18}\text{F}$ -PEG6-IPQA.

Summaries of safety data will present tabulations for the whole safety population and for each tumor type. All continuous safety variables will be summarized by descriptive statistics and discrete variables will be summarized by counts and percentages.

The investigators will evaluate the normal or abnormal of the results from clinical laboratory, vital sign, and ECG results for the following:

- An outlying result for any numeric laboratory result, vital sign result, or ECG interval measurement will be any post-treatment change from baseline that meets either of the following criteria:  
<25<sup>th</sup> percentile – 1.5 x (interquartile range) or  
>75<sup>th</sup> percentile + 1.5 x (interquartile range).
- An extreme value for any numeric laboratory result, vital sign result, or ECG interval measurement will be any post-treatment change from baseline that meets either of the following criteria:  
<25<sup>th</sup> percentile – 3 x (interquartile range) or  
>75<sup>th</sup> percentile + 3 x (interquartile range).

Post-treatment changes from baseline will be summarized by mean, standard deviation, minimum, and maximum at each time point and for each tumor type. Plots and shift tables of all post-treatment changes from baseline for each tumor type versus time will be generated and examined for trends and relatively large individual changes from baseline.

#### **3.7.4.1 Clinical laboratory evaluation**

For each clinical laboratory variable and each time point, the following safety endpoints will be summarized by counts and percents by tumor type:

- The occurrence of one or more changes from baseline, at each post-treatment time point, greater than 40% and 80% of the span of the normal limits (not applicable to qualitative parameters).
- The occurrence of post-treatment values that are changes greater than 80% of the span of the normal limits (not applicable to qualitative parameters).

#### **3.7.4.2 Vital signs**

For each vital sign variable and each time point, the following safety endpoints will be summarized by counts and percents by tumor type:

- The occurrence of one or more changes from baseline, at each post-treatment time point, greater than a pre-specified magnitude (20 mm Hg for systolic blood pressure, 10 mm Hg for diastolic blood pressure, 10 beats per minute for heart rate, 1.5 C for body temperature, and 10 breaths per minute for respiration rate.
- The occurrence of post-treatment values outside the normal limits.

#### **3.7.4.3 Electrocardiograms**

For each time point, ECG parameters will be evaluated by the cardiologist and documented on the hard copy of the ECG. CTC Version 3 Toxicity Criteria will be used to grade abnormalities.

#### **3.7.4.4 Physical examination**

The number and percent of subjects with changes in physical examination status from normal at baseline to abnormal at each post-treatment time point will be presented by tumor type.

#### **3.7.4.5 Pre-treatment events**

The number and percent of subjects with one or more pre-treatment events will be summarized by tumor type.

#### **3.7.4.6 Adverse events**

The number and percent of subjects with one or more AEs will be summarized by tumor type. Exact 95% confidence intervals about the percent of subjects with an AE will also be presented.

There will be discussions of other significant AEs, defined as laboratory abnormalities that qualify as AEs (other than those meeting the definition for serious) and any events that led to an intervention (including premature discontinuation of <sup>18</sup>F-PEG6-IPQA, dose reduction, or significant additional concomitant therapy), in addition to those reported as SAEs.

#### **3.7.4.7 Significance level**

Statistical tests will use a 0.05 significance level and will be 2-sided unless otherwise noted. Confidence intervals, both individual and simultaneous, will be at 95% confidence level unless stated otherwise.

### **3.7.5 Procedures for missing, unused and spurious data**

Missing values will not be substituted by estimated values, but treated as missing in the statistical evaluation. All data from all subjects dosed in the study will be included in all listings, plots, summary tables, and statistical analysis when appropriate.

### **3.7.6 Rules for excluding subjects from analysis**

A subject will be excluded from relevant analysis if a subject has failed to complete all procedures required by the study protocol for a corresponding efficacy population. If the subject has received any <sup>18</sup>F-PEG6-IPQA, all available safety data will be used. The reason(s) for any exclusion will be described in the report.

### **3.7.7 Procedures for reporting deviations from original statistical plan**

Any deviations from the statistical analysis outlined in this protocol will be described, and reasons for the deviations listed, in the final Clinical Study Report.

## ***3.8 Study Administration and Investigator Obligations***

### **3.8.1 Institutional Review Board**

This study must have the approval of a properly constituted Hospital Ethics Committee, Regional Ethics Committee, or other Institutional Review Board (IRB).

The investigator must submit an annual review report and a final study report to the Institutional Review Board (IRB) for approval. Copies of the continuing review report and final study report must also be forwarded to the HSRRB.

The investigator must also report all serious and medically significant adverse events to the IRB or Ethics Committee, as well as the USAMRMC Human Research Protection Office.

### **3.8.2 Informed Consent**

All study participants must sign and date an informed consent form prior to any study related procedures. The investigator will be responsible for designing the consent form using appropriate National or Regional Guidelines (equivalent to the American Federal Guidelines Federal Register July 27, 1981, or 21 CFR Part 50, or International Committee on Harmonization-Good Clinical Practice).

The informed consent form must be approved by the IRB or Ethics Committee and the USAMRMC Human Subjects Research Review Board (HSRRB). State and local laws, and/or institutional requirements may require the disclosure of additional information on the informed consent form. A copy of the informed consent form will be given to the participant. The investigator will keep each participant's signed informed consent form on file for inspection by a regulatory authority at any time.

### **3.8.3 Modification of the Protocol**

The investigator will only alter the protocol to eliminate apparent immediate hazards to the participant. If preliminary or interim statistical analysis indicated that the experimental design, dosages parameters, or selection of participants should be modified, these changes will be described in an amendment to be approved by the institution's and other appropriate review committees after consultation with the statistician and Study Chairman. Any amendments cannot be enacted unless approved by the HSRRB and/or USAMRMC Human Research Protection Office. All revisions made to protocols previously approved by the IRB will be submitted to the IRB for approval prior to implementation of the revision. If the IRB decides to disapprove a research activity, it shall include in its written notification a statement of the reasons for its decision and give the investigator an opportunity to respond in person or in writing. No changes to the protocol will be initiated unless also approved by the Human Subjects Research Review Board.

### **3.8.4 Protocol Deviations**

In the event of a protocol deviation and/or violation, the principal investigator will notify the Institutional Review Board, U.S. Army Medical Research and Materiel Command, Human Subjects Research Review Board (HSRRB), M.D. Anderson, and the study Medical Monitor (Eric Strom, M.D.). This notification will occur as soon as the deviation is identified and will be included in the annual review and final study report.

### **3.8.5 Concomitant Medications**

#### **3.8.5.1 Allowed**

Supportive treatment will be given as medically indicated. All concomitant medications will be specified in the case report form.

#### **3.8.5.2 Not Allowed**

Any treatment that might interfere with the biological activity, the efficacy, or the evaluation of the proposed study treatment is not allowed throughout patient participation in the study. Agents that may not be administered to patients while they are on this trial include other anticancer therapy and other investigational therapy.

### **3.8.6 Radiation Safety Procedures**

A copy of the radiation safety procedures approved by the IRB and/or Safety Committee will be kept on file in the Investigator Study File and the Pharmacy Study File. This document will be updated and revised as necessary to remain current with institutional guidelines.

### **3.8.7 Pregnancy**

The risk to a fetus is unknown, and information from animal studies may or may not predict what will happen in humans. Patients in this study should make every effort to avoid pregnancy both for themselves and with their partner while on the study. If pregnancy occurs in a subject or their partner, the investigator must notify the Principal Investigator immediately.

### **3.8.8 Case Report Forms**

All data will be entered into PDMS (or the system that is currently being designed to replace it at MD Anderson), which will serve as the electronic case report form (CRF).

### **3.8.9 Termination of the Study**

If, in the judgment of the investigators, the continued exposure to the study agent represents a significant risk to patients, the study will be terminated. The HSRRB and/or USAMRMC Human Research Protection Office, FDA and M. D. Anderson will retain the right to terminate the study and remove all study materials from the study site at any time. Specific instances that may precipitate such termination are as follows:

- Unsatisfactory participant enrollment with regard to quality or quantity

- Deviation from protocol requirements, without prior approval from HSRRB and M. D. Anderson.
- Inaccurate and/or incomplete data recording on a recurrent basis
- The incidence and/or severity of adverse drug events in this or other studies indicating a potential health hazard caused by the treatment

### **3.8.10 Records Retention**

The investigator and other appropriate study staff will be responsible for maintaining all documentation relevant to the study. Such documentation includes:

- Case Report Forms—must be accurate and up-to-date.
- Copies of all Serious AE reporting forms faxed to the USAMRMC Human Research Protection Office.
- Participant Files—should substantiate the data entered in PDMS with regard to laboratory data, participant histories, treatment regimens, etc.
- Participant Exclusion Log—should record the reason any participant was screened for the study and found to be ineligible.
- Drug Dispensing Log—should record the total amount of study drug received and returned to sponsor, and the amount distributed and returned or destroyed. This information must agree with the information entered in PDMS.
- Informed Consent Forms—completed consent forms from each participant must be available and verified for proper documentation.
- Informed Consent Log—must identify all participants who signed an Informed Consent Form so that the participants can be identified by audit.

The Investigator must keep on file protocols, amendments, IRB approvals, all copies of Form FDA 1572, all correspondence, and any other documents pertaining to the conduct of the study for a minimum of two (2) years after notification by USAMRMC Human Research Protection Office of either FDA approval or discontinuation of the IND.

### **3.8.11 Study Monitoring**

The University of Texas M.D. Anderson Cancer Center IND Office will monitor the study investigators to assure satisfactory enrollment rate, data recording, and protocol adherence. The investigator and staff are expected to cooperate and provide all relevant study documentation in detail at each site visit on request for review. M.D. Anderson Cancer Center will monitor and/or audit to assure satisfactory protocol adherence and enrollment.

### **3.8.12 Medical Monitoring**

The medical monitor will review all serious and unexpected adverse events associated with this protocol and provide an unbiased written report of the event within ten (10) calendar days of the initial report. At a minimum, the medical monitor will comment on the outcomes of the adverse event (AE) and relationship of the AE to the study. The medical monitor will also indicate whether he/she concurs with the details of the report provided by the study investigator.

The medical monitor for this study will be Eric Strom, MD:

Eric A. Strom, M.D.  
University of Texas M.D. Anderson Cancer Center  
Medical Research Monitor  
1220 Holcombe Blvd. ACBP1.2849  
Houston, Texas 77030 USA  
Phone: 713/563-5466  
Fax: 713/563-5468  
Email: [estrom@mdanderson.org](mailto:estrom@mdanderson.org)

The medical monitor will forward reports to the U.S. Army Research and Material Command, ATTN: MCMR-HRPO, 504 Scott Street, Fort Detrick, Maryland, 21702-5012.

### **3.8.13 Ethical and Legal Considerations**

This study will undergo full approval in accordance with the human surveillance requirements of each institution. Blood samples will be obtained for the evaluations as described in the protocol. Data collected on paper forms will be stored in locked file cabinets with restricted access. Data collected on electronic media will be stored in computer files with restricted password access. All staff members in the study will be informed prior to employment and at regular intervals of the necessity for keeping all data confidential. Computers will not be accessible to the public and will be located in locked offices. Subjects will be assigned a separate study number to protect subject identification. No patient identifiers will be used in any publications of this research.

### **3.8.14 Risks/Benefits**

#### **3.8.14.1 Risks**

<b>Procedure</b>	<b>Risks</b>	<b>Measures to Minimize Risks</b>
PET/CT scans	Radiation exposure	These diagnostic tests are medically necessary to monitor the patient; however, low risk of radiation exposure as part of participation in the study.
Intravenous administration of the trial imaging agent	1) Bruising, swelling, blood blister, pain and /or infection out of placing the needle in vein. 2) Chemical exposure due to the new imaging agent injected to patient's body	This is a similar procedure for patient who receives the standard of care PET imaging scan. The risk of getting these side effects due to needle puncture is low. The amount of chemical as the API (active pharmaceutical ingredient) administered is extremely low, in the order of 15 microgram/dose or less. It should not induce any pharmacologic or toxicological effects.
Blood draws	Pain, bleeding, bruising, infection, and/or fainting	The blood draw is necessary to characterize the property of the agent and amount of the blood draw is within the typical range.

### **3.8.14.2 Benefits**

The potential future benefits of the trial are:

- To enable better noninvasive PET imaging diagnoses of tumor types for patients who have the NSCLC
- To stratify patients based on the imaging results for different and most effective treatments accordingly
- To enable noninvasive PET procedure for monitoring treatment response

### **3.8.15 Gender and Minority Inclusion**

Women and minorities will be actively recruited to participate in the trial. The first cohort of 3 patients in this trial will be women who meet all eligibility criteria. However, since only 42% of lung cancer participants and 22% of laryngeal cancer participants are female, we expect to have more male than female subjects on the study. We expect that the ethnic distribution of the enrolled participants will reflect the local ethnic mixture of each institution's surrounding community.

### **3.8.16 Subject Records**

FDA, HSRRB and/or USAMRMC, Human Research Protection Office, M.D. Anderson or their representatives may have access to subject records.

### **3.9.13 Publication Statement**

Data will be reviewed by the collaborating biostatistician prior to publication. HSRRB and/or USAMRMC, Human Research Protection Office will have 30 days to review all definitive publications, such as manuscripts and book chapters, and a minimum of 10-15 days to review all abstracts.

### **3.9.14 Roles and Responsibilities of Key Study Personnel**

**Dr. Donald A. Podoloff** will serve as Study Chairman of this protocol at M. D. Anderson Cancer Center. He will coordinate and supervise all aspects of the clinical trial, supervise the biological correlate studies, and the preparation of results for presentations and publication. He will assume primary responsibility for the study.

**Dr. David J. Stewart** will serve as a Study Co-Chairman of this protocol at M. D. Anderson Cancer Center. He will coordinate and supervise all aspects of the clinical trial, and preparation of results for presentations and publication.



## Informed Consent

# Please Do Not Use for Patient Consent

Go to the PDOL Homepage to access the  
Informed Consent Printer Database

## INFORMED CONSENT/AUTHORIZATION FOR PARTICIPATION IN RESEARCH

A phase I study of 18F-Fluoro-PEG6-IPQA as a PET Imaging Agent for  
Active/Mutant EGFR Expression in Tumors  
2009-0832

**Study Chair: Donald Podoloff**

1.

Participant's Name

Medical Record Number

You are being asked to take part in this [clinical](#) research study at The University of Texas M. D. Anderson Cancer Center ("M. D. Anderson"). This consent form explains why this research study is being done and what your role will be if you choose to take part. This form also describes the possible risks connected with being in this study. After reviewing this information with the person responsible for your enrollment, you should know enough to be able to make an informed decision on whether you want to take part in the study.

You are being asked to take part in this study because [you may have a tumor in your lung](#).

This research study is financially supported by the United States Department of Defense.

## DESCRIPTION OF RESEARCH

### 2. PURPOSE OF STUDY

**NOT FOR USE IN CONSENTING PATIENTS**

The goal of this clinical research study is to learn if an imaging solution called 18F-PEG6-IPQA can help to find tumors when used in positron emission tomography (PET) scans. The safety of the solution and how the solution is processed by your body will also be studied.

### **3. DESCRIPTION OF STUDY**

**18F-PEG6-IPQA** is a solution that is designed to be attracted to tumor cells. The imaging solution has a small dose of radiation added to it, which may help doctors see the cancer cells better during imaging scans. This is the first study using 18F-PEG6-IPQA in humans.

#### **Screening Tests**

Signing this consent form does not mean that you will be able to take part in this study. You will have "screening tests" to help the doctor decide if you are eligible to take part in this study. The following tests and procedures will be performed:

- Blood (about 2 tablespoons) will be drawn for routine tests.
- You will have a physical exam, including measurement of your vital signs (blood pressure, heart rate, temperature, and breathing rate).
- Your medical history and demographic information (such as your marital status, job status, and education) will be recorded.
- You will be asked about any drugs you have taken in the past or are taking.
- You will have an electrocardiogram (ECG -- a test that measures the electrical activity of the heart).
- If you are able to become pregnant, you will have a blood (about 2 tablespoons) pregnancy test. To take part in this study, you must not be pregnant.

The study doctor will discuss the screening test results with you. If the screening tests show that you are not eligible to take part in the study, you will not be enrolled.

#### **Study Imaging**

If you are found to be eligible to take part in this study, you will visit the clinic on Day 1 for the injection of the study solution and PET scans.

For up to 6 hours before the PET scans and computed tomography (CT) scans, you must not eat or drink anything except water. This is called fasting.

A small tube will be placed in your arm and you will receive an injection of 18F-PEG6-IPQA.

After the injection, you will need to rest quietly until it is time for the scan. About 2 hours after the injection, you will have 3 PET scans with a PET/CT scanner. Before

each PET scan, you will have a CT scan to make sure you are in the right position for the PET scans. Each PET scan may last up to 1 hour. Each positioning CT scan should take about 5 minutes. You will have a 10 minute "rest period" between each PET scan.

### **Study Visits**

#### **On Day 1:**

- Before the imaging solution is injected, you will have an ECG and your vital signs will be measured.
- Blood (about 2 tablespoons total) will be drawn for pharmacokinetic (PK) testing. PK testing measures the amount of study solution in the body at different time points. Blood will be drawn at 1, 3, 8, 16, 30, 45, 60, 90, and 150 minutes after the injection of 18F-PEG6-IPQA for a total of 9 draws.
- About 30 minutes after the injection, your vital signs will be measured and the injection site will be checked.
- Urine will be collected during the 10 minute rest periods in between scans.
- After the scans are completed (about 5 hours after the injection) your vital signs and injections site will be checked again and you will have an ECG. Blood (about 2 tablespoons) and urine will also be collected for routine tests.

#### **On Days 2 and 7:**

- Blood (about 2-3 tablespoons) will be drawn for routine tests.
- Your vital signs and the injection site will be checked
- You will be asked about any side effects you may be having since the injection.

### **End-of-Study Visit**

The end-of-study visit will be about 14 days after the injection of 18F-PEG6-IPQA and imaging scans. The following tests and procedures will be performed:

- Blood (about 2-3 tablespoons) will be drawn for routine tests.
- You will have a physical exam, including measurement of your vital signs.
- The injection site will be checked.
- You will have an ECG.

### **Length of Study**

You will be in this study for about 14 days. You will be taken off study early if intolerable side effects occur.

**This is an investigational study.** 18F-PEG6-IPQA is not FDA-approved or commercially available for use in imaging scans. Its use in this study is investigational.

The scans performed with 18F-PEG6-IPQA are also considered investigational and will not be used for planning any of your future cancer treatment.

All study procedures and imaging scans will be performed at no cost to you while you are on study.

Up to 15 patients will take part in this study. All will be enrolled at M. D. Anderson.

#### 4. RISKS, SIDE EFFECTS, AND DISCOMFORTS TO PARTICIPANTS

While on this study, you are at risk for side effects. These side effects will vary from person to person. You should discuss these with the study doctor. Many side effects go away shortly after the study injection, but in some cases side effects may be serious, long lasting, or permanent, and may even result in hospitalization and/or death.

Tell the study staff about any side effects you may have, even if you do not think they are related to the study solution.

**This is the first study of 18F-PEG6-IPQA in humans, so the side effects are not well known.** Based on studies in animals, 18F-PEG6-IPQA may cause the following side effects:

● increased level of the substance in the blood that keeps the blood from leaking out of blood vessels	● increased blood platelet count (possible blood clotting problems)	● abnormal liver function tests (possible liver damage)
--	---	---

18F-PEG6-IPQA has a small amount of radiation, which means you will be exposed to radiation during the study. All radiation from the imaging solution and imaging scans adds up over a lifetime and may increase the risk of new cancer forming.

The radioactive solution does not remain in your system for a long period of time. However, you should wait 2 hours before holding an infant or getting close to a pregnant woman to avoid exposing them to radiation. You should drink fluids after the scan to help remove the solution from your system.

Bruising, swelling, pinching, blood blisters, pain, and/or an infection may occur at the injection site.

**PET and CT scans** may cause you to feel “closed in” while lying in the scanner. However, the scanner is open at both ends and an intercom allows you to talk with doctors and staff. If you feel ill or anxious during scanning, doctors and/or technicians will give comfort or the scanning will be stopped.

**Fasting** may cause your blood sugar to drop. You may feel tired, hungry, and/or nauseous. If you have diabetes, it is important to talk to your doctor about managing your blood sugar while fasting.

**Blood draws** may cause pain, bleeding, and/or bruising. You may faint and/or develop an infection with redness and irritation of the vein at the site where blood is drawn. Frequent blood collection may cause anemia (low red blood cell count), which may create a need for blood transfusions.

This study may involve unpredictable risks to the participants.

### **Pregnancy Related Risks**

- 4a. Because taking part in this study can result in risks to an unborn or breastfeeding baby, you should not become pregnant, breastfeed a baby, or father a child while on this study. You must use birth control during the study if you are sexually active.

Birth Control Specifications: If you are able to become pregnant or father a child, you must use birth control while on study. Acceptable forms of birth control include hormonal (such as birth control pills) or barrier method (such as a condom or diaphragm).

Females: If you are pregnant, you will not be enrolled on this study. If you become pregnant or suspect that you are pregnant, you must tell your doctor right away.

Getting pregnant **may** result in your removal from this study.

Males: Tell the doctor right away if your partner becomes pregnant or suspects pregnancy.

## **5. POTENTIAL BENEFITS**

Future patients may benefit from what is learned. There **are** no benefits for you in this study.

## **6. ALTERNATE PROCEDURES OR TREATMENTS**

You may choose not to take part in this study.

### **I understand that the following statements about this study are true:**

7. M. D. Anderson may benefit financially from my participation and/or from what is learned in this study.
8. This study is supported by: Department of Defense.
9. I may ask the study chair any questions I have about this study, including questions

about the costs. I may contact the study chair, Dr. Donald Podoloff, at 713-745-1160. I may also contact the Chair of M. D. Anderson's IRB at 713-792-2933 with any questions that have to do with this study or my rights as a study participant.

10. My participation in this research study is strictly voluntary. I may refuse to take part in this study without any penalty or loss of benefits to which I am otherwise entitled. I may also withdraw from participation in this study at any time without any penalty or loss of benefits. I should first discuss leaving the study with my doctor. If I withdraw from this study, I may still be treated at M. D. Anderson.
11. I understand that the study may be changed or stopped at any time by the study chair, Department of Defense, the U.S. Food and Drug Administration (FDA), the Office for Human Research Protections (OHRP) (a regulatory agency that oversees research in humans), or the IRB of M. D. Anderson.
12. I will be informed of any new findings that might affect my willingness to continue taking part in the study.
13. M. D. Anderson will take appropriate steps to keep my personal health information private. However, there is no guarantee of absolute privacy. Federal agencies (such as the FDA and the OHRP), Department of Defense, Cyclotop, and the IRB of M. D. Anderson might review my record to collect data or to check that the research is being done safely and correctly. In some situations, the FDA could be required to reveal the names of participants.
14. If I suffer injury as a direct result of taking part in this study, M. D. Anderson will provide medical care. However, this medical care will be billed to my insurance provider or me in the ordinary manner. I understand that I will not be reimbursed for expenses or compensated financially by M. D. Anderson or Department of Defense for this injury. I may also contact the Chair of M. D. Anderson's IRB at 713-792-2933 with questions about study-related injuries.
15. Certain tests, procedures, and/or medications that I may receive as part of this study may be without cost to me because they are for research purposes only. However, my insurance provider or I may be financially responsible for the cost of supportive care and treatment of any complications resulting from the research tests, procedures, and/or medications, including hospitalization, nausea, vomiting, low blood cell counts, and dehydration. Standard medical care that I receive under this research study will be billed to my insurance provider and/or me in the ordinary manner. I should learn before taking part in this study which parts of the research-related care will be provided without charge, which costs my insurance provider will pay for, and which costs will be my responsibility. I may ask to speak with a financial counselor about the costs of this study.
16. I understand that there are no plans to compensate me for any patents or

discoveries that may result from my participation in this research. I will receive no compensation for taking part in this study.

**Authorization for Use and Disclosure of Protected Health Information:**

- A. During the course of this study, the research team at M. D. Anderson will be collecting information about you. This information may include your medical history, study schedule, and the results of any of your tests, therapies, and/or procedures. The purpose of collecting and sharing this information is to learn about how the study procedures may affect the disease and any study-related side effects. Your doctor and the research team may share your study information with the parties named in Section E below. [If you withdraw from the study, data collected about you up to the time you withdrew may have to remain in the study database for inclusion in the data analysis.](#)
- B. If you refuse to provide your authorization to disclose your protected health information, you will not be able to participate in this research study.
- C. Your protected health information will be protected according to state and federal law. However, there is no guarantee that your information will remain confidential, and it may be re-disclosed at some point.
- D. All identifying information such as your name and address will be kept private. This information may be kept at M. D. Anderson forever. You will be assigned a code number so that your name will not be used. The research team at M. D. Anderson will be able to link the code number to your name. In some instances, in order to ensure the scientific value of the study, the parties named in Section E below will be able to view your study record but will not be permitted to copy any identifying information contained in your record.
- E. Your information may be shared with the following parties:
- Department of Defense
  - Cyclotope
  - The FDA
  - The OHRP
  - The IRB of M. D. Anderson
  - Officials of M. D. Anderson
  - Clinical study monitors who verify the accuracy of the information
  - Individuals with medical backgrounds who determine the effect that the study procedures may have on the disease
  - Individuals who put all the study information together in report form
- F. You have the right to see and reproduce your records related to the research study, and ask for corrections, for as long as this information is held by the study chair and/or M. D. Anderson. However, in some studies, in order to ensure the scientific

value of the study, participants are not able to view or reproduce their study records until the research has been completed with all participants in the study. If possible for this study, your doctor will be able to discuss your clinical test results with you.

- G. There is no expiration date for the use of your protected health information. You may withdraw your authorization to share your protected health information at any time in writing. Instructions on how to do this can be found in the M. D. Anderson Notice of Privacy Practices (NPP). You may contact the IRB Staff at 713-792-2933 with questions about how to find the NPP. If you withdraw your authorization, you will be removed from the study and the study chair and staff will no longer use or disclose your protected health information in connection with this study, unless the study chair or staff needs to use or disclose some of your research-related protected health information to preserve the scientific value of the study. The parties listed in Section E above may use any study data that were collected before you canceled your authorization.
- H. Information about this research study may be submitted to ClinicalTrials.gov, a publicly available online database managed by the U. S. National Institutes of Health. None of your identifying information will be submitted to ClinicalTrials.gov. If information from this study is submitted, none of it will be able to be directly linked to you.

# Please Do Not Use for Patient Consent

Go to the PDOL Homepage to access the  
Informed Consent Printer Database

## CONSENT/PERMISSION/AUTHORIZATION FOR TREATMENT

Having read and understood the above and having had the chance to ask questions about this study, think about the study, and talk with others as needed, I give the study chair permission to enroll me on this study. By signing this consent form, I am not giving up any of my legal rights. I have been given a signed copy of this consent document.

### **SAMPLE -- NOT FOR USE IN CONSENTING PATIENTS**

\_\_\_\_\_  
SIGNATURE OF PARTICIPANT

\_\_\_\_\_  
DATE

I was present during the explanation of the research to be performed under Protocol **2009-0832**.

### **SAMPLE -- NOT FOR USE IN CONSENTING PATIENTS**

\_\_\_\_\_  
SIGNATURE OF WITNESS TO THE VERBAL CONSENT PRESENTATION  
(OTHER THAN PHYSICIAN OR STUDY CHAIR)

\_\_\_\_\_  
DATE

### **SAMPLE -- NOT FOR USE IN CONSENTING PATIENTS**

\_\_\_\_\_  
SIGNATURE OF PERSON RESPONSIBLE & RELATIONSHIP

\_\_\_\_\_  
DATE

I have discussed this clinical research study with the participant and/or his or her authorized representative, using language that is understandable and appropriate. I believe that I have fully informed this participant of the nature of this study and its possible benefits and risks and that the participant understood this explanation.

### **SAMPLE -- NOT FOR USE IN CONSENTING PATIENTS**

\_\_\_\_\_  
SIGNATURE OF STUDY CHAIR OR PERSON OBTAINING CONSENT

\_\_\_\_\_  
DATE

**NOT FOR USE IN CONSENTING PATIENTS**

**Translator**

I have translated the above informed consent as written (without additions or subtractions) into \_\_\_\_\_ and assisted the people obtaining/providing  
(Name of Language)  
consent by translating all questions and responses during the consent process for this participant.

**SAMPLE -- NOT FOR USE IN CONSENTING PATIENTS**

NAME OF TRANSLATOR \_\_\_\_\_

SIGNATURE OF TRANSLATOR \_\_\_\_\_

DATE \_\_\_\_\_

- ☐ Please check here if the translator was a member of the research team. (If checked, a witness, other than the translator, must sign the witness line.)

**NOT FOR USE IN CONSENTING PATIENTS**